The Living Murray
One River. One Life. Our Future.

Koondrook–Perricoota Forest Flood Enhancement Project

Hydraulic Modelling

FORESTS NSW

MURRAY-DARLING BASIN COMMISSION

NSW Government
Department of Water & Energy

Department of **Environment & Climate Change** NSW

The Living Murray
One River. One Life. Our Future.

Koondrook–Perricoota Forest Flood Enhancement Project

Hydraulic Modelling

FORESTS NSW

MURRAY-DARLING BASIN COMMISSION

NSW Government
Department of Water & Energy

Department of **Environment & Climate Change** NSW

Acknowledgments

We wish to acknowledge the support provided by a number of people from Forests NSW; Murray Darling Basin Commission (MDBC); NSW Department of Water and Energy (DWE); NSW Department of Environment and Climate Change (DECC); NSW Department of Commerce; DHI Pty Ltd; Salient Solutions Pty Ltd; Water Technology Pty Ltd; Murray Catchment Management Authority, NSW; and North Central Murray Catchment Management Authority, Victoria. Lindsay Johnson, Gary Miller, Jin Teng, Jai Vaze, Vince Kelly, Andrew Keogh, Andy Close, Robert Clark, Grantley Smith, Ray Evans, John Lenehan, George Samios and Bronson McPherson provided technical and field support. Digby Jacobs, Mike Emy, Jolanta Skawinski, Linda Broekman, Peter Barker, Ross Williams and Mick Dwyer provided administrative support. The report was reviewed by Andy Close (MDBC) and Ana Deletic (Monash University). Ann Munroe and Diane Robinson provided editorial support and guided critical transition from manuscript to final publication. MDBC, DECC and DWE provided financial support for this work under The Living Murray Initiative.

Prepared by: Dr Narendra Kumar Tuteja

Contributions:
Dr Narendra Kumar Tuteja (DECC, eWater CRC) – **Hydraulic Modelling, Spatial Analysis, Soils**
Mustak Shaikh (DWE) – **Remote Sensing Analysis**
Brian Jenkins (DECC) – **Soils**
Paul Spiers (DECC) – **Vegetation Mapping**

Published by:
Department of Environment and Climate Change NSW
59–61 Goulburn Street
PO Box A290
Sydney South 1232

Phone: (02) 9995 5000 (switchboard)
Phone: 131 555 (environment information and publications requests)
Phone: 1300 361 967 (national parks information and publications requests)
Fax: (02) 9995 5999
TTY: (02) 9211 4723

Email: info@environment.nsw.gov.au
Website: www.environment.nsw.gov.au

ISBN 978 1 74122 672 0
DECC 2008/561
April 2008

Printed on recycled paper

Contents

Figures

Tables

Preface

There are about 4.5 million hectares of wetlands in NSW, most of which are located west of the Great Dividing Range and cover an area of about 6% of the State. The wetlands in NSW are divided into three broad groups: coastal, tableland and inland, on the basis of geographic location. Within these groups, wetlands vary in their hydrologic, geomorphic and vegetation characteristics. Wetlands are very sensitive to changes in both water and land management, which may result in their degradation or improvement.

An inter-governmental treaty, called 'The Ramsar Convention on Wetlands', was signed in 1971 to provide a framework for national action and international cooperation for the conservation and sustainable use of the wetlands of national and international significance. Koondrook–Perricoota Forest is in the NSW part of the Ramsar-listed Murray floodplain wetland 'Gunbower–Koondrook–Perricoota Forests'. It is the second largest red gum forest in Australia and is located along the River Murray between the towns of Echuca and Barham. It is one of the six icon sites that will benefit from environmental watering under The Living Murray initiative signed in 2002 by the Australian, New South Wales, Victorian, South Australian and Australian Capital Territory governments.

This report describes a major effort in hydraulic modelling of the Koondrook–Perricoota Forest undertaken by the Scientific Services Division of the Department of Environment and Climate Change in collaboration with NSW Department of Water and Energy, Forests NSW, the Murray Darling Basin Commission and NSW Department of Commerce. The work has been done to support development of the environmental watering plans envisaged in The Living Murray Initiative, engineering designs of the Torrumbarry Cutting, and to assist in implementation of basin-scale hydrological models to incorporate the effects of environmental flow diversions from the Murray River. A comprehensive hydraulic model for the Koondrook–Perricoota Forest has been developed in this work by using a multi-disciplinary approach, and the science that underpins the hydraulic model has been externally reviewed and is described in detail in this report. A robust technology in wetland modelling has been developed and demonstrated for the Koondrook–Perricoota Forest, and its generalisation to other important wetlands warrants consideration.

Len Banks
Executive Director
Scientific Services Division, DECC

Summary

Koondrook–Perricoota Forest (KPF) is one of the six Icon sites that will benefit under The Living Murray Initiative established by the Murray Darling Basin Ministerial Council in 2002. Within The Living Murray Initiative and The Environment Works and Measures Program coordinated by MDBC, it is proposed to construct a channel called the Torrumbarry Cutting to provide environmental flows to the KPF. This report describes the development and implementation of the MIKE suite of hydraulic models for the KPF. Key issues relating to the design capacity of the Torrumbarry Cutting; inflow to the KPF under historical and likely future flooding conditions; flood inundation mapping and remote sensing analysis; soils investigations; flood inundation patterns and inundation depth; partitioning of the water balance components; and return flows are discussed in this report.

On the basis of analysis of flow data in the Murray, a design capacity of 5000 to 6000 ML/day is recommended for the Torrumbarry Cutting. Extensive soils investigations were done in the KPF to prepare a soils map and to establish surface infiltration rates and soil depth across different soil types. Infiltration rate varies in the range 5 to 20 mm/day across the bulk of the areas likely to be inundated under enhanced flooding conditions. Calibration datasets for the KPF floodplain inundation patterns under historical conditions were obtained from remote sensing analysis of 12 images from the Landsat satellite for three historical flood events under 1991, 1993 and 2000 conditions. For a range of historical flow conditions in the Murray (3500 to 57 000 ML/day), inundation areas in the range 0.7% to 69% were estimated from the remote sensing analysis. Additionally, an inundation area of about 73% was estimated from mapping of the KPF floodplain; this corresponded to 55 000 ML/day flow in the Murray in August 1946.

The KPF floodplain modelling was performed in three stages, moving progressively from simple to more complex forms. Knowledge of the KPF flood inundation processes was improved in each stage to better formulate more complex model forms. It was considered mandatory to commence simulations with simple model forms using MIKE 11 (Stage 1: quasi-2D) and then conduct targeted simulations using MIKE 21 (Stage 2: 2D) and MIKE FLOOD (Stage 3: combined 1D flow in the runners and 2D flow on the floodplain). On the basis of the results from the MIKE 11, MIKE 21 and MIKE FLOOD models, we concluded that up to a flow of about 28 000 ML/day all three hydraulic models provided similar estimates of the inundation area in the range 0% to 10%. As flow increased further, the results from the models tended to differ. The accuracy of inundation areas predicted by each model under a range of hydrological conditions in the Murray is discussed in this report. We show that an ecological target of 30% inundation of the KPF can be achieved from diversion flow of 6000 ML/day from the Torrumbarry Cutting. Inundation areas in the KPF simulated under steady state conditions for flow diversions of 2000, 3000, 5000 and 6000 ML/day from the Torrumbarry Cutting for 45 days were 12%, 17%, 28% and 32% respectively. Return flows from short- and long-duration enhanced flooding of the KPF are likely to vary in the range 70% to 84%.

A hysteretic inundation response model is proposed for the KPF. The proposed inundation response model consists of primary wetting and drying curves that define the lower and upper bounds of the wetland inundation. All possible wetland inundation processes that depend on the hydrological conditions in the Murray can be defined by the secondary wetting and drying curves. Results from complex hydraulic modelling of the KPF are synthesised into simple and practical tools for use by environmental water managers and to help implement basin-scale hydrological models to incorporate the effects of environmental flow diversions within The Living Murray Initiative.

1 Introduction

The Living Murray (TLM) initiative was established in 2002 by the Murray Darling Basin Ministerial Council in response to concerns about the environmental and economic health of the River Murray system (MDBC 2006). An inter-government agreement was signed in 2003 to commit $500 million to the first step of TLM, which aims to recover an average of up to 500 GL/year new water over 5 years and thus improve environmental flows and achieve ecological objectives at six Icon sites along the River Murray. The six Icon sites that will benefit under the TLM initiative are: Barmah–Millewa Forest; Gunbower–Koondrook–Perricoota Forests; Hattah Lakes; Chowilla Floodplain and Lindsay–Wallpolla Islands; the Lower Lakes, Coorong and Murray Mouth; and the River Murray Channel. This report deals with hydraulic modelling of the Koondrook–Perricoota Forest (KPF) to support development of the environmental watering plans and engineering design of the structural works at this Icon site.

Koondrook–Perricoota Forest is in the NSW part of the Ramsar-listed Gunbower–Perricoota Forest (Figure 1). It is the second-largest red gum forest in Australia and covers about 33 750 ha along the Murray River. It is located south-west of Deniliquin between the towns of Echuca in the east and Barham in the west. Before river regulation was introduced in the early 1900s, the KPF experienced regular flooding for 3 to 5 months once every 4 years. Nowadays, the flood frequency duration is approximately once every 12 years; this change has meant a decline in both the productivity of the wetland and the health of the ecosystem. The forest's wetlands and floodplains provide habitat for many species of plants, fish, reptiles, birds and marsupials that are endangered. The forest is also valued for its cultural heritage and its economic and recreational uses.

1.1 PROJECT BACKGROUND AND OBJECTIVES

The Living Murray Environmental Works and Measures Program (EWMP) was formulated by the Murray Darling Basin Commission (MDBC) to develop and implement a program for the structural works and operational measures that are required to deliver and manage environmental water to meet the ecological objectives at the Icon sites. Within the TLM and EWMP initiatives, it is proposed to construct a channel in the KPF to allow water from Torrumbarry Weir to take its natural course through the forest, eventually returning to the Murray and its tributary Wakool to efficiently utilise the available Murray River water. Although the natural volume and pattern of water flow to the forest can't be restored, the project's ultimate aim is to provide water releases that will inundate at least 30% of river red gum forest and keep the KPF in an ecologically healthy condition. Benefits include breeding opportunities for thousands of colonial waterbirds in at least 3 years out of 10, and there will be healthy populations of resident native fish in the wetlands.

A preliminary study was carried out by Murray Irrigation Limited (part of the study was subcontracted to URS Australia) to investigate the performance of a range of channel and flow options and to estimate the flood inundation areas associated with the options (MIL 2004). Alignment of the channel, called the Torrumbarry Cutting, is shown in Figure 3. Murray Irrigation Limited developed some preliminary options for the proposed layout of the channel; they focused on minimising the cut and fill volumes and minimising the overall environmental impact associated with constructing the channel through the forest.

Figure 1. Location map of the Koondrook and Perricoota Forests adjoining the Murray

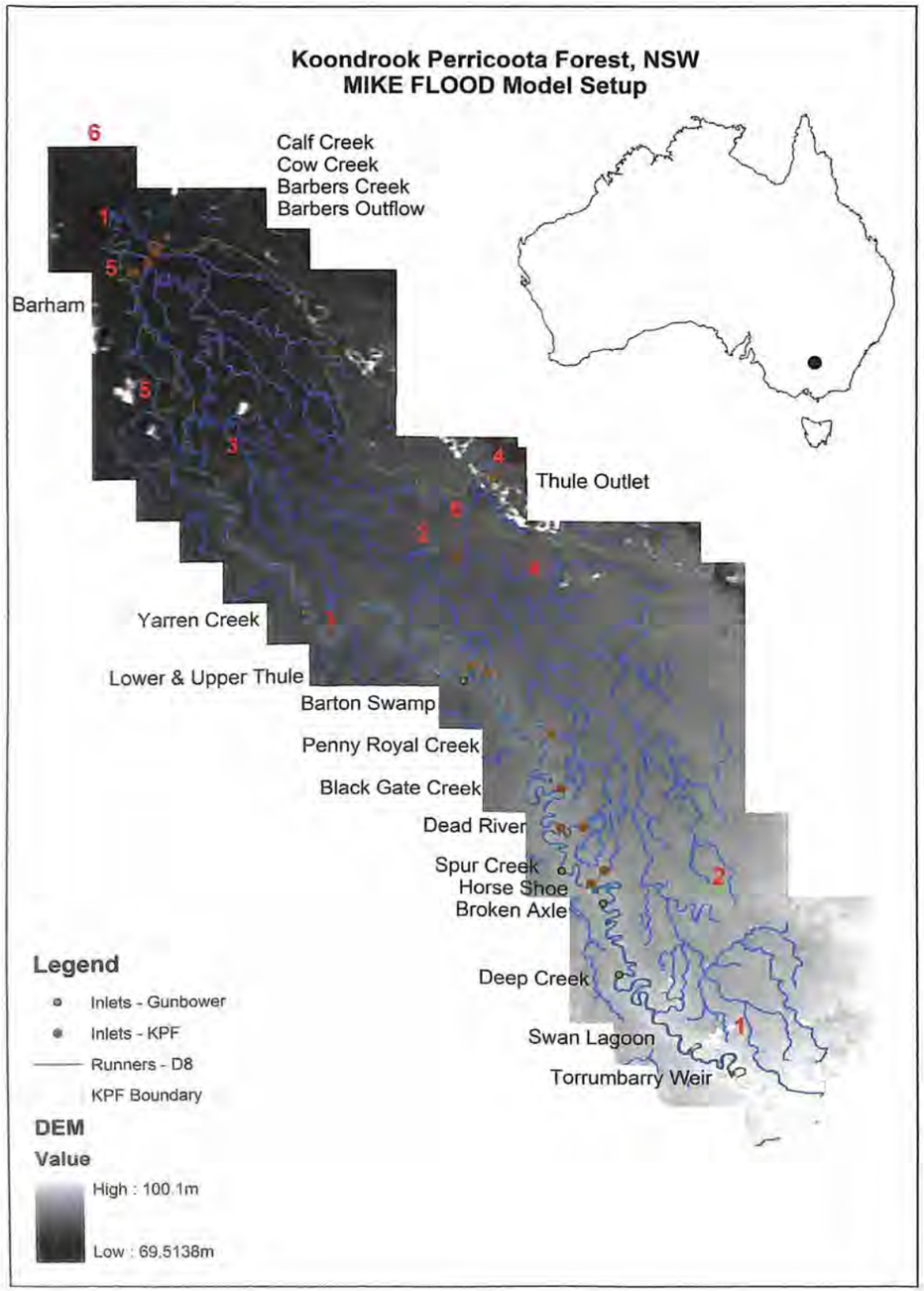

URS Australia used the Hydrologic Engineering Center River Analysis System (HEC-RAS) to undertake one-dimensional hydraulic modelling of the various options to assess the capacity of the channel and the extent of flooding into the surrounding areas. Each channel alignment option was modelled under flow conditions of 4000 ML/day and 6000 ML/day to determine the extents of flooding achieved through the forest and any potential inundation of the Murray River and Swan Lagoon, which is located approximately 3 km west of the Bullock Head Creek discharge point.

Three assumptions were made: free flow occurs from the channel banks; the levee bank along the eastern boundary was assumed to be continuing along the forest boundary; and no flow condition occurs in Bullock Head Creek. Assumptions of Manning's coefficient, a measure of riverbed friction, were made, and no sensitivity analyses of the impact of riverbed friction on water surface profiles were investigated.

The results of the hydraulic modelling by URS Australia indicated that the construction of a channel through the Koondrook–Perricoota forest and the use of Torrumbarry Weir Pool to achieve the desired flooding regime within the forest are feasible (for details see the URS Australia report 'Torrumbarry Cutting – Hydraulic Modelling, October 2004').

On the basis of preliminary hydraulic modelling, URS Australia put forward a number of recommendations. The most critical recommendations were:

- Further hydraulic investigations need to be undertaken to determine the most feasible option for the channel alignment and cross-section to minimise the overall costs associated with the project.
- Further 2D modelling (in plan) should be undertaken using a model capable of handling complex topography. Given the complexity of the locations where the Swan Lagoon depressions and Bullock Head Creek intersect, undertaking further modelling with a 1D HEC-RAS model would not be suitable. This is because the model cannot accurately determine how the flows are likely to split where Bullock Head Creek joins the existing drainage depressions at a number of locations downstream. Further 2D modelling will provide a more accurate indication of the level of flood inundation expected in the forest and Swan Lagoon, the flow split, and the volume of water required to effectively flood the forest for the desired period of time.

In July 2005, MDBC commissioned this project for the KPF under the Environmental Works and Measures Program to develop a 2D hydraulic model using MIKE FLOOD (DHI 2007) with the following specific objectives to determine:

- The design capacity of the Torrumbarry Cutting on the basis of water availability in the Murray
- overbank flow from the Murray into the KPF and Gunbower Forest under historical conditions
- the areal extent of inundation and the depth and velocity distribution in the KPF under historical conditions
- the areal extent of inundation and the depth and velocity distribution in the KPF under likely future conditions for a range of diversion flows from Murray into the Torrumbarry Cutting
- the likely inundation of the KPF against ecological targets: 30% inundation of the forest and maximising the inundation of high-quality red gum species

- partitioning of the water balance components during flooding of the KPF under historical and future conditions
- likely return flow from outlets to the Murray and Wakool following enhanced flooding of the KPF
- transformation of the hydraulic problem into a hydrological problem by linking of the results from hydraulic modelling of the KPF with the MDBC hydrological model (MDBC 2002, 2007).

NSW Department of Environment and Climate Change (DECC, which now undertakes some of the tasks performed by the former Department of Natural Resources) has undertaken the hydraulic modelling work in collaboration with NSW Department of Water and Energy (DWE; formerly DNR), Forests NSW, the Department of Commerce (DOC) and MDBC. An operational MIKE FLOOD hydraulic model has been developed for the complete KPF by DECC. In addition to the hydraulic modelling work in the KPF, two major investigations completed in this project are:

- salinity impacts of enhanced flooding in the KPF (Evans and Barnett 2007)
- soils investigations to support KPF hydraulic modelling (Jenkins et al. 2006).

In a separate but closely related project, Manly Hydraulic Laboratory (MHL) of the Department of Commerce has developed a 1D hydraulic model, MIKE 11, for different flow conditions in the Torrumbarry Cutting (DOC 2006). DECC's 2D floodplain hydraulic model of the KPF and MHL's 1D hydraulic model of the Torrumbarry Cutting interact explicitly, and the inflow boundary conditions of the DECC model are derived from the MHL model.

1.2 WETLAND HYDROLOGY AND FLOOD INUNDATION PROCESSES

The role of wetlands to provide for stable water supplies, improved water quality and a range of ecological benefits has been demonstrated in a number of recent studies (Richardson et al. 1997; Borin et al. 2001; Moore et al. 2002; Mitchell et al. 2002; Kazezyilmaz-Alhan et al. 2007). Consequently, there has been an increase in the research effort aimed at understanding wetland hydrology, water quality and environmental flows.

Wetland hydrology and flood inundation processes are generally investigated under the riparian zone hydrological processes wherein interactions of the floodplain with the river are examined to study issues such as proportioning of pre-event and event stormwater runoff and reversal of flow in the floodplains. Riparian zones provide distinct connectivity between the river and the floodplains that play a significant role in spatial and temporal connectivity of water fluxes in and through the riparian zone (Bishop et al. 1990; McDonnell et al. 1991; Cirmo and McDonnell 1997).

Developments in wetland hydrology models are very recent. In contrast, high-resolution distributed hydrology models from hillslope to catchment scales with varying levels of complexity have been developed and applied for several decades (Abbott et al. 1986; Wigmosta et al. 1994; Bates et al. 2000; Watson et al. 2001; Tuteja et al. 2007). Philosophical problems in contemporary physically based hydrological modelling are continually debated over the following key issues (Cloke et al. 2006): acquisition of necessary input data (Sieben and McDonnell 2002), effective parameterisation (Beven 2000; Beven and Freer 2001), model evaluation and calibration (Anderson and Bates 2001), scale dependency (Blöschl and Sivapalan 1995) and uncertainty estimation (Beven and Freer 2001).

Although there has been much fieldwork in the science of wetland and riparian zone isotope hydrology (Claxton et al. 2003; Summerell et al. 2006) and remote sensing analysis of wetland inundation and environmental flows (Smith 1997; Bates et al. 2006; Shaikh et al. 1998, 2001), there has been little progress in the development and implementation of sound hydrological models for wetlands and riparian zones. There has been no generalised modelling methodology for riparian zones with a high enough resolution to capture the detailed processes that are fundamental to understanding wetland and floodplain hydrology (e.g. rapid soil moisture dynamics, spatial and temporal patterns of flood inundation and velocity fields, pre-event and event water sources and mixing of water parcels). The development of state of the art flow and transport hydrological models for wetlands and riparian zone hydrology are very recent. Cloke et al. (2006) proposed coupling of the random walk particle method (RWMP) with the subsurface flow numerical model ESTEL2D, a subset of the TELEMAC modelling system of Hervouet (2000). Kazezyilmaz-Alhan et al. (2007) have proposed the wetland model WETSAND, which consists of a diffusion wave approximation for the overland flow and the advection-dispersion-reaction equations for water quality.

Models for simulating overland flow and flood inundation solve some form of the Navier-Stokes equations, such as the Saint Venant equation for shallow water depth, in association with assumptions. These assumptions relate to small water surface slope, sub-critical flow conditions, and larger wavelengths of flow rather than to water depth, boundary friction and turbulence.

Such simulations are invariably very complex and require careful consideration of the hydraulic processes operating over a range of time and length scales (Bates and Anderson 1993, 1996). Computational demand for complete solution of the Saint Venant equations may be substantial, and the solution may contain large accumulated error (Singh, 1996). For most practical flow routing problems, analytical solutions of the Saint Venant equations are not tractable. Therefore, simplified flow routing approximations of the hydraulic models based on Saint Venant equations are also popularly used. These model approximations include: kinematic wave (Dooge and Harley 1967; Woolhiser and Liggett 1967; Ponce et al. 1978), diffusion wave (Dooge and Napiórkowski 1987; Singh 1996) and gravity wave (Yen 1979; Singh, 1996). Linearised routing forms of the Saint Venant equations are also popularly used (Dooge 1980; Napiórkowski 1992).

Developments in numerical simulation using two- and three-dimensional modelling approaches to free surface flow problems started in the early 1990s (Bates et al. 1997). The main aim is to develop predictive models by comparing their performance with field data and with the results of simulations by means of the Saint Venant equations. Hydraulic models based on Saint Venant equations divide the river into a number of reaches. The hydraulic equations (mass and momentum) are applied to each reach, and the system of equations corresponding to all reaches is solved simultaneously with suitable initial and boundary conditions. Codes have been developed using varying levels of numerical complexity, including finite difference (Zeilke and Urban 1981; Bates and De Roo 2000; DHI 2007), finite element (Gee et al. 1990; Bates et al. 1992, 1996) and finite volume (Lane et al. 1994). These models tend to use stable numerical schemes (Brooks and Hughes 1982; Abbott et al. 1986), moving inundation extent boundaries (Lynch and Gray 1980; King and Roig 1988) and element-by-element storage of the mass and momentum stiffness matrix to optimise computer storage requirements (Carey and Jiang 1986; Hervouet 1992; Binley and Beven 1993). Such models include momentum transfer between in-channel flows and out-of-bank flows in the floodplain to account for significant two- and three-dimensional effects (Knight and Shiono 1996).

The current generation of flood inundation models, aided by advances in computer power, is capable of adequately representing the dynamic hydraulic processes of floodplain problems of practical interest (10–60 km reach scales). Two issues—the uncertainty and preparation of the validation datasets—are central to any flood inundation problem.

Most distributed models have parameters that are difficult to measure from field observations even though they are theoretically measurable (Grayson et al. 1992; Beven 2001). Flood inundation models contain enough sources of error to affect the results in the idealisation of a floodplain problem (e.g. parameters, floodplain geometry, inflow hydrographs and lateral fluxes, observed inundation patterns and numerical approximations inherent in the flow equations). In recent times efforts have been made to address the uncertainty issues in flood inundation modelling (e.g. Romanowicz and Beven 2003; Horritt 2006). These developments make use of the GLUE methodology of Beven and Binley (1992), which is used extensively in distributed hydrological modelling.

In-situ measurements of flood extent and depths, although very useful, are generally difficult to obtain for large floodplain problems that are of practical interest for environmental management. Therefore, considerable attention has been given to remote sensing analysis of the extent of flood inundation over large areas (Bates et al. 1997; Smith 1997; Shaikh et al. 2001; Bates et al. 2006). Satellite and airborne platforms provide useful flood inundation maps that can act as validation datasets for hydraulic flood inundation models. Bates et al. (2006) used airborne synthetic aperture radar to map flood inundation at 1.2 m resolution along a 16km reach of the River Severn in west-central London. Bates et al. (1997) and Smith (1997) present a good review of the active and passive remote sensing studies of flood inundation. Shaikh et al. (2001) classified wetlands of the Lower Darling River in south-eastern Australia on the basis of broad commence-to-flow discharges and the inundation effects at different discharge magnitudes. To date, remote sensing of floodplain inundation from satellite platforms has not offered a solution to the recording of dynamic flood inundation processes, because multiple images at fine resolution are generally not available (e.g. 35 days for ERS1 and ERS2 satellites, 14 days for Landsat, 7 to 10 days for RADARSAT). Nevertheless, these techniques indeed provide very useful calibration datasets for the flood inundation hydraulic models that can simulate a variety of historical and likely future conditions.

1.3 OVERVIEW OF THE ANALYSIS AND MODELLING APPROACH

A schematic diagram of the KPF hydraulic modelling study, including all the input and output data and the developed models, is shown in Figure 2. The digital elevation model (DEM), as well as the spatial extents of the soil types and surface infiltration rates obtained from soils investigations, a vegetation species map, evaporation rates and streamflow data, was used to develop the KPF hydraulic model (Section 2). Water availability analysis was first done to explore the opportunity for diverting a range of discharges into the Torrumbarry Cutting on the basis of the existing observed flow (1950–2000) and flows modelled from the MDBC Model BIGMOD/MSM (1891–2000) in the Murray at Torrumbarry Weir. The data were analysed to estimate the proportion of time in each year in which demand for a diversion flow varying from 2000 to 7000 ML/day in steps of 1000 ML/day could be satisfied. The suitability of the design carrying capacity of the Torrumbarry Cutting from a water availability perspective was explored from this analysis (Section 4).

Three flood events—one each from 1991, 1993 and 2000—were selected to develop the KPF hydraulic model for historical conditions. In total, 12 Landsat TM (Thematic Mapper)

images across the three historical events were used in the remote-sensing analysis to develop flood inundation maps (Section 5). Additionally, mapped flood extents of the 1946 flood event and the Murray streamflow data downstream of Torrumbarry Weir and Barham were used for validation of the KPF hydraulic model.

A three-stage modelling approach was developed for the KPF hydraulic model to progressively move from simple model forms of the hydraulic model to more complex model forms (Section 6). Knowledge of the KPF flood inundation processes was improved in each stage, and a better understanding of the parameters and hydraulic processes was developed to better formulate more complex and comprehensive hydraulic models. When flow in the Murray exceeds about 17 000 ML/day, water is naturally diverted from the Murray to the KPF in the north and Gunbower in the south. The overbank flow into the Murray floodplains varies depending on the magnitude of flow in the Murray. Therefore, a 1D MIKE 11 model was first developed and calibrated to quantify overbank flow from each inlet point of the floodplain along the left bank (Gunbower inlets) and right bank (KPF inlets) of the Murray. The calibrated MIKE 11 model for the Murray provided inflow into the KPF under historical conditions for the three flood events.

Figure 2. Schematic diagram of components of the Koondrook–Perricoota Forest Hydraulic Modelling Project

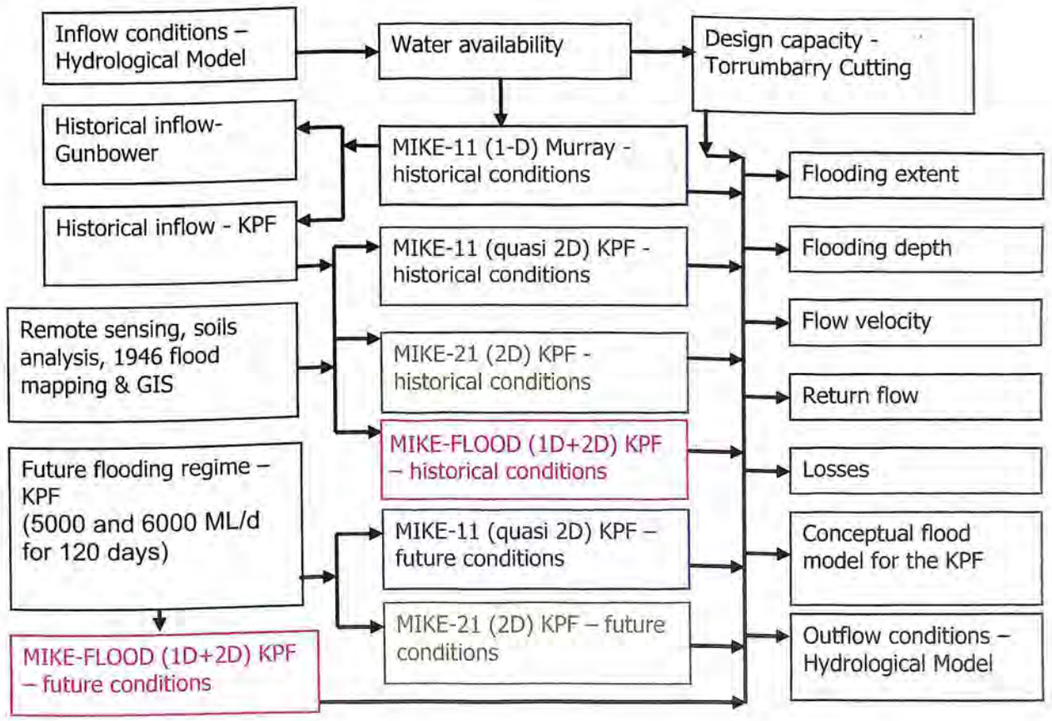

In stage 1, a quasi-2D MIKE 11 hydraulic model was developed for the KPF floodplain along the flow paths for historical and likely future conditions with water diverted from the Torrumbarry Cutting. Sensitivity of the model to floodplain resistance parameters and infiltration rates on outflow from the KPF, as well as flood inundation extents and flow velocity, were examined. In stage 2, a 2D MIKE 21 hydraulic model was developed for the KPF floodplain for the historical and likely future conditions. The model was implemented at 40 m grid cell resolution, and model simulations were performed at 10 s time steps for each historical and future flooding event. Flood inundation extent maps obtained from Stage 1 and Stage 2 modelling were compared with the maps from remote sensing analysis and 1946 mapped flood extents. The relative importance of channel flow in the runners of the KPF and floodplain for different inflow boundary conditions was evaluated. In Stage 3, a final comprehensive MIKE FLOOD model was developed for the KPF; it combines the strengths of 1D modelling using MIKE 11 for adequate representation of the channel conveyance and 2D modelling using MIKE 21 to properly represent two-dimensional effects in the out-of-bank flows. The model internally allows for dynamic exchange in both directions between the 1D channel and 2D floodplain flow components. Results from the MIKE FLOOD model were then used for the likely future conditions to assess whether the given level of diversion from the Torrumbarry Cutting could meet the ecological objectives of the Koondrook–Perricoota Icon site.

Finally, a hysteretic concept of the KPF floodplain inundation process is proposed. Simplified parametric forms of the hysteretic flood inundation model were developed (Section 7). Results from the KPF hydraulic model were synthesised to develop relationships between storage and outflow, inflow and return flow/losses and water depth and inundation area. These functional relationships in parametric forms enable the linking of information from the KPF hydraulic model into the hydrological model.

2 Study area

The River Red Gum forest of Koondrook–Perricoota is located on the River Murray floodplain in south-west NSW, between the towns of Echuca in the east and Barham in the west. The forest study area is about 33 750 ha. The eastern boundary of the KPF is located upstream of Torrumbarry Weir and provides suitable opportunity for the diversion of water through the Torrumbarry Cutting. There are eight inlet locations on the right bank of the Murray from which water can naturally enter the KPF (NSW) and five inlet locations on the left bank of the Murray from which water can enter the Gunbower Forest (Victoria) when flow in the Murray exceeds 17 000 ML/day (Figure 3). The KPF inlets are Swan Lagoon upstream, Swan Lagoon downstream, Horseshoe Lagoon, Dead River Lagoon, Black Gate, Penny Royal, Upper Thule and Lower Thule. The Gunbower inlets are Deep Creek, Broken Creek, Spur Creek, Barton Creek and Yarren Creek. Five outlets from which water can potentially leave the KPF are Barbers Outflow, Barbers Creek, Cow Creek, Calf Creek and Thule Creek. Thule Creek outflow is located on the northern boundary of the KPF, whereas the remaining outflow points are located towards the western boundary of the KPF. Downstream of the KPF Forest boundary all outflow streams/runners towards the western boundary join Barbers Creek.

2.1 DIGITAL ELEVATION MODEL

The DEM for the KPF was developed using remote sensing technologies for high-resolution terrain mapping (Figure 3). The DEM at 1 m grid cell resolution was developed by using a LiDAR (Light Detection And Ranging) survey (MDBC 2005). The survey was part of the Hume-Euston Project covering 1.7 million hectares along the Murray stretching between Lake Hume in the east and Robinvale in the west, and between Moulamein in NSW and Shepparton in Victoria. The report considered a three-tiered accuracy assessment that compared LiDAR data with more traditional photogrammetry techniques. Anticipated accuracy of the LiDAR survey is ±15 cm vertical and ±50 cm horizontal, with vertical accuracy being the primary measure. MDBC (2005) reports an overall vertical accuracy of the Hume-Euston LiDAR-generated DEM of 17 cm on open ground, measured at 1 standard deviation by the root mean squared error (RMSE) method. The error was affected by the terrain conditions, and the largest errors were associated with the presence of water bodies and saturated soils.

Additional ground survey work was done in the KPF as a component of this project at the following locations: Torrumbarry Cutting, KPF inlets and outlets, Bullock Head Creek and Swan Lagoon. Differences in elevation at various locations between 1 m LiDAR DEM and the survey data are shown in Figure 4. The scatter plots in Figure 4 show unsystematic differences between the DEM and survey data, with the bulk of the differences within ±0.5 m. At 1 standard deviation, the accuracy varied between the two datasets in the range 13 to 41 cm. All terrain data for the KPF hydraulic model was derived from the DEM, and the survey data were used to verify the geometry around the KPF inlets and outlets and around the Torrumbarry Cutting.

Five cross-sections across the width of the KPF and perpendicular to the general flow path were obtained from the DEM to assess the average slope of the KPF floodplain (Table 1, Figure 5). The average elevation along the width of the forest towards the eastern boundary, where the cutting discharges into Bullock Head Creek, is 84.70 m; towards the western boundary it is 76.56 m. The average slope of the KPF floodplain along the flow path varies from 1 in 4613 at the upstream end (eastern boundary) to 1 in 7310 at the downstream end (western boundary). The southern boundary of the KPF floodplain adjoining the Murray is generally higher than the northern boundary, and the general flow direction in the KPF floodplain is north-west.

Figure 3. Digital Elevation Model of the KPF at 1 m grid cell resolution, obtained from LiDAR survey

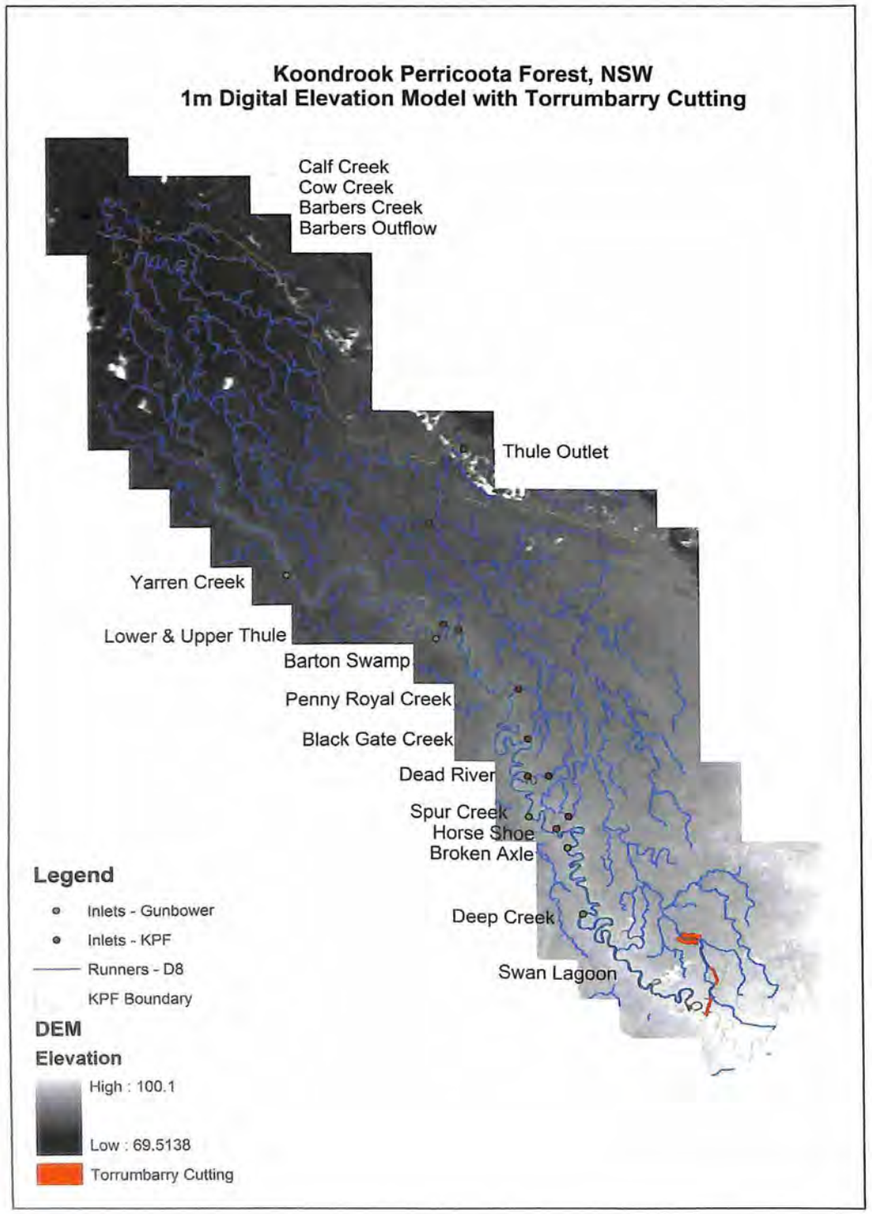

Figure 4. Comparison of elevations from the 1 m LiDAR DEM and the survey data

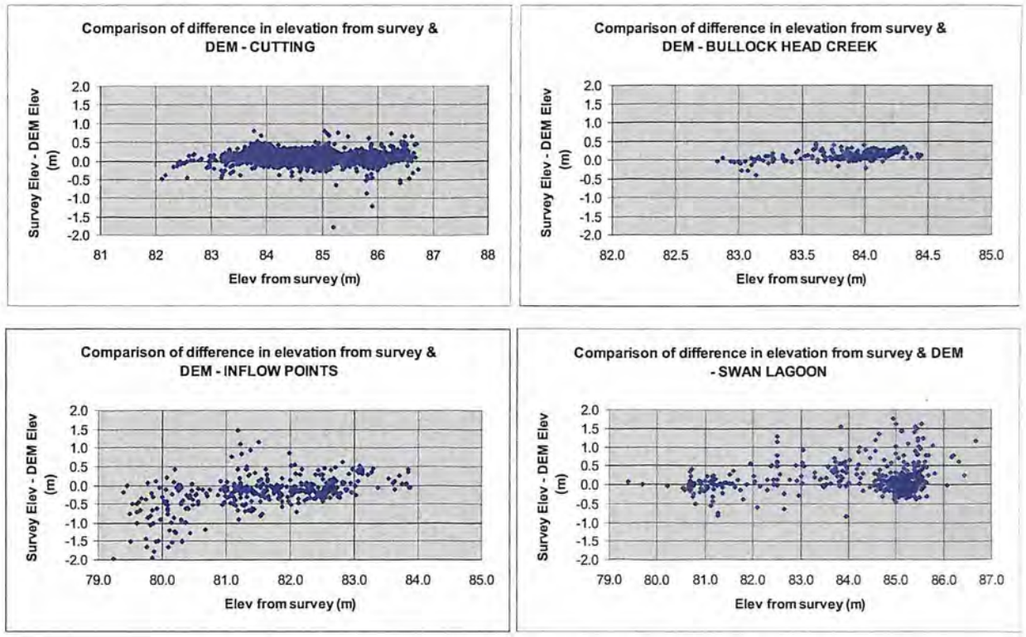

Figure 5. Cross-sections across the KPF floodplain, obtained from the 1 m LiDAR DEM (RD: reduced distance from the right bank of the Murray)

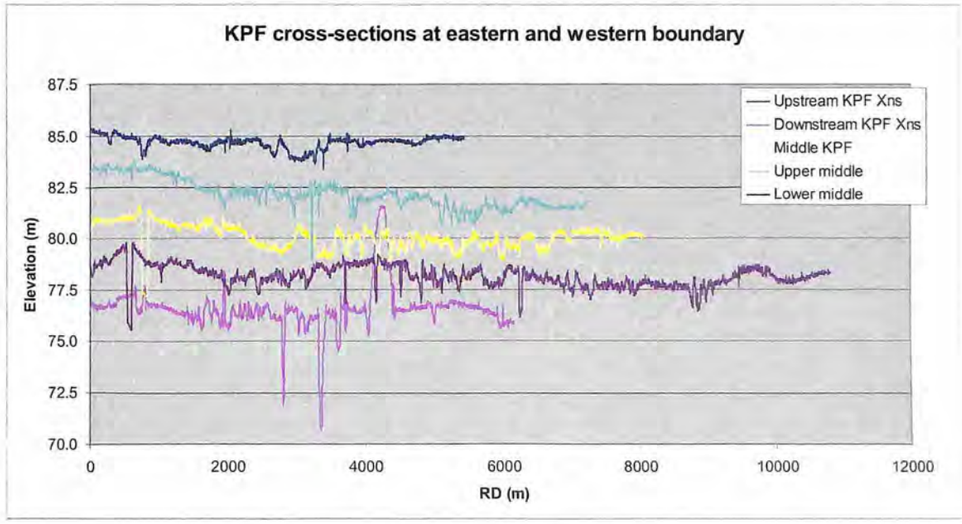

2.2 LAND USE DATA

The land use map of the KPF is sourced from Forests NSW (Figure 6).

The main vegetation species/land use categories in the KPF are: Box, Box/Red Gum, Red Gum SQ1 (high productivity), Red Gum SQ2 (low productivity), Red Gum SQ3 (low productivity), Open Plains or Swamp. In general, the vegetation species map indicates the degree of wetness in the KPF, with more frequent wetting of the areas under SQ1 (downstream end) and least wetting under Box vegetation (upstream end). The bulk of the area in the KPF is under low productivity Red Gum SQ2.

Figure 6. Vegetation map of the KPF (data sourced from Forests NSW)

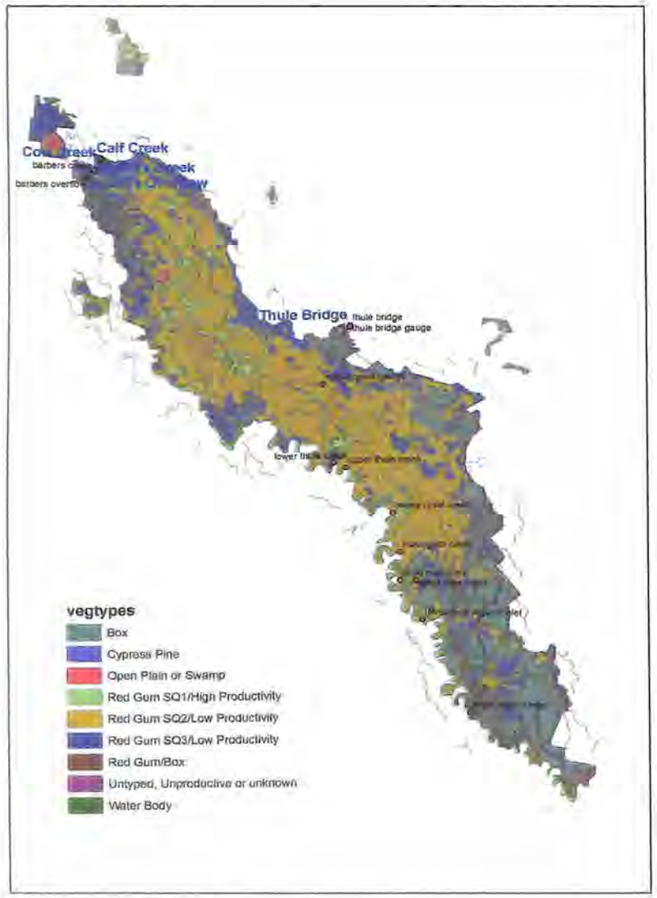

Table 1. Average elevations and slopes of the KPF floodplain, obtained from the 1 m LiDAR DEM (see Figure 5 for cross-section locations)

Cross-section	RD (m)	Width (m)	Av. elevation (m)	Slope
Upstream KPF	0	5448	84.70	
Upper middle	11 650	7235	82.17	1 in 4613
Middle	23 300	8088	80.08	1 in 5556
Lower middle	34 950	10 817	78.15	1 in 6048
Downstream KPF	46 600	6161	76.56	1 in 7310

RD: reduced distance from right bank of the Murray

2.3 SOILS AND SURFACE INFILTRATION DATA

Extensive soils investigations, including a soil survey and surface infiltration experiments, were done in the KPF to support the hydraulic modelling work (see Jenkins et al. 2006 for details). Soils data was collected in three phases. Soil profile descriptions were first done at 26 strategically selected locations (Figure 7) across the forest to represent different soils and landscape elements that closely related to the vegetation patterns in the KPF (Phase 1). Deep drilling up to 10 m was done at 12 sites to check for ancestral streams and determine the salinity profiles (Phase 2). Surface infiltration experiments were then done at 10 of the 26 soil survey locations (Phase 3).

Soils data collected at the 26 sites were analysed in the laboratory for the following : cation exchange capacity (CEC) (Pleysier and Juo 1980); exchangeable cations (Pleysier and Juo 1980); dispersion percentage (Ritchie 1963); electrical conductivity of 1:5 soil water extract (EC1:5) (Rayment and Higginson 1992); Emerson aggregate test (EAT) (Charman and Murphy 2000), particle size (Craze et al. 2003) and pH (Rayment and Higginson 1992). A total of 93 soil samples were analysed in the laboratory. Results from soil survey and laboratory analysis were used in conjunction with vegetation maps, remote sensing and aerial photographic interpretation to prepare a spatial map of different soil types in the KPF (Figure 7).

Soils in the KPF consist mostly of alluvial sediments deposited during formation of the alluvial plain. They vary greatly in depth and extent, depending on the complex drainage patterns in a braided environment. Typically, the majority of the soils have a medium to heavy clay layer within the top 30 cm of the profile. KPF soils were classified into six major soil hydrological groupings that reflect the relative infiltration rates of the most representative impermeable near-surface horizon. The six soil hydrological groupings are Bonum (sand hills), Bullock Head (high floodplain with gilgai), Fence Trail (high floodplain with minimal gilgai), Rusty Gate (mid floodplain with grey clays), Iron Punt (low floodplain with grey clays) and Borrumbarry (depressions and swamps).

Hydraulic flood inundation modelling of the KPF requires spatially distributed estimates of the surface infiltration rates from prolonged flooding under a ponding situation with a positive hydraulic head. The presence of heavy cracking clays in the KPF renders the conventional methods of measuring surface infiltration and hydraulic conductivity unsuitable (e.g. constant head well permeameter, Talsma and Hallam 1980; cylinder infiltrometers, Bouwer 1986; or disc infiltrometer, Peroux and White 1988).

Figure 7. Soils map of the KPF

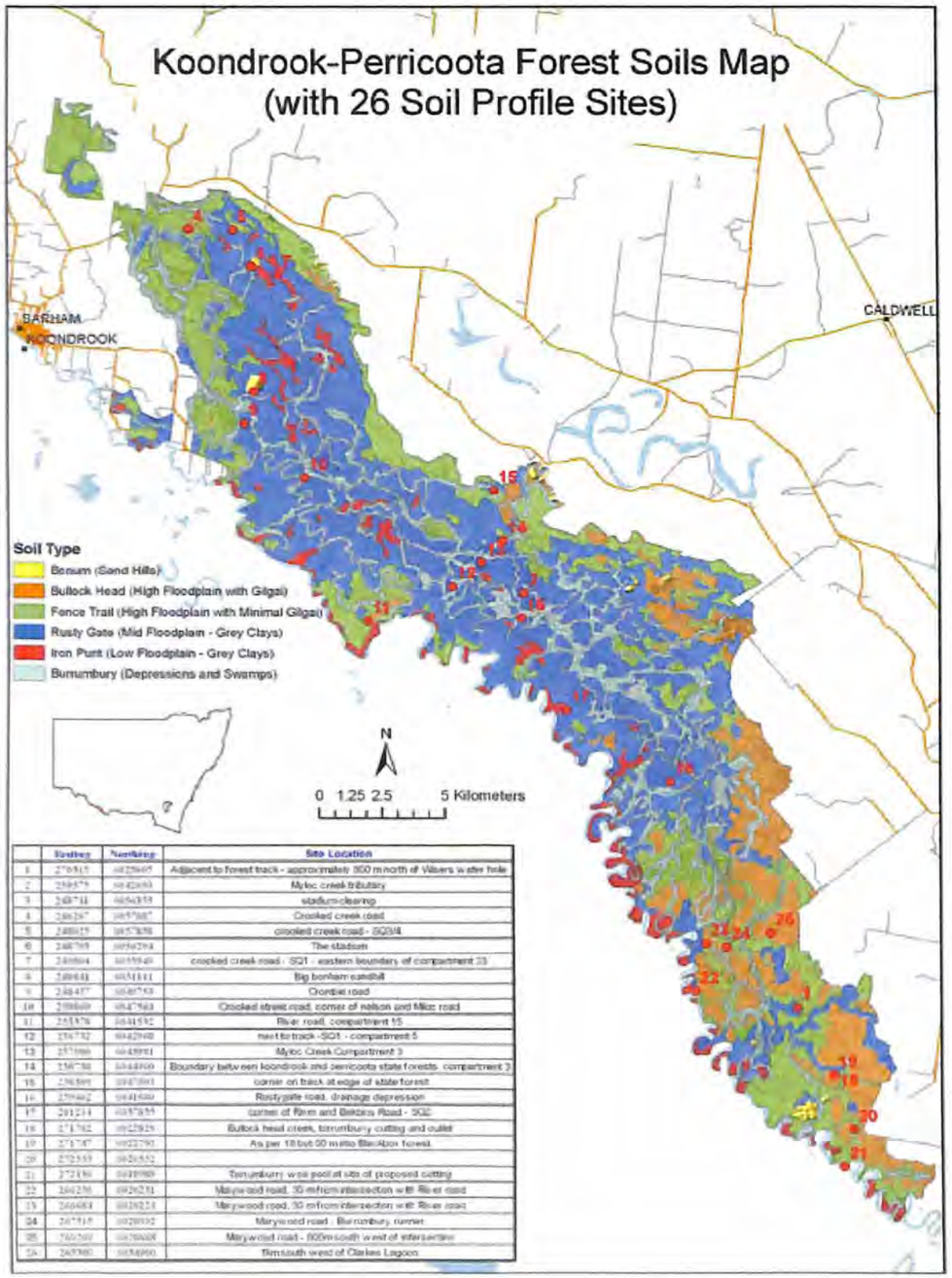

	Eastings	Northings	Site Location
1	276915	6025905	Adjacent to forest track - approximately 300 m north of Waters water hole
2	276879	6042693	Mylec creek tributary
3	268718	6050359	stadium clearing
4	280267	6057988	Crooked creek road
5	280815	6057838	crooked creek road - SQ3/4
6	280769	6056294	The stadium
7	280804	6055549	crooked creek road - SQ1 - eastern boundary of compartment 33
8	280641	6051111	Big bonham sandhill
9	280487	6050753	Crombie road
10	279869	6047563	Crooked street road, corner of nelson and Mlec road
11	278876	6041592	River road, compartment 15
12	278782	6042948	next to track - SQ1 - compartment 5
13	277986	6043951	Mylec Creek Compartment 3
14	278736	6044850	Boundary between koondrook and perricoota state forests. compartment 3
15	279599	6047001	corner on track at edge of state forest
16	279462	6041680	Rustygate road, drainage depression
17	281214	6037634	corner of River and Bekkers Road - SQ2
18	271762	6022825	Bullock head creek, burrumbury cutting and outlet
19	271747	6022790	As per 18 but 50 m into Blackburn forest.
20	272559	6026552	
21	272180	6028969	Tarrumbury weir pool at site of proposed cutting
22	284236	6029231	Marywood road, 30 m from intersection with River road
23	284683	6028233	Marywood road, 30 m from intersection with River road
24	287519	6028932	Marywood road - Burrumbury tunnel
25	286269	6029668	Marywood road - 800m south west of intersection
26	283980	6034890	1km south west of Clarkes Lagoon

An experimental setup was specifically designed for this project. A metal tube measuring 225 mm in diameter (Jenkins et al. 2006) was hammered into the ground using a modified hydraulic corer (Jenkins et al. 2006). The severely dense nature of the soils (mostly heavy clays) constrained the depth of penetration to the range 80 to 390 mm at the 10 sites where surface infiltration experiments were conducted (see Ksat sites, Figure 6, for location). In an attempt to saturate the soil, water was poured onto each site from a water tanker on three separate days in the week prior to setting up the experimental sites.

Water was added to each metal tube to 1 m height above the ground, and for the following 2 weeks the level was topped up to 1 m once a day following measurements. A steady state was reached at most sites over the 2 weeks following setting up of the experiment, and the surface infiltration rate was estimated from the measurements. The 10 sites at which infiltration experiments were conducted were numbers 5, 8, 10, 12, 13, 16, 17, 18, 24 and 26 (Figure 7). Sites 10, 12, 18 and 26 are located on Grey to Brown Vertosols (soil classification system of Isbell 1996). No infiltration rates could be established for Sites 18 and 26, largely because of lateral flow from large cracks in the surface soils. Site 8 is located on an Aeolian or wind-blown soil (Arenic Rudosol) and Sites 5, 13, 16, 17 and 24 are located on Alluvial soils (Stratic Rudosol). Steady state surface infiltration rates were generally low for most profiles, with the exception of sand hills. Because of problems with lateral flow and cracking, some of the rates were slightly modified on the basis of field knowledge and pedo-transfer functions derived from results of the laboratory analysis. Details of the pedo-transfer functions and indices used are given by Jenkins et al. (2006). Steady state infiltration rates for each soil type are shown in Table 2 and Figure 8. Saturated hydraulic conductivity was estimated by the approach of Green and Ampt (1911). Steady state modified infiltration rates from Table 2, in conjunction with the soils map, were used in hydraulic modelling.

Table 2. Steady state infiltration rate and saturated hydraulic conductivity for different soil types on the KPF floodplain

Soil unit	Area (%)	Site no.	Measured infiltration[1]	Modified infiltration[2]	Hydraulic conductivity[3]
Bonum – sand hills	0.7	8	906.8	907.0	888.0
Bullock Head – high floodplain with gilgai	13.3	18	–	30.0	26.0
Fence Trail – high floodplain with minimal gilgai	23.9	–	–	20.0	17.0
Rusty Gate – mid floodplain with Grey Clays	39.0	5, 26	371.6,-	15.0	13.0
Iron Punt – low floodplain with Grey Clays	4.8	17	4.7	5.0	4.0
Burrumbury – depressions and swamps	18.3	10,12,13,16,24	43.4,2.5,23.2,13 7.7,19.2	22.0	19.0
Area weighted average				25.0[4]	22.2[4]

[1]Steady state infiltration rate was estimated from measured data (mm/day)

[2]Modified infiltration rate was based on laboratory tests and field knowledge to account for lateral flow and cracking (mm/day)

[3]Saturated hydraulic conductivity was estimated from measured data and the Green and Ampt Approach (1911) (mm/d)

[4]Area weighted average value was calculated for the entire KPF floodplain and included areas that may or may not be inundated.

Figure 8a. Measured cumulative infiltration (mm) and infiltration rates (mm/day) at Sites 5, 8 and 13 (see Figure 7 for location)

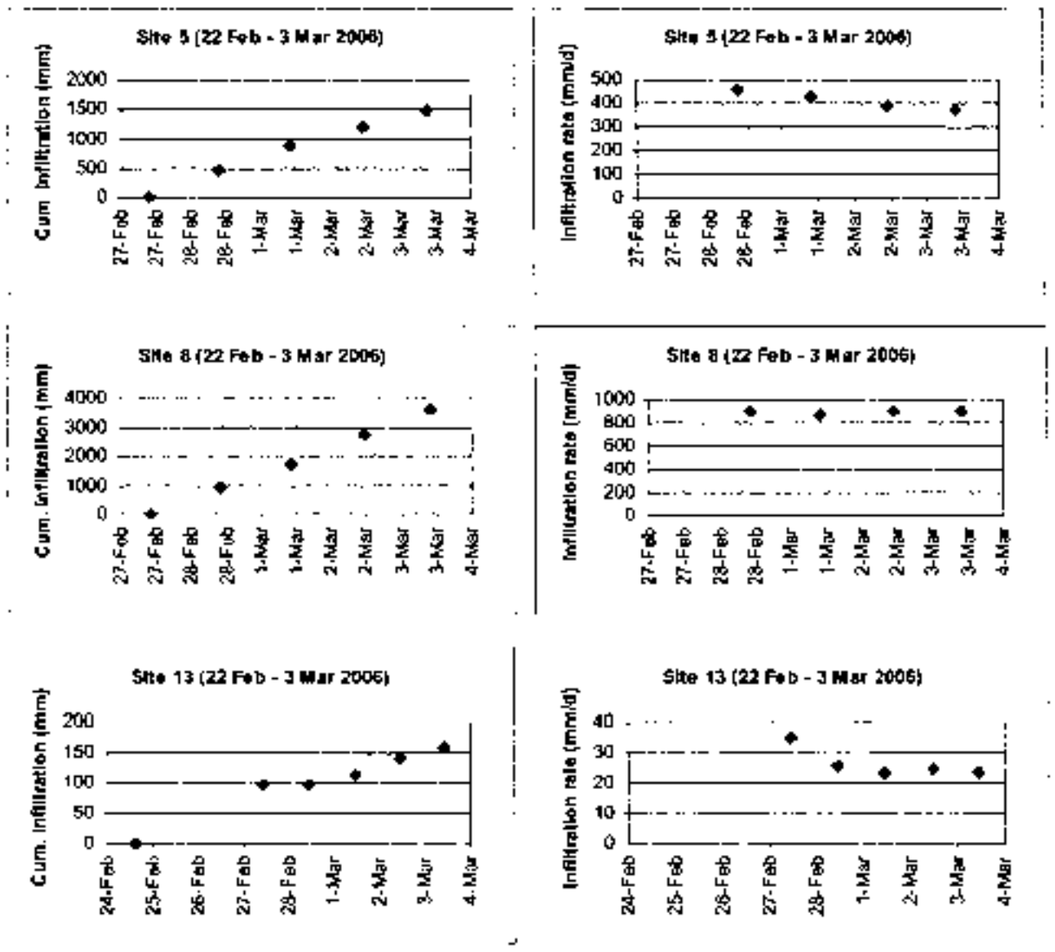

Figure 8b. Measured cumulative infiltration (mm) and infiltration rates (mm/day) at Sites 16, 17 and 24 (see Figure 7 for location)

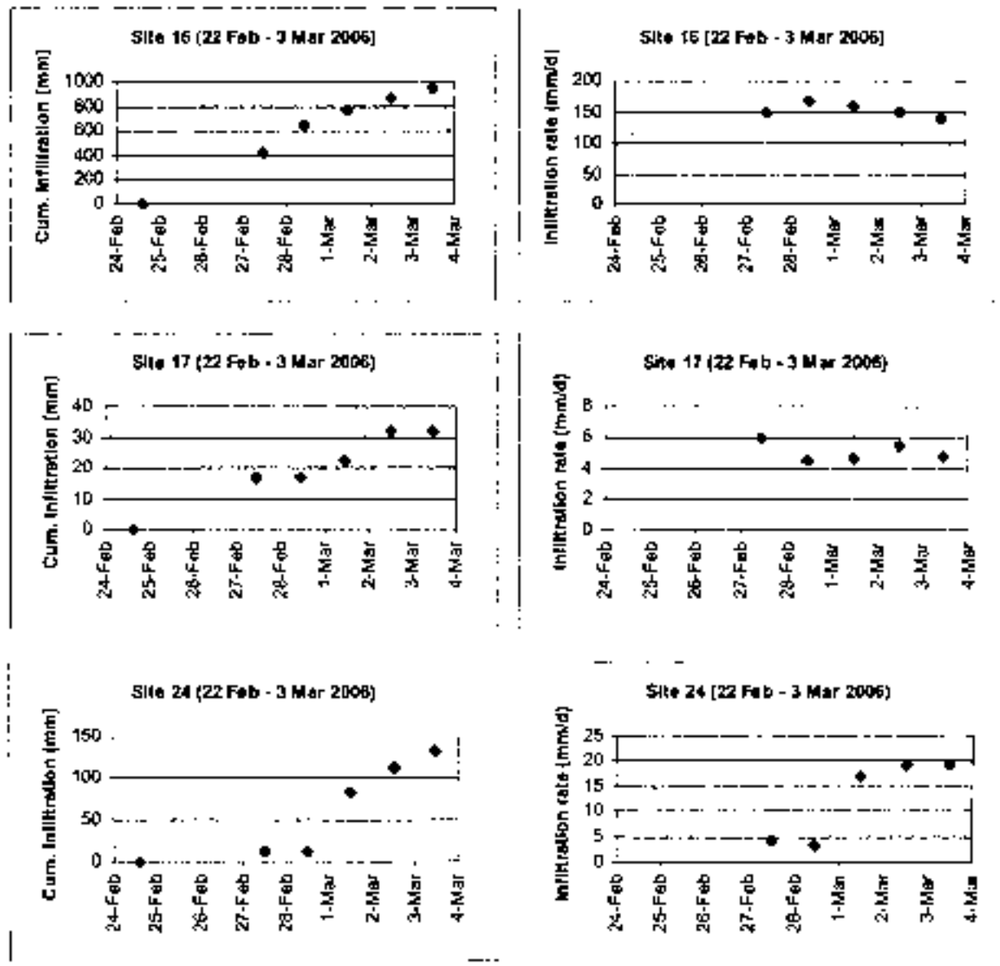

2.4 FLOOD INUNDATION AND REMOTE SENSING DATA

The source data maps for the KPF floodplain inundation and the prevailing vegetation patterns, prepared from an aerial survey on 7 August 1946 by the RAAF, are available in the Forests NSW archives. This flood event corresponds to 55 000 ML/day flow in the Murray and forms a useful dataset. Maps from the aerial survey were produced at a scale of 20 chains to the inch, equivalent to 1:15 840. These maps were scanned and ortho-rectified to match SPOT 5 satellite imagery with the datum set for GDA94 Zone 55.

Ortho-rectification is a procedure for digitally matching the scanned Forestry Commission maps. The maps are scanned to produce a digital file and are then digitally stretched to match corresponding features on the SPOT image. This process puts the maps into the

same frame of reference and makes then 'correct in space'. The features of the maps can now be directly traced over by using the data capture and edit tools in ArcGIS.

A flood inundation map was digitised by the following procedure. A line feature was first created by tracing over the features of the rectified maps. The lines mark the outline of the boundaries of the inundated and vegetation composition areas. This was checked for obvious anomalies by aerial photo interpretation (API). The line feature was then converted to a polygon feature and the feature annotated. Each area in the KPF floodplain was identified as water or dryland to prepare a mapped area of the inundation as it was on 7 August 1946.

API was then used to verify the accuracy of the original mapping. In the API process two slightly overlapping photos (60% overlap) are viewed through a stereoscope to produce a 3D image.

This mapping was supplemented with the following data to produce a final flood inundation map of the KPF for the 1946 event (Figure 30):

- **Land and Property Information (LPI) map, Cohuna sheet**. These photos are produced by the NSW Department of Lands as part of its state-wide coverage of aerial photography. These are standard production contact prints produced at 1:50 000 scale with 60% forward overlap and are suitable for API.
- **Campbells Island – Koondrook and Perricoota Air Photos**. These photos were supplied by Forests NSW and were produced in 1993. They are high-detail photos at 1:15 000 scale and are suitable for API.
- **LiDAR**. These are colour infra-red photos produced in conjunction with the production of a DEM for the Murray River channel. The photos are in digital format and were used to further verify areas prone to inundation within the KPF.
- **SPOT imagery**. SPOT was selected as the base imagery on which to overlay the maps. This satellite imagery was supplied as part of a whole-of-government purchase of state-wide imagery. It has a 2.5 m spatial resolution, which gives an effective scale of 1:10 000.

In addition to the inundation mapping for the 1946 flood event, 12 remote sensing images from the Landsat satellite were analysed by the methodology discussed in Section 5. The Landsat TM images used in the remote sensing analysis work fall within the period of three historical flood events in the Murray: for 1991, 1993 and 2000 (Table 3, and see Figure 23).

Table 3. Flood events in the Murray used for remote sensing analysis (Section 5) and hydraulic modelling (Section 6)

Event year	Event duration	Landsat TM image
1991	1 August to 30 November	1 August ([1]DN: 20; cloud-affected), 17 August (DN: 22), 2 September (DN: 28), 4 October (DN: 30,31,32), 21 November (DN: 40)
1993	1 July to 10 December	10 January (DN: 45), 22 August (DN: 24,25), 23 September (DN: 35), 26 November (DN: 40)
2000	1 August to 15 December	3 September (DN: 40; cloud-affected), 4 October (DN: 34,35,36), 7 December (DN:41)

[1] DN: Digital number threshold used for image processing to delineate the wet areas (see Section 5).

2.5 CLIMATE AND STREAMFLOW DATA

Three time series of flow are available downstream of Torrumbarry Weir from the calibrated water allocation and routing model for the Murray River (BIGMOD/MSM, MDBC 2002). These are: observed flow (1950 to 2000); natural flow conditions (1891 to 2000); and current conditions (1891 to 2000) (Figure 9a, b).

The **natural conditions flow** time series represents the likely flow downstream of Torrumbarry Weir if no storage were available in the Murray system and water were routed naturally from the drainage network under 1891–2000 climate conditions. The **current conditions flow** time series represents the likely flow downstream of Torrumbarry Weir if the current storage and water management procedures were applicable under 1891–2000 climate conditions. The mean annual flows for the period 1891–2000 for the natural and current conditions downstream of Torrumbarry Weir were 7333 GL/year and 3999 GL/year, respectively, i.e. 55% flow for the current conditions relative to the natural conditions.

Climate surfaces are available for the Australian continent from the SILO database using the widely accepted methodology of Jeffrey et al. (2001). Daily climate data from SILO at a 5 km grid included 17 locations within the KPF where data were available from 1956 onwards (Figure 10). Average daily pan evaporation and rainfall data for 1956 to 2000 at each location were estimated (Figure 11). The spatial variability in climate data was found to be negligible relative to temporal variability.

A smoothened daily pan evaporation and rainfall for the average year was obtained by using Fourier Transforms (Tuteja et al. 2002). First, four significant harmonics of the fitted Fourier Transform were used in smoothing the pan evaporation and climate data. Average daily values for pan evaporation were tightly packed around the mean for pan evaporation, whereas they varied substantially for rainfall, and this is reflected in the respective low and high values of the coefficient of variation, C_v (Figure 11). A pan factor value of 0.85 was used to convert pan evaporation into potential evapotranspiration and used in hydraulic modelling across the whole forest (pink line in the evaporation plot, Figure 11).

Figure 9. Flow data in the Murray downstream of Torrumbarry Weir under natural and current conditions

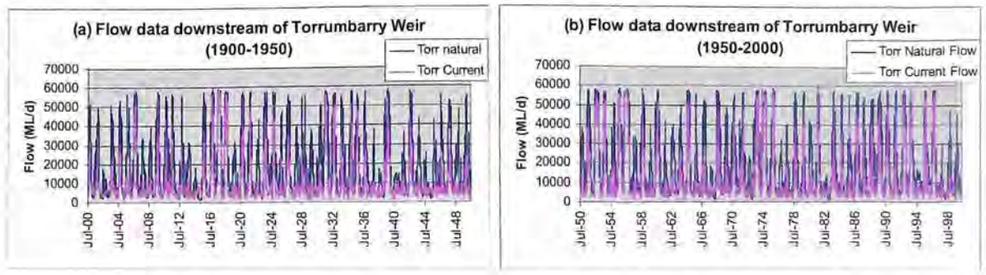

Figure 10. Climate data grid point locations in the KPF

Figure 11. Climate data for the KPF (legend numbers correspond to grid point locations shown in Figure 10)

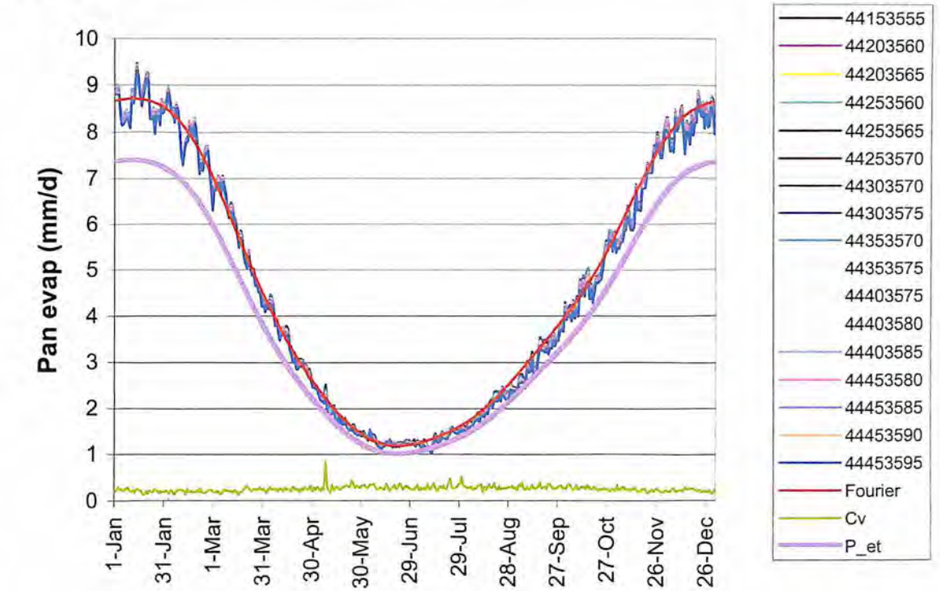

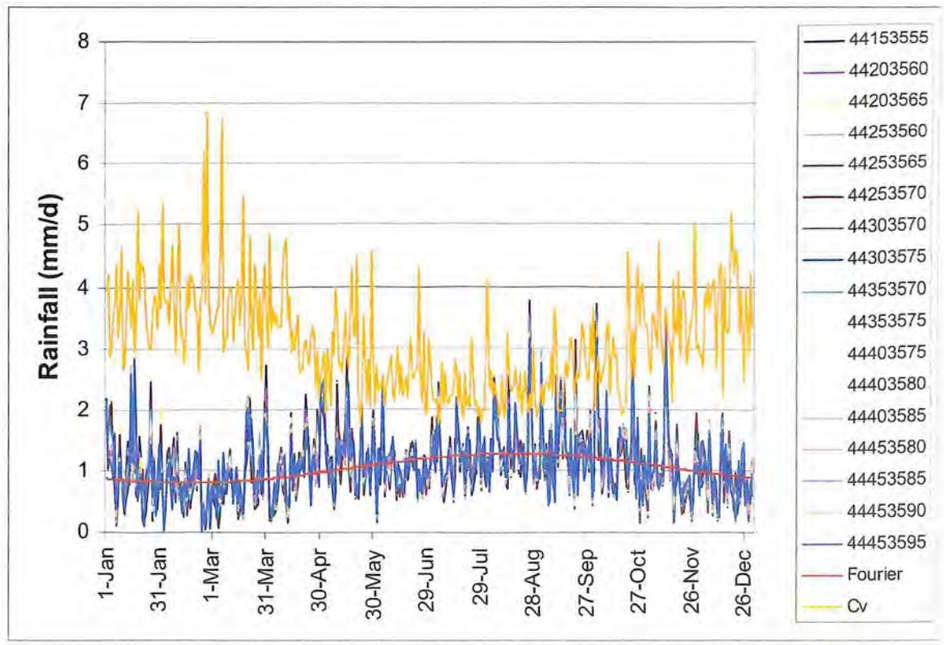

3 MIKE FLOOD hydraulic model components

The MIKE FLOOD hydraulic model consists of three sub-models: MIKE 11, MIKE 21, and a coupling model that links MIKE 11 and MIKE 21 (DHI 2007). A brief description of these models is given below.

3.1 MIKE 11 MODEL

MIKE 11 is a 1D model that can be used for modelling river flows, tidal effects, flood extent, duration and depth, flow exchange and flood mapping (DHI 2007). It includes options for incorporating simple and advanced structures for performing hydraulic simulations. The model is primarily developed for hydraulic modelling of flow in rivers, channels and runners. However, MIKE 11 modelling can also be performed across floodplains by using wide cross-sections for the preliminary assessment of floodplain behaviour. Flood mapping can be achieved in MIKE 11 by draping the DEM over the simulated water levels from 1D modelling at the desired time steps. The model projects a 2D water level on the basis of simulated water level across each cross-section (from MIKE 11) on to the DEM and estimates inundated grid cells that have projected water levels higher than the ground surface elevation. This type of modelling forces a 1D hydraulic modelling methodology onto a 2D process and is referred to as quasi-2D hydraulic modelling of the floodplain.

The model solves the following Saint Venant equations.

Mass balance: $$\frac{\partial Q}{\partial x}+\frac{\partial A}{\partial t}=q \qquad (1)$$

Momentum balance: $$\frac{\partial Q}{\partial t}+\frac{\partial\left(\alpha\frac{Q^2}{A}\right)}{\partial x}+gA\frac{\partial h}{\partial x}+\frac{gQ|Q|}{M^2AR^{4/3}}=0 \qquad (2)$$

where, x = distance along the direction of flow (m), t = time (s), $Q(x,t)$ = discharge across the cross-section (m^3s^{-1}), $A(x,t)$ = cross-sectional area (m^2), $h(x,t)$ = water level (m), $R(x,t)$ = hydraulic radius (m^2m^{-1}), q = lateral flow ($m^3s^{-1}m^{-1}$), $M = 1/n$ = Manning number, n = Manning roughness coefficient, α = velocity distribution coefficient (–).

Using the relationship between cross-section area, storage width and water level, both mass and momentum balance equations are transformed in terms of Q and h. The system of equations is solved for Q and h by using the six-point fully implicit numerical scheme of Abbott (1979). The mass balance equation is centred at water level between the current and next time step, whereas the momentum balance equation is centred at discharge between the time steps (Figure 12). The model is solved with suitable initial and boundary conditions. Invariably, the upstream boundary condition is a specified flux boundary condition (Neuman Type II), whereas the downstream boundary condition is a system-dependent boundary condition and is specified as a rating curve. The model estimates outflow on the basis of the dynamic simulated water level at the outflow boundary. Key model input data include the stream/river network, cross-section geometry, riverbed friction, and initial and boundary conditions. Key model output data include the water level at the cross-sectional locations and the discharge at mid-points between the successive cross-sections. A number of additional internal state variables can also be obtained (e.g. velocity, flow width, resistance, mass balance error).

Figure 12. Numerical approximation approach used in the MIKE 11 Model

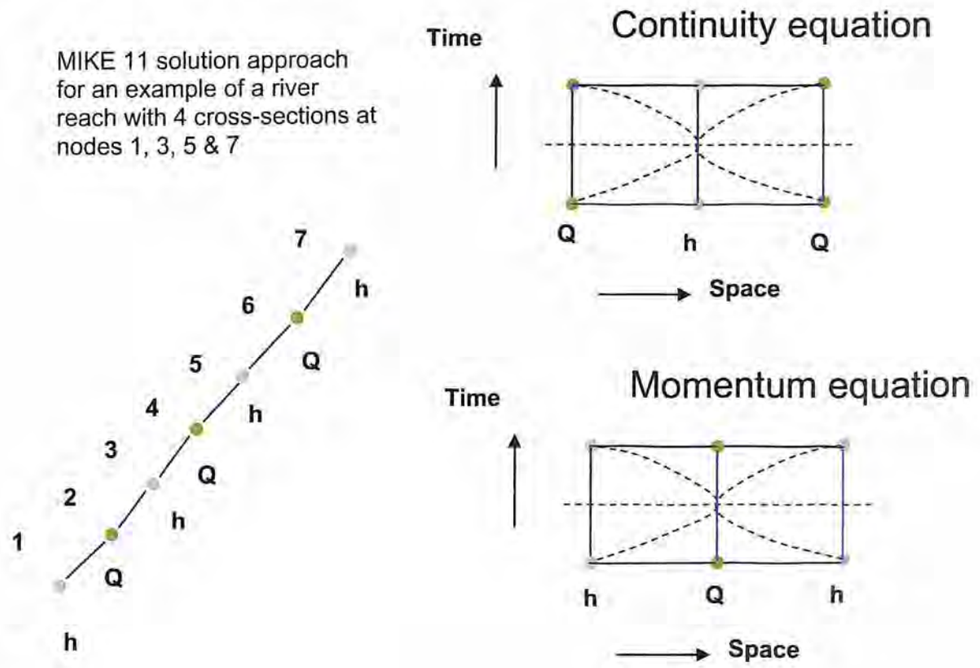

3.2 MIKE 21 MODEL

MIKE 21 is a 2D model that can be used for modelling river flows, tidal effects, flood extent, duration and depth, flow exchange and 2D flood mapping in GIS (DHI 2007). It includes options for incorporating simple structures for performing hydraulic simulations.

The model solves the following Saint Venant equations.

Mass balance: $$\frac{\partial p}{\partial x}+\frac{\partial q}{\partial y}+\frac{\partial \varsigma}{\partial t}=S \qquad (3)$$

Momentum balance in x-direction:

$$\frac{\partial p}{\partial t}+\frac{\partial}{\partial x}\left(\frac{p^2}{h}\right)+\frac{\partial}{\partial y}\left(\frac{pq}{h}\right)+gh\frac{\partial \varsigma}{\partial x}+\frac{gp\sqrt{p^2+q^2}}{C^2h^2}-\frac{1}{\rho_w}\left[\frac{\partial}{\partial x}(h\tau_{xx})+\frac{\partial}{\partial y}(h\tau_{xy})\right]$$

$$-\Omega q-fVV_x+\frac{h}{\rho_w}\frac{\partial p_a}{\partial x}=S_{fx} \qquad (4)$$

Momentum balance in y-direction:

$$\frac{\partial q}{\partial t}+\frac{\partial}{\partial y}\left(\frac{q^2}{h}\right)+\frac{\partial}{\partial x}\left(\frac{pq}{h}\right)+gh\frac{\partial \zeta}{\partial y}+\frac{gq\sqrt{p^2+q^2}}{C^2h^2}-\frac{1}{\rho_w}\left[\frac{\partial}{\partial y}\left(h\tau_{yy}\right)+\frac{\partial}{\partial x}\left(h\tau_{xy}\right)\right]$$

$$-\Omega p-fVV_y+\frac{h}{\rho_w}\frac{\partial p_a}{\partial y}=S_w \qquad (5)$$

where, $h(x,y,t)$ = water depth (m), $\zeta(x,y,t)$ = surface elevation (m), $p,q(x,y,t)$ = flux density in x- and y-directions ($m^3 s^{-1} m^{-1}$), $C(x,y)$ = Chezy's resistance ($m^{0.5} s^{-1}$), g = acceleration due to gravity (ms^{-2}), $f(V)$ = wind friction factor (–), $V, V_x, V_y(x,y,t)$ = wind speed and components in x- and y-directions (ms^{-1}), Ω = Coriolis parameter (s^{-1}), $p_a(x,y,t)$ = atmospheric pressure ($kgm^{-1}s^{-2}$), ρ_w = density of water (kgm^{-3}), S, S_u, S_v = source mass, source momentum components (m^2s^{-2}), $\tau_{xx}, \tau_{xy}, \tau_{yy}$ = components of effective shear stress (m^2s^{-2}).

Equations 3, 4 and 5 are expressed in terms of water depth and flux densities in the x- and y-directions and are solved numerically by using a fully implicit finite difference scheme. The MIKE 21 numerical procedure uses the Alternating Direction Implicit (ADI) technique to solve the mass and momentum stiffness matrix at each time step (Abbott et al. 1973, 1981). For each direction of the ADI scheme, the system of equations is resolved by using a double sweep numerical algorithm to achieve convergence. Both types of boundary condition (specified water level Dirichlet Type I and specified flux Neuman Type II) can be used in MIKE 21. The boundary conditions can vary in both time and space. Point sources and sinks can also be incorporated into the MIKE 21 Model. Model input data include bathymetry (obtained from the DEM), boundary conditions, wind speed and direction (constant and/or varying in time and space), atmospheric pressure maps, bed resistance (constant or spatially variable), flux- or velocity-based eddy viscosity and radiation stresses. Rainfall, evaporation and surface infiltration data varying in time and space can be incorporated into MIKE 21. Model output includes spatial and temporal variations of water depth and flux densities in the x- and y-directions.

3.3 MIKE FLOOD MODEL

MIKE FLOOD model combines the strengths of 1D modelling using MIKE 11 for adequate representation of the channel conveyance and floodplain modelling using MIKE 21 to properly represent 2D effects in the out-of-bank flows. The model allows for dynamic exchange internally in both directions between the 1D channel and 2D floodplain flow components. The model can be used for floodplain applications, storm surge studies, urban drainage, dam break, hydraulic design of structures and broad-scale estuarine applications. The three main types of link permissible in MIKE FLOOD are listed below.

3.3.1 Standard link

This type of link allows connection between the end of a MIKE 11 branch and a series of MIKE 21 grid cells. Discharge is extracted from the MIKE 11 boundary and is imposed in MIKE 21 as a source term, thus affecting the continuity and momentum equations in MIKE 21 (equations 3 to 5). MIKE 21 in turn provides the water level boundary to MIKE 11 at the next time step.

3.3.2 Lateral link

This type of link allows connection between the end of one MIKE 11 reach within one branch and a series of MIKE 21 grid cells (Figure 13). Flow through MIKE 11 and vice-versa is via a lateral boundary which is applied into MIKE 21 via a source term. Flow through the link is dependent on a structure equation and water levels in MIKE 11 and MIKE 21. Flow through the link is distributed into several MIKE 11 water level points and several MIKE 21 grids cells. Lateral link is explicit and does not guarantee momentum conservation.

Lateral links can be specified along the centre line, left levee line or the right levee line of the MIKE 11 cross-sections. A structure required to calculate flow exchange between the two models is typically a weir that represents overtopping of a river bank or a levee.

Figure 13. Lateral flow link over either left or right banks between MIKE 11 branches and MIKE 21 grid cells in MIKE FLOOD (from DHI 2007).

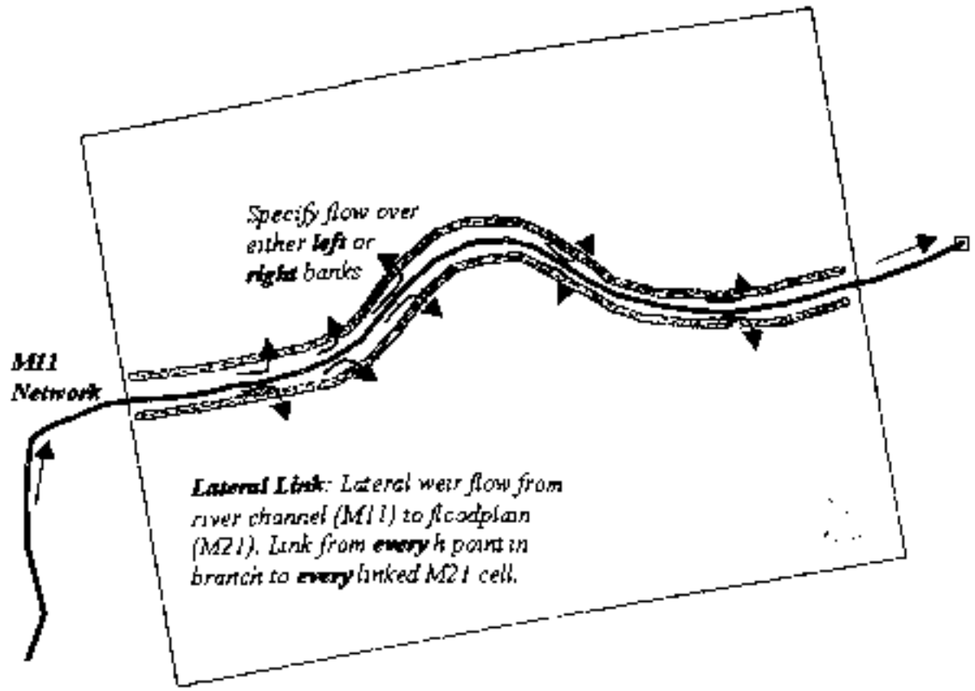

The geometry of the structure can be determined from MIKE 11 cross-sections or MIKE 21 cell bed levels, or from a combination representing the highest level from MIKE 11 and MIKE 21, or from the user specified geometry. Transfer between the two models can be implemented by using either a 'Simple Method' or a 'Cell to Cell Method'. In the first method, transfers between the two models occur through one structure between each reach, with average representative structure geometry. However, in the second method the structure geometry is subdivided into a series of internal structures. Each internal structure has a bed level and a width determined from the resolution of points defined along the structure.

3.3.3 Structure links

This type of link allows connection between the end of a MIKE 11 branch and a series of MIKE 21 grid cells. The structure link is similar to the standard link. However, unlike the with the standard link, two links are required for each structure link: one for the left or bottom grid cell and another for the top or right grid cell. The structure link takes the implicit terms describing momentum through a three-point MIKE 11 branch and uses them to replace or modify the implicit terms describing momentum across the face of a MIKE 21 cell. In this way, the flow properties from one MIKE 21 cell to another MIKE 21 cell are modified to represent the structure.

4 Water availability and Murray streamflow analysis

Water availability analysis was done to explore the opportunity for diverting a range of discharges into the Torrumbarry Cutting on the basis of existing observed flow (1950–2000) and modelled flows from the MDBC Model BIGMOD/MSM (1891–2000) in the Murray at Torrumbarry Weir (see Tuteja and Close 2006 for details). The flow duration curves for observed flow downstream of Torrumbarry Weir and Barham, along with the flow duration curves for the natural and current conditions time series downstream of Torrumbarry Weir, are shown in Figure 14. Difference between the flow duration curves for observed flow downstream of Torrumbarry Weir and Barham show the volume of water lost to diversion flow between the Gunbower and Koondrook–Perricoota Forests (major component), direct evaporation and infiltration. When the observed flow downstream of Torrumbarry Weir is 20 000, 30 000, 40 000, 50 000 or 65 000 ML/day, the proportion of combined flow naturally diverted to the Gunbower and Koondrook–Perricoota Forests is 0%, 14%, 30%, 41% and 46%, respectively. According to Forests NSW, flow in the Koondrook–Perricoota Forests commences at 17 000 ML/day flow downstream of Torrumbarry Weir (Lindsay Johnson, pers. comm.). This value is lower than the 20 000 ML/day flow commencement value for the forests evident in the flow duration curves.

Figure 14. Flow duration curves downstream of Torrumbarry Weir for the observed flow (1950–2000), under natural conditions (1891–2000), and under the current conditions (1891–2000), and flow duration curve for the observed flow at Barham.

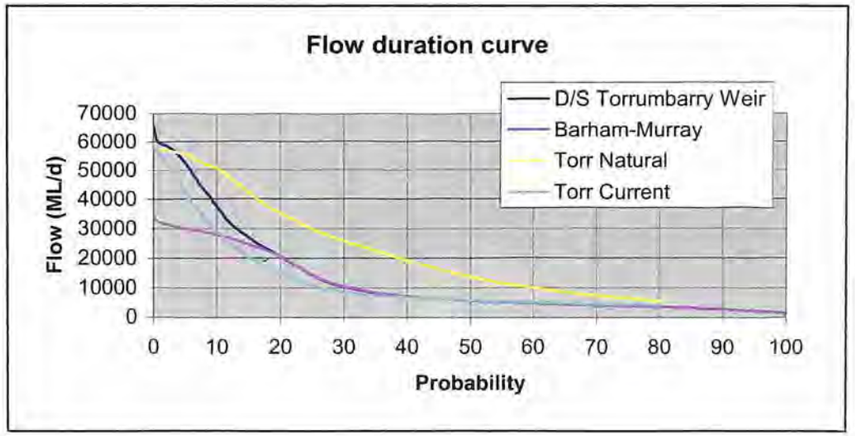

Water availability analysis for diversion into the Torrumbarry Cutting was conducted in the following manner by using the flow time series downstream of Torrumbarry Weir under **current conditions** (1891–2000).

A threshold discharge was assumed such that all diversions into the Torrumbarry Cutting were considered only when flow downstream of Torrumbarry Weir under **current conditions** exceeded the threshold discharge. It was assumed that the Environmental Watering Group

(EWG) and the TLM Committee will consider a range of dry and wet conditions in the basin, taking into account environmental and irrigation water requirements in an integrated manner.

Threshold discharges of 0, 5000, 10 000, 15 000, 17 000 and 20 000 ML/day were assumed. The carrying capacity of the Torrumbarry Cutting was assumed to vary between 2000 and 7000 ML/day in increments of 1000 ML/day.

For each threshold discharge (six values) and for each carrying capacity of the Torrumbarry Cutting (six values), the **number of days in a year** (May of year one to April of the following year) when water is available for diversion into the Torrumbarry Cutting was estimated.

These data were then used to estimate the exceedence probability, corresponding to the number of days in a year a given demand for diversion into the Torrumbarry Cutting can be satisfied.

The volume of water (GL/year) that can potentially be diverted into the Koondrook–Perricoota Forest each year (1891–2000), corresponding to a threshold discharge of 17 000 ML/day and a carrying capacity of the cutting varying between 2000 to 7000 ML/day was estimated. The number of years (or exceedence probability) a given annual demand of 600 GL/year can be satisfied was then estimated.

The number of days a given demand can be satisfied corresponding to an exceedence probability of 33% (1 in 3 years) and 25% (1 in 4 years) are shown in Tables 4 and 5, respectively. Duration curves for the annual runoff volumes (GL/year) that can potentially be diverted into the Koondrook–Perricoota Forest are given in Figure 15. Figure 16 shows the results of the analysis for a threshold discharge of 10 000 ML/day and a carrying capacity of the Torrumbarry Cutting in the range 2000 to 7000 ML/day.

Figure 15. Duration curves for the volume of water that can potentially be diverted into the Koondrook–Perricoota Forest with different carrying capacities of the Torrumbarry Cutting.

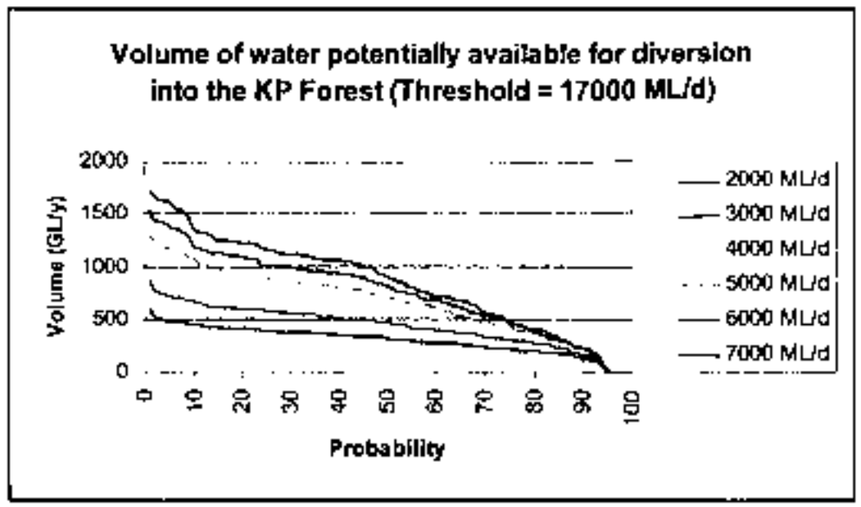

Table 4. Number of days in a year a given demand for diversion flow into the cutting can be satisfied, corresponding to a 33% exceedence probability (1 in 3 years) for various magnitudes of the threshold discharge[1].

	Threshold discharge in the Murray downstream of Torrumbarry Weir					
	0 ML/day	5000 ML/day	10000 ML/day	15000 ML/day	17000 ML/day	20000 ML/day
Flow (Cutting)	No. of days					
2000 ML/day	365	285	227	194	186	165
3000 ML/day	365	280	220	189	179	160
4000 ML/day	362	260	212	186	171	156
5000 ML/day	339	246	207	179	165	153
6000 ML/day	309	235	203	171	160	145
7000 ML/day	285	227	194	185	156	142

[1]Flow is diverted into the Torrumbarry Cutting only when flow in the Murray exceeds the threshold discharge.
Note: When flow in the Murray at Torrumbarry Weir exceeds 40 000 ML/day, about 6000 ML/day is naturally diverted to the KPF. The Cutting offers the option of diverting flows of up to 6000 ML/day when flow in the Murray is less than 40 000 ML/day

Table 5. Number of days in a year a given demand for diversion flow into the cutting can be satisfied, corresponding to a 25% exceedence probability (1 in 4 years) for various magnitudes of the threshold discharge.

	Threshold discharge in the Murray downstream of Torrumbarry Weir					
	0 ML/day	5000 ML/day	10000 ML/day	15000 ML/day	17000 ML/day	20000 ML/day
Flow (Cutting)	No. of days					
2000 ML/day	365	310	239	205	198	176
3000 ML/day	365	286	233	202	191	168
4000 ML/day	365	272	224	198	182	166
5000 ML/day	355	258	222	191	176	160
6000 ML/day	322	246	210	182	168	156
7000 ML/day	310	239	205	176	166	152

The results of the analysis show that it is possible to meet the demand 33% of the time (1 in 3 years) for a diversion flow of 6000 ML/day into the Torrumbarry Cutting on **160 days of the year**, corresponding to a threshold discharge of 17 000 ML/day (Figure 15). For the same diversion flow and threshold discharge, the demand can be satisfied 25% of the time (1 in 4 years) for **168 days**.

This analysis does not consider water requirements for irrigation and other environmental assets that the EWG and TLM will need to consider. The issue of return flow will also need to be considered. Because of the pressing demand on water in the Murray system, it is likely that, at most, water would be available for diversion into the Cutting on between 90 and 120 days (e.g. 6000 ML/day for 100 days or 5000 ML/day for 120 days) (Andy Close, pers. comm).

Assuming annual environmental water requirements of about 600 GL/year (6000 ML/day for 100 days or 5000 ML/day for 120 days = 600 GL/year), to achieve the ecological objectives

for the Koondrook–Perricoota Forest, exceedence probabilities of 0.92%, 17%, 50%, 60%, 65% and 68% are estimated for carrying capacities of the Torrumbarry Cutting equal to 2000, 3000, 4000, 5000, 6000 and 7000 ML/day, respectively. The respective flooding frequencies to meet the annual ecological demand of 600 GL/year are 1 in 109, 1 in 5.9, 1 in 2, 1 in 1.7, 1 in 1.54 and 1 in 1.47 years, respectively.

The desired flooding of the Koondrook–Perricoota Forest is at a frequency of 1 in 3 years and an areal extent of at least 30% of the forest. A carrying capacity of the Torrumbarry Cutting in the range of 4000 to 7000 ML/day can potentially achieve the desired ecological outcomes provided the assumption of 600 GL/y is correct. The hydraulic efficiency of the flooding is likely to be greater at a carrying capacity of 5000 to 6000 ML/day relative to 4000 ML/day. Therefore, a design discharge capacity of 5000 to 6000 ML/day would appear reasonable for the Torrumbarry Cutting. However, if the EWG and TLM Committee consider that a very small proportion of the available water downstream of the Torrumbarry Cutting can be diverted into the KPF, then this will likely dictate the design discharge for the Cutting (from a water availability perspective). Predictions of the areal extent of the flood inundation of the KPF were obtained from MIKE FLOOD model simulations (Section 5).

Figure 16. Number of days in a year on which a specified demand for diversion flow into the Torrumbarry Cutting can be satisfied under the current conditions (1891–2000) (threshold discharge: 10 000 ML/day)

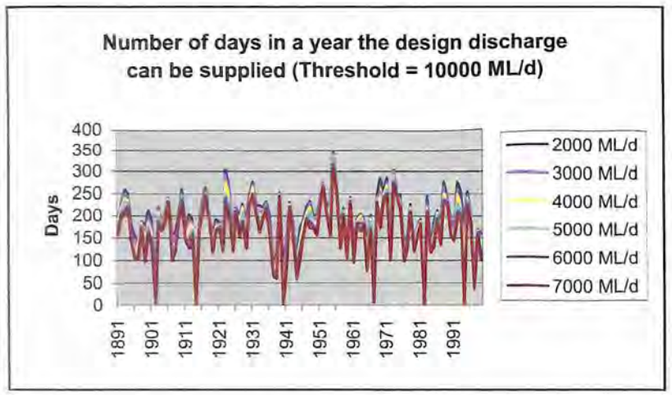

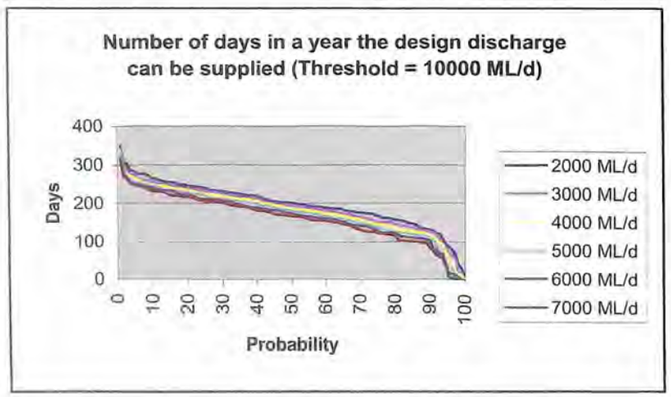

5 Remote sensing analysis of floodplain inundation

Remote sensing analysis using 12 Landsat TM images spanning across three historical flood events (see Table 3) was done to determine the flood extent of the KPF by the methodology of Shaikh et al. (2001, 1998) and Green et al. (1998). Cloud-free satellite images were selected on the basis of hydrologically significant dates (see Section 6.1.2 for details) within the three historical events during 1991, 1993 and 2000. All the geo-referenced images had a root mean square (rms) error of less than a pixel. The methodology uses the spectral responses of water, vegetation and bare soil in association with image-processing techniques to delineate dry and wet areas of the floodplain (Figures 17, 18).

Figure 17. Spectral responses of water, vegetation, soil and snow in four wavelength bands of the SPOT satellite (blue: 0.4 to 0.5 µm; green: 0.5 to 0.6 µm; red: 0.63 to 0.69 µm; and near-infrared: 0.7 to 1.1 µm) (courtesy SPOT Imaging)

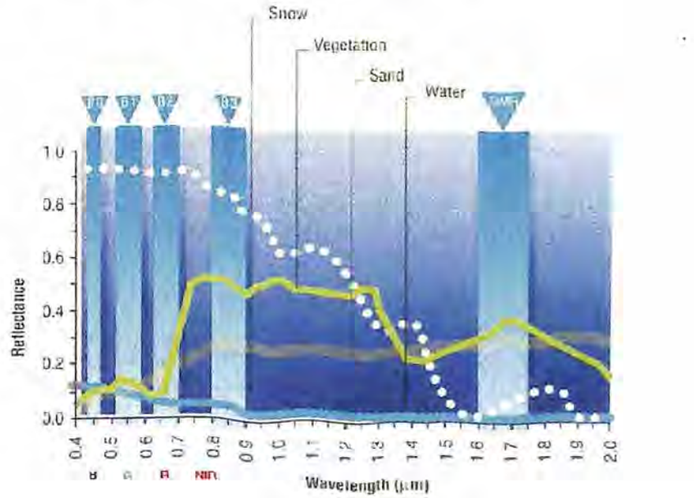

The digital number (DN) is a measure of the strength of the signal received from the object. Water is less reflective than adjacent bare soil in the green (TM2, 0.52–0.6 mm) and red (TM3, 0.63–0.69 mm) spectral bands. During flooding the contrast is low because of the presence of large sediment loads in the water. Wetlands present further difficulties due to their shallow water depths and the resultant reflectance off bottom sediments (Shaikh et al. 2001). In such cases the near-infrared (TM4, 0.7–0.9 mm) and middle infrared (TM5, 1.55–1.75 mm) are superior to any of the other wavelengths, as these wavelengths are absorbed even by shallow water, resulting in much greater tonal contrast in the infrared bands (Johnston and Barson 1993). Therefore, the most useful bands for demarcating water bodies are the near-infrared (TM4) and middle infrared (TM5).

Density slicing is an enhancement technique whereby an image is processed to display a new image in which the pixels have only one of two DNs: either 1 (wet) or 0 (dry). The values are assigned on the basis of whether the original image pixel had a DN greater or less than the nominated threshold. Density slicing has been found to be very reliable in delineating inundated and non-inundated wetlands (Bennett 1987; Johnston and Barson 1993; Shaikh et al. 1998). Johnston and Barson (1993) used a DN of 40 as a threshold to map inundated areas using TM5.

Table 6. Inundation areas estimated from a remote sensing analysis of Landsat TM images and from the MIKE 11, MIKE 21 and MIKE FLOOD hydraulic models.

Date	Flow (ML/day)	DN threshold	Wet area (%)			
			Remote sensing	MIKE 11	MIKE 21	MIKE FLOOD
1 August 1991	4861	20	1.3			
17 August 1991	12 698	22	0.7	2.1	0.14	0.14
2 September 1991	23 048	28	0.7	4.7	5.0	1.9
4 October 1991		30	12.6			
		31	17.5			
	43 065	32	23.2	21.9	53.4	36.0
21 November 1991	3496	40	1.7			
10 January 1993		45	1.5			
22 August 1993	36 319	24	6.0			
		25	8.4	11.7	31.9	18.8
23 September 1993	56 970	35	68.8	33.9	65.9	51.9
26 November 1993	27 678	40	4.8	7.5	42.4	28.8
3 September 2000	15 977	40	6.3		0.16	
4 October 2000	28 309	34	11.2	7.7	25.0	
		35	12.5			
		36	12.6			
7 December 2000	16 987	41	3.1	3.4	33.2	

[a] Adopted Density Number (DN) threshold values following comparison with reconnaissance survey data and discussions with Forests NSW field staff

In this study, the DN for water in the range 20 to 45 was used for different images (see Table 3). Note that the threshold value is not always the same; it changes from image to image, and sometimes even within the same image. These values vary from one image to another because the images were acquired in different seasons and under different atmospheric conditions. Radiometric normalisation can be performed on an image to ensure that all images have digital values as if acquired in similar conditions. However, this requires atmospheric correction algorithms along with associated atmospheric data, which are difficult to collect (Cantya et al. 2004). Thus, an appropriate value was decided on for each image on the basis of a visual interpretation of the false colour composite image. In this application, a threshold value was determined by examining the data values for flooded and non-flooded areas. For each image the exact DN value was confirmed by comparison with an approximation relationship of the KPF flood inundation developed by Forests NSW on the basis of a reconnaissance survey following flooding from high flows in the Murray. A

sensitivity analysis was also performed on three images for 4/10/91 (DN: 30, 31 and 32), 22/8/93 (DN: 24 and 25) and 4/10/00 (DN: 34, 35 and 36). The inundation area corresponding to each image was thus estimated from the remote sensing analysis (Table 6).

Forests NSW field staff conducted a reconnaissance surveys during historical flood conditions in the KPF. Following flooding in the KPF, field staff surveyed representative areas for all vegetation types in different parts of the forest by boat. Visual assessment of the percentage flooded area was then applied to the complete forest for each vegetation type to estimate the extent of flooding of the whole forest. The field staff established a relationship between flood inundation of the KPF and the 30-day minimum flow in the Murray prior to the date when the reconnaissance survey was conducted (Gary Miller, Forests NSW staff, pers. comm.).

Unfortunately, the dates of the reconnaissance survey are not available. Therefore, the inundation area estimates obtained from the remote sensing analysis need to be compared with the reconnaissance data in the same format (i.e. 30-day minimum flow in the Murray prior to the image date; Figure 19). Comparison between the two datasets for the 30-day minimum flow in the Murray is meaningful for high flow values and inundation areas in excess of about 15%. This is because for low flows a significant proportion of the flow leaves the KPF via runners, and this is not captured well when inundation areas are related to 30-day minimum flow information in the Murray. Good agreement between the two datasets for inundation areas in excess of 15% indicates that the remote sensing data can be used for further comparison with the results of hydraulic modelling (Section 6). The results of the remote sensing analysis provide a good indication of the overall flooding patterns in the KPF but need not be treated as an absolute representation of flooding in specific parts of the KPF. Flood inundation maps prepared from the results of the remote sensing analysis are given in Figure 20.

Figure 18. Scatter diagram of digital numbers (DNs) in the near-infrared band and the red band and their relationship with the ground surface (vegetation, water bodies and bare soil)

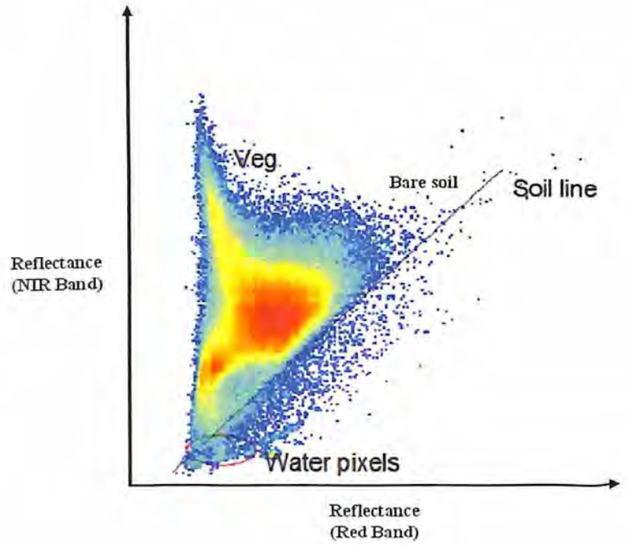

Figure 19. Comparison of flood inundation areas in the KPF during historical events, as determined by the remote sensing analysis and the reconnaissance survey

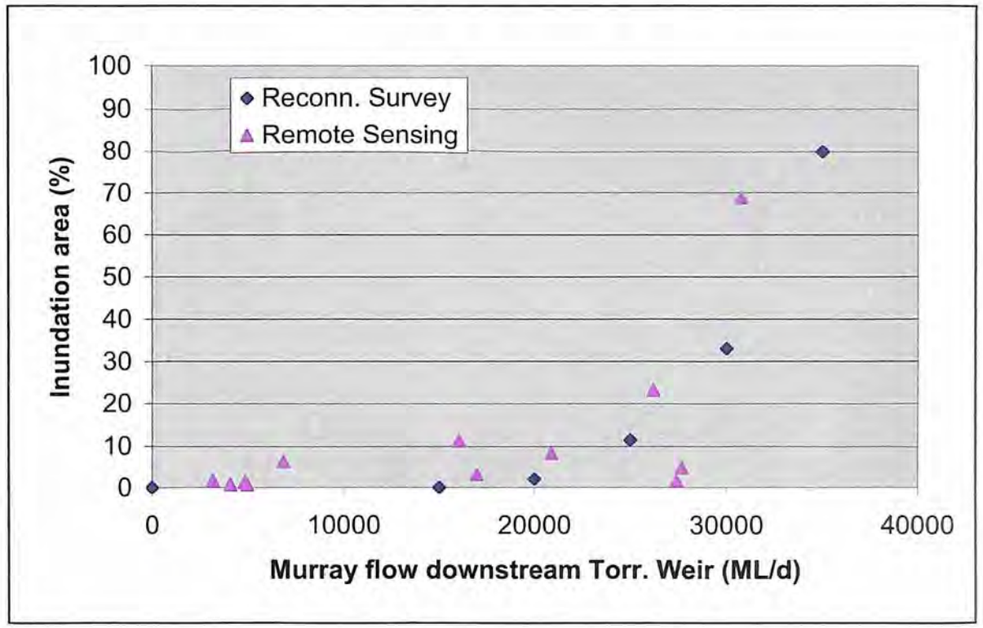

Note: The flow data for the Murray downstream of Torrumbarry Weir in Figure 19 are the 30-day minimum flows prior to the date when the reconnaissance survey was conducted by Forests NSW. Dates for the reconnaissance survey are not available from Forests NSW archives; therefore, the inundation data from the remote sensing analysis need to be compared with the survey data against 30-day minimum flows in the Murray.

Figure 20. Flood inundation maps of the KPF during historical events. Prepared from results of the remote sensing analysis

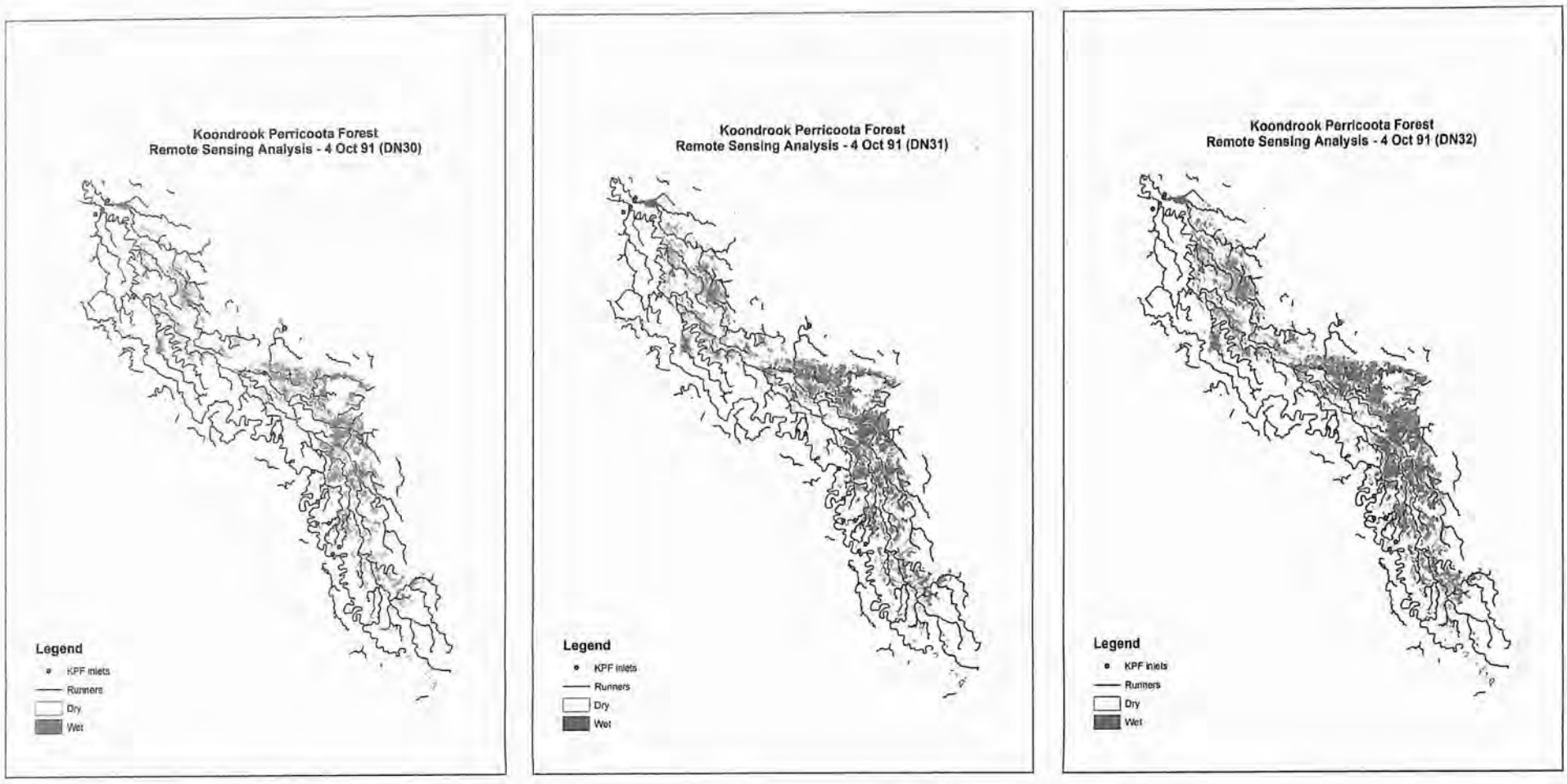

Figure 20. Flood inundation maps of the KPF during historical events. Prepared from results of the remote sensing analysis (continued)

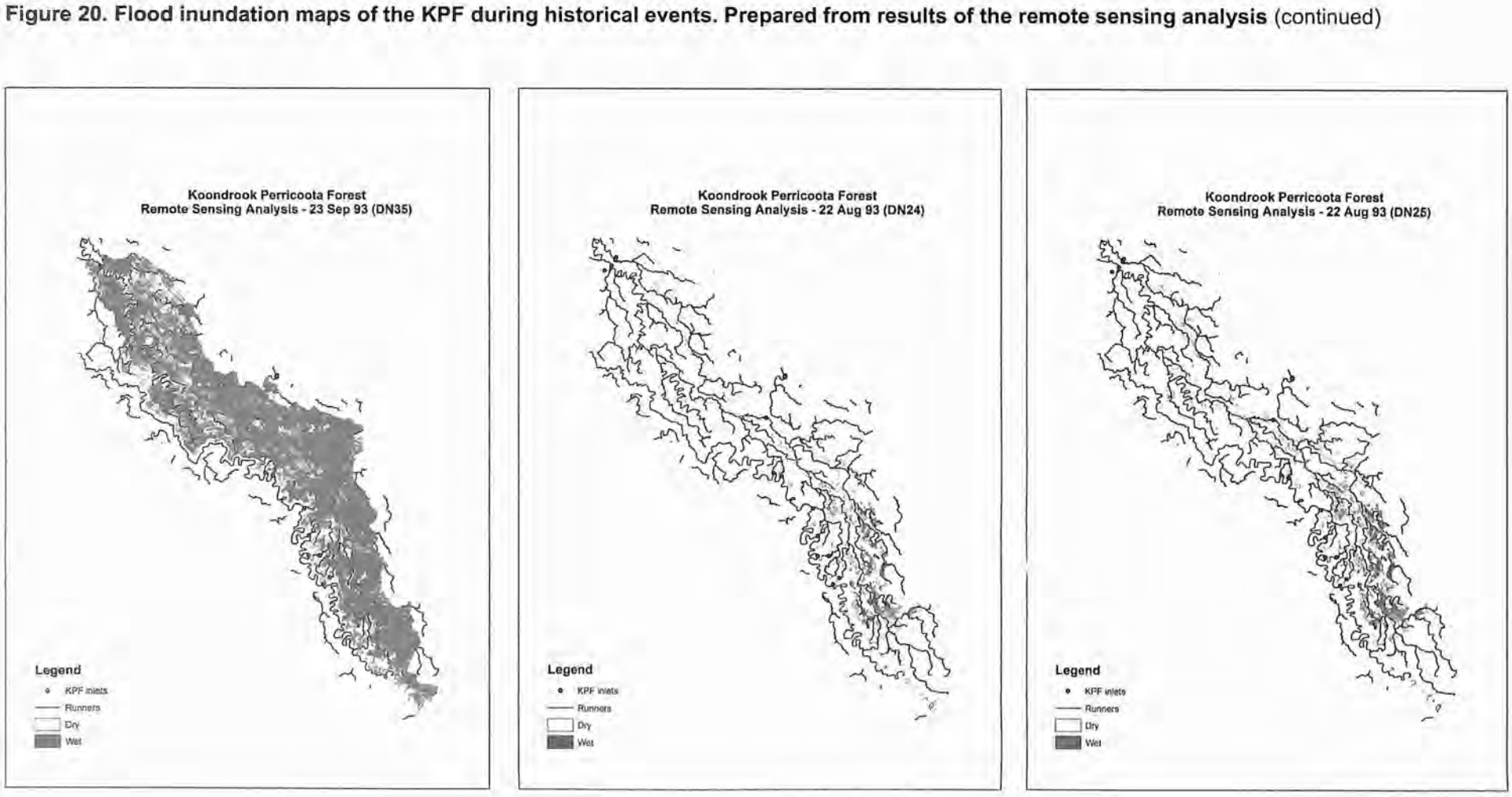

6 Hydraulic modelling

6.1 OVERBANK FLOW INTO THE MURRAY FLOODPLAIN

Water is diverted naturally into the KPF (NSW) and Gunbower (Victoria) forests when flow in the Murray is high (see Figure 14). Natural flow diversion from the Murray into the forests commences at about 17 000 ML/day, and flow diversions increase substantially with an increase in flow in the Murray from 20 000 to 65 000 ML/day. When the observed flows downstream of Torrumbarry Weir are 20 000, 30 000, 40 000, 50 000 and 65 000 ML/day, the proportions of combined flow naturally diverted to the Gunbower and Koondrook–Perricoota Forests are 0%, 14%, 30%, 41% and 46%, respectively.

6.1.1 KPF and Gunbower inlets

There are eight KPF inlet locations on the right bank of the Murray and five Gunbower inlet locations on the left bank of the Murray between Torrumbarry Weir and Barham (see Figure 3). The KPF inlets are Swan Lagoon upstream, Swan Lagoon downstream, Horseshoe Lagoon, Dead River Lagoon, Black Gate, Penny Royal, Upper Thule and Lower Thule. The Gunbower inlets are Deep Creek, Broken Creek, Spur Creek, Barton Creek and Yarren Creek. Swan Lagoon upstream and downstream inlets are the largest KPF inlets, whereas Deep Creek and Yarren Creek are the largest Gunbower inlet locations. Cross-sections at the upstream end of the Lower Thule inlet adjoining the Murray and the downstream end where the inlet runner merges with the floodplain are shown in Figure 21. Typically, water always enters the KPF and Gunbower from within the inlet cross-sections and not from the banks of the Murray directly into the floodplain (Lindsay Johnson, Forests NSW, pers. comm.). In general, the inlet runners merge with the forest floodplain within about 50 to 300 m. Conveyance of the runners reduces gradually, and water in excess of runner capacity spills out of the runners into the KPF floodplain. Rating curves at all inlet locations were developed by using cross-sections obtained from the DEM and survey data, Manning's n of 0.04, local representative slopes, and the Manning's formula (Figure 22). The rating curves indicate that up to 20000 ML/day combined flow from all inlets can potentially enter the KPF under high flow conditions of about 75000 ML/day in the Murray.

Figure 21. Upstream end of the Lower Thule inlet adjoining the Murray (left), and the downstream end where the inlet runner merges with the KPF floodplain (right)

Figure 22. Rating curves at all inlet locations of the KPF and the Gunbower Forest (see Figure 3 for locations of the inlets)

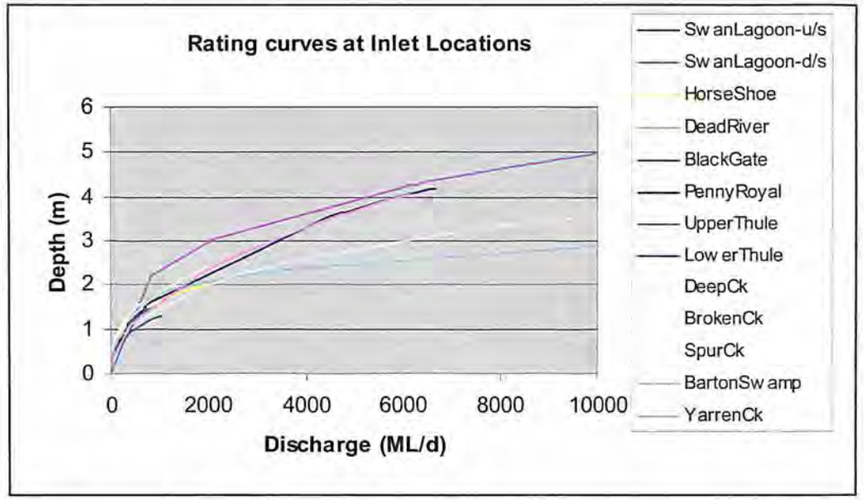

6.1.2 Historical flood events and partitioning of flow into the KPF and Gunbower

For historical modelling of the KPF floodplain, it was necessary to first determine diversion flow from each inlet location during different historical events (see Table 3). Therefore, a 1D MIKE 11 model was set up for the Murray between downstream of Torrumbarry Weir and Barham, an area that includes all the KPF and Gunbower inlets. Four historical events (1991, 1993, 2000 and 2003) were used to set up and calibrate the MIKE 11 model for the Murray (Figure 23). The flood events for 1991, 1993, 2000 and 2003 correspond to peak flows of about 43 000, 60 000, 47 000 and 23 000 ML/day, respectively. These events were strategically chosen for hydraulic modelling of the KPF to represent a range of historical conditions (e.g. single and multiple peak hydrographs representing flows up to 60 000 ML/day).

The available data for these flood events includes cross-sections along the Murray (sourced from Water Technology Pty Ltd.), cross-sections at the KPF and Gunbower inlets (sourced from the DEM and survey data discussed in Section 2.1), hydrographs and rating curves at Torrumbarry Weir and Barham (sourced from MDBC) and the Landsat TM images (see Table 3). A total of 26 cross-sections between Torrumbarry Weir (upstream) and Barham (downstream) were used to describe a total of 108 km of the Murray (average reach length 4.14 km). The bed levels at the upstream and downstream boundaries are 76.65 m and 71.84 m, respectively, and the average representative slope is 1 in 22380.

The bed level at each KPF and Gunbower inlet location is higher than the bed level of the Murray at the junction, and this can lead to divergence problems in MIKE 11. Therefore, to avoid divergence problems in the numerical solution of the Saint Venant equations, a broad crested weir was introduced at the junction of each KPF and each Gunbower inlet with the Murray. Implementation of the broad crested weir allows for explicit simulation of the flow through each inlet corresponding to the dynamic water level in the Murray. Cross-sections obtained from the DEM were used to describe the weir geometry, thereby accounting for the representative conveyance of each inlet runner. MIKE 11 calculates the *Q–h* relationships for

critical flow conditions at the weir and incorporates the effects of structure into balance equations 1 and 2. Flow was permissible in both directions, and an inflow head loss factor of 0.5 was used.

Manning's n, a measure of the riverbed friction, was varied in the range 0.03 to 0.05, and the calibrated parameter values for the historical events of 1991, 1993, 2000 and 2003 were 0.04, 0.036, 0.04 and 0.042, respectively. Peak flows for the respective flood events were about 43 000, 60 000, 47 000 and 23 000 ML/day. The calibrated Manning's n values are consistent with the magnitudes of flow, with high values corresponding to high-magnitude historical flood events. Calibrated historical flood events compare very well with the observed flow at Barham (Figure 23).

Figure 23. Historical flood events in the Murray downstream of Torrumbarry Weir and Barham (arrows indicate dates corresponding to the remote sensing images)

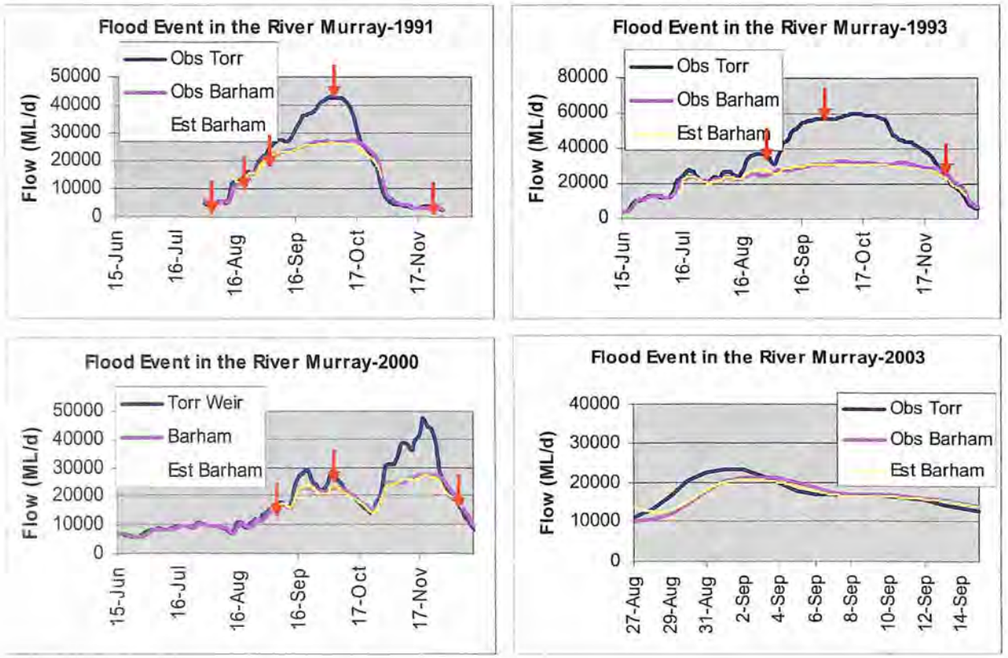

Simulated inflows into the KPF floodplain during historical events are shown in Figure 24. The mass balance error for all the historical flood events was negligible (<0.001%). The simulated volume of water diverted naturally into the KPF and Gunbower floodplains through the respective inlets varied among events in the range 2.1% to 12.4% of the flow in the Murray downstream of Torrumbarry Weir (Table 7). For a given flood event, flow diversions between the KPF and Gunbower are broadly comparable with the marginally larger flow diversions into the Gunbower. The simulated combined inflows from all inlets of the KPF for each of the flood events in 1991, 1993 and 2000 are much more than the volume of water in the range 4000 to 6000 ML/day planned for diversion into the KPF from the Torrumbarry Cutting (Figure 24). Inflow hydrographs for each inlet, obtained from the MIKE 11 model of the Murray, were used for hydraulic modelling of the KPF floodplain.

Figure 24. Inflows into the KPF floodplain during historical flood events in the Murray (simulated by the MIKE 11 model)

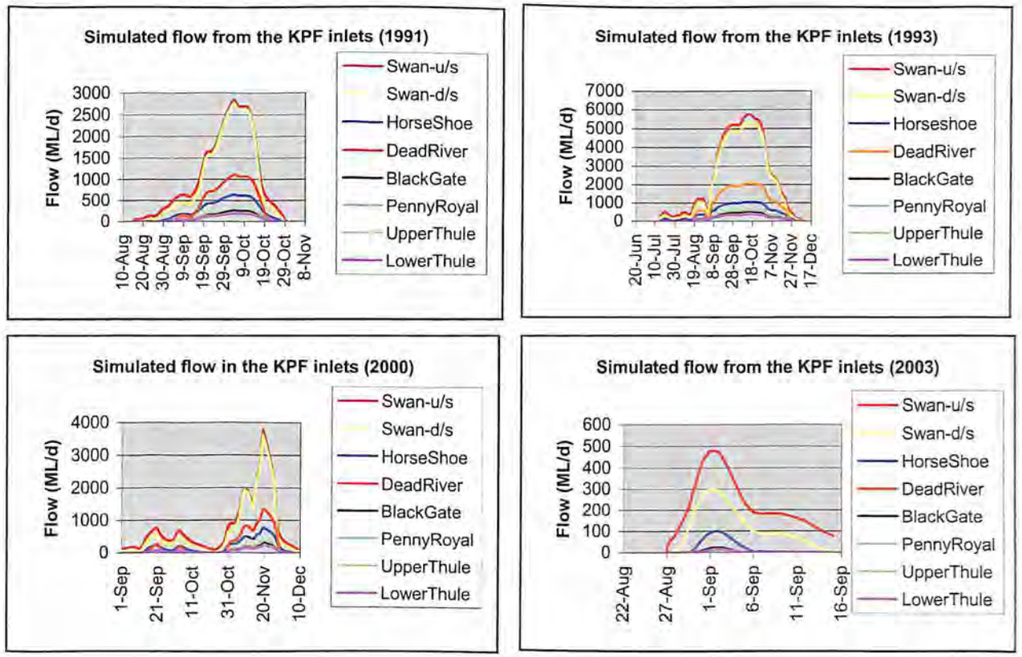

Table 7. Percentages* of flow diverted from the Murray into the KPF and Gunbower floodplains

Event	Diversion into Gunbower (%)	Diversion into KPF (%)
1991	12.4	10.3
1993	11.2	9.0
2000	9.9	8.1
2003	2.1	2.1

*Flow diversions are shown as percentages of the flow in the Murray downstream of Torrumbarry Weir

6.2 FLOODPLAIN MODELLING

KPF floodplain modelling was performed in three stages, moving progressively from simple to more complex forms. Knowledge of the KPF flood inundation processes was improved in each stage to better formulate more complex model forms. The primary reason for the choice of a staged approach was to account for the scale of the problem. The total area of the KPF is about 33 750 ha, and the total area included within the KPF DEM is 68 971 ha. The total number of grid cells in the KPF DEM at 1 m resolution is about 690 million. Historical and likely future flood events required for hydraulic modelling vary between 3 and 6 months' duration. Non linear overland flow simulations using the Saint Venant equations are generally required in time steps of a few seconds to overcome the numerical instability issues. Therefore, the size of the hydraulic modelling problem is huge and involves significant numerical overheads. On the basis of prototype benchmarking, it was estimated that the

simulation times for implementation of the MIKE FLOOD model would be very long (>30 days). It was considered mandatory to begin simulations with simple model forms using MIKE 11 (quasi-2D) and to then conduct targeted simulations using MIKE 21 (2D) and MIKE FLOOD (combined 1D flow in the runners and 2D flow in the floodplain).

6.2.1. Stage 1—quasi-2D floodplain modelling using coarse MIKE 11

A coarse quasi-2D MIKE 11 floodplain model was set up for the KPF (Figure 25). This type of modelling involves 1D simulation of the water surface profiles using wide cross-sections aligned perpendicularly to the direction of flow for representation of the floodplain geometry in MIKE 11. Simulated water levels at a given instance of time are draped over the DEM to produce inundation maps of the floodplain. In this approach a 1D representation is imposed on essentially a 2D process; therefore, this approach requires *a priori* information on the flow path and flow direction across the floodplain. In the case of KPF, the runners mapped across the floodplain are discontinuous and cannot be used directly for representing the flow paths. Therefore, spatial analysis techniques were required to predict drainage patterns across the KPF floodplain.

The earliest and simplest method for specifying flow directions is to assign flow from each pixel to one of its eight neighbours, either adjacent or diagonally, in the direction with the steepest downward slope. This method, designated D8 (8 flow directions), was introduced by O'Callaghan and Mark (1984) and has been widely used (Marks et al. 1984; Band 1986; Jenson and Domingue 1988; Mark 1988; Morris and Heerdegen 1988; Tarboton et al. 1988; Tarboton 1989; Jenson 1991; Martz and Garbrecht 1992). In the context of a grid, the upslope area is the area contributing to each pixel and may be estimated as the product of the number of pixels draining through each pixel and the pixel area. The D8 approach has disadvantages arising from the discretisation of flow into only one of eight possible directions, separated by 45° (e.g., Fairfield and Leymarie, 1991; Quinn et al., 1991; Costa-Cabral and Burges, 1994). Tarboton (1997) proposed robust, precise and useful multiple flow path algorithms, called the D∞ method, to minimise dispersion and avoid grid bias in determining the upstream contributing area. The D∞ method was unsuccessful when it was applied to the KPF floodplain DEM at 1-, 2- and 5-m resolutions owing to memory overflow in the recursive algorithms of the area accumulation procedure. Flow direction and flow accumulation algorithms using the D8 method were then used with the 1 m DEM to delineate the runners and the upslope contribution areas (Figure 25). The runners obtained from the D8 method matched very well with the spatial patterns of the mapped runners. Additionally, they enhanced the discontinuous drainage patterns of the mapped runners.

The coarse quasi-2D MIKE 11 setup includes a total of five runners and eight inlet runners, covering a combined reach length of about 82 415 m (Table 8). A total of 100 geo-referenced cross-sections were used, with an average reach length of 824 m. These cross-sections were aligned perpendicularly to the runners delineated by the D8 method. Link channels were provided between Runner 1 and all other runners to include the effects of flux transfer between the runners in either direction. Flood hydrographs for the 1991, 1993, 2000 and 2003 events at each KPF inlet were used as the specified flux (inflow) boundary conditions (see Figure 24). At the downstream end of Runners 1 and 4, a system-dependent boundary condition was used by specifying the rating curve, and the model estimates flux (outflow) depending on the dynamic water levels.

Table 8. Network details of the quasi-2D MIKE 11 model of the KPF floodplain (see Figure 25 for layout of the runners and the cross-sections)

	No. of sections	Reach length (m)	Upstream connection		Downstream connection	
			Name	Distance (m)	Name	Distance (m)
Runner 1	27	49 489				
Runner 2*	4	6361			Runner 1	
Runner 3*	4	6925			Runner 1	34 067
Runner 4*	4	4710				
Runner 5*	4	5340			Runner 1	45 535
Swan-d/s	7	785	Murray	90 139	Runner 1	0
Swan-d/s	7	785	Murray	90 246	Runner 1	0
Horse Shoe	8	1100	Murray	109 063	Runner 2	0
Dead River	7	1370	Murray	118 531	Runner 2	1721
Black Gate	7	1522	Murray	120 884	Runner 2	4018
Penny Royal	7	1396	Murray	129 857	Runner 1	14 631
Upper Thule	7	1184	Murray	137 493	Runner 1	18 971
Lower Thule	7	1648	Murray	139 378	Runner 1	19 926

*Link channel with Runner 1 included, providing for flux transfer in either direction.

MIKE 11 allows for surface infiltration through the cross-section specific leakage factor parameter, expressed in units per second. Initial model simulations were done with no surface infiltration and a Manning's roughness coefficient of 0.05 for all the floodplain cross-sections. Water levels simulated at different times within each historical flood event were draped over the DEM at 10 m resolution. All historical flood events were simulated and inundation area statistics prepared from output grids of the water depth. A scatter diagram of flow versus inundation area was developed from the quasi-2D MIKE 11 outputs and was compared with the results of the remote sensing analysis (Figure 26a). The results indicated that for no leakage and a Manning's n value of 0.05, MIKE 11 overestimates the inundation area relative to those from the remote sensing study up to 45 000 ML/day; it significantly underestimates the inundation area for higher flow values.

The depth of flooding in the KPF floodplain tends to vary between 0 and 2 m (Lindsay Johnson, pers. comm.). The variation in the leakage factor with depth of flooding for surface infiltration rates of 18, 20 and 25 mm/day is shown in Figure 26b. Assuming an average depth of inundation across the KPF floodplain in the range 0.2 to 0.4 m, the plausible range of the leakage factor is likely to vary between 5.0×10^{-7} s^{-1} and 1.0×10^{-6} s^{-1}. Therefore, a sensitivity analysis was conducted to analyse the impact of surface infiltration rate on the pattern and extent of floodplain inundation; the leakage factor was varied in the range 0 to 1.0×10^{-6} s^{-1}. The results show a reduction in the simulated inundation area of up to 15% as the leakage factor increased from 0 to 1.0×10^{-6} s^{-1} (Figure 26c). This is because an increase in the leakage factor results in less water being available for the overland flow. The corresponding reduction in outflow volume from the KPF can be substantial (up to 50%). The area weighted average value of the infiltration rate (with a 1 m hydraulic head) and saturated the hydraulic conductivity of the KPF floodplain are 25 and 22.2 mm/day, respectively (see Table 2). Therefore, for an area weighted depth of about 0.3m, a leakage factor in the range 6×10^{-7} s^{-1} to 8×10^{-7} s^{-1} is very likely for the KPF (Figure 26b).

Figure 25. Layout of the KPF floodplain quasi-2D MIKE 11 hydraulic model (floodplain runners generated by the D8 method are shown in blue)

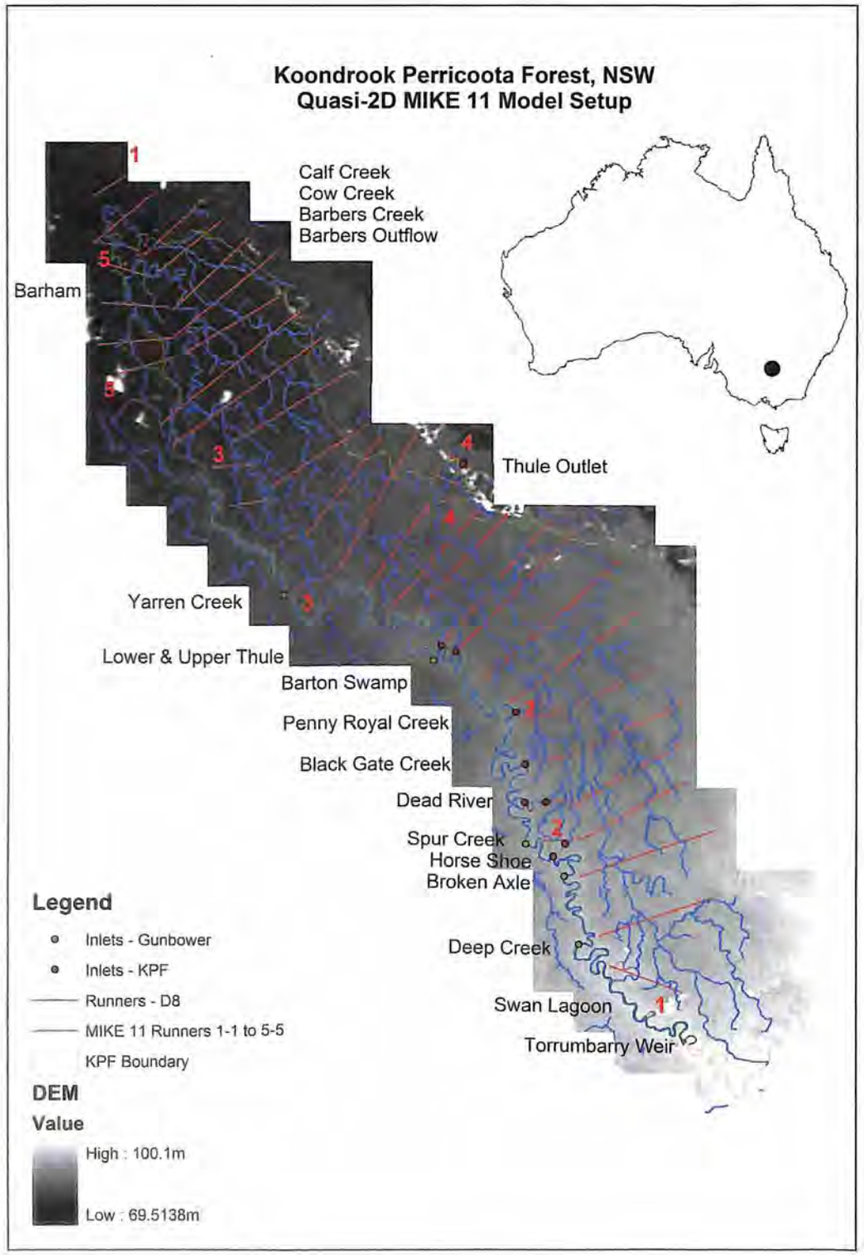

Figure 26. Results of sensitivity analysis from the quasi-2D MIKE 11 hydraulic model. (a) Flow versus inundation area (RS: Remote sensing; MIKE 11-A: Results with Manning's n = 0.05 and leakage factor = 0 s^{-1}; MIKE 11B: Results with Manning's n = 0.042 and leakage factor = 7×10^{-7} s^{-1}). (b) Water depth versus leakage factor corresponding to surface infiltration rate of 18 mm/d, 20 mm/d and 25 mm/d. (c) Leakage factor versus reduction in inundation area (Area) and reduction in outflow (Volume). (d) Roughness coefficient versus reduction in inundation area for 4 October 2000 and 7 December 2000

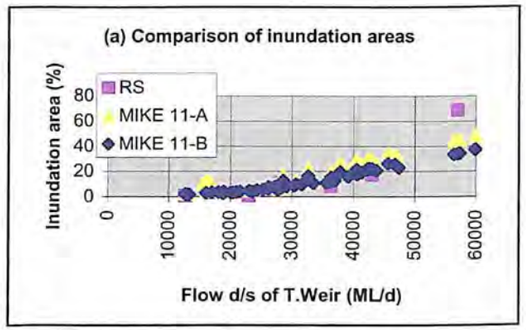

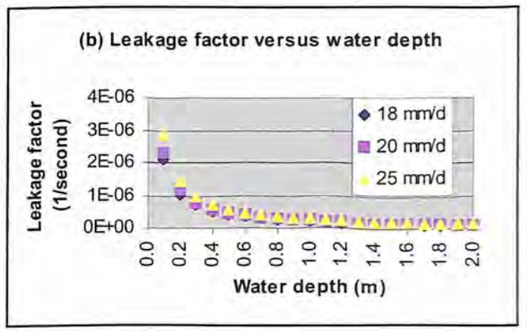

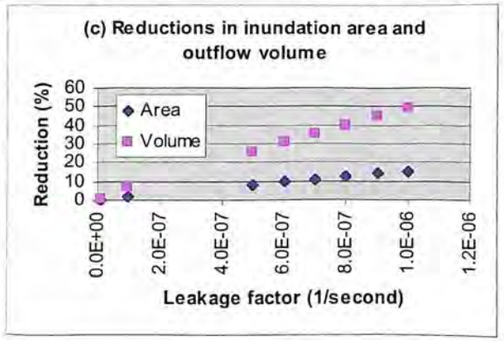

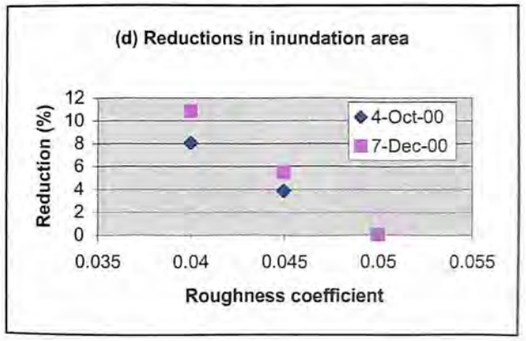

Three Manning's n values—0.04, 0.045 and 0.05—were used to conduct a sensitivity analysis of the bed resistance. Decreasing Manning's n from 0.05 to 0.04 increases the velocity of water and results in lower values of the inundation area relative to those from Manning's n of 0.05 (Figure 26d). On the basis of the direction of change in inundation area evident from the sensitivity analysis and a comparison with the results of the remote sensing analysis, the leakage factor of 7×10^{-7} s^{-1} and Manning's n of 0.042 were optimised for the KPF study. Simulations for all historical events were done with the optimised values and a relationship of flow versus inundation area was developed (see Figure 26a). The results from the quasi-2D MIKE 11 show a good match with those from the remote sensing study up to about 35 000 ML/day. Thereafter, the results drift apart and lower estimates for the inundation area are obtained from the model relative to those from the remote sensing study.

6.2.2 Stage 2—2D floodplain modelling using MIKE 21

MIKE 21 is a 2D model, and for large areas like the KPF there can be significant numerical overheads. The total area of the KPF is about 33 750 ha, and the total area included within the KPF DEM is 68 971 ha. The sizes of the ASCII grid files for the KPF DEM at 5, 25 and 40 m resolution are 418, 17 and 8 MB respectively. Ideally, MIKE 21 grids up to 5 MB can be handled effectively for long-term simulations (about 6 months) with the currently available versions of the model operational on high-end PCs. This is because the model needs to hold

about 12 grid arrays in banded form in the memory (points in the model domain that can potentially get wet): three arrays each of the state variables water depth and flux density (in both the x- and y-directions), one array for bathymetry, one array for friction and one array for infiltration. At 5, 25 and 40 m resolution, the memory requirements for the KPF are about 3.5 GB, 140 MB and 55 MB, respectively. Additionally, for the simulations to run smoothly, the Courant number must be constrained to less than or equal to 1 for floodplain problems that can potentially have high Froude number flows. The Courant number represents how fast the fluid is travelling through the computational domain. It is defined as the ratio of the speed of the fluid to the speed of the computation.

$$C_r = \frac{U_{\max}}{\Delta x / \Delta t} \qquad (6)$$

where, C_r = Courant number (–), $U_{\max}$ = maximum fluid velocity (m s^{-1}), Δx = grid spacing (m) and Δt = time (s).

Assuming a maximum local fluid velocity of 4 m s^{-1}, a grid spacing of 40 m and a Courant number value of 1, a simulation time step estimate of 10 s is obtained. The spatial and temporal resolutions chosen for the MIKE 21 simulations were 40 m and 10 s, respectively. Although the 40 m grid scale is considerably coarser than that of the available DEM data, it still pushes the model computations to limits while keeping the simulation times within a practical range (5 to 15 days on an Intel® Dual Core™ PC with a 2.13-GHz processor speed and 3.25 GB RAM).

Two types of boundary conditions were used in setting up the MIKE 21 model. Each of the eight KPF inlets was treated as a point source (see Figure 3), and simulated hydrographs at each inlet location obtained from the MIKE 11 model for the Murray for 1991, 1993 and 2000 were used to describe the source terms (see Figure 24). A constant head boundary condition was used at the western boundary (Barbers Creek outflow) and the northern boundary (Thule Creek outflow). The respective water levels maintained in the simulations were 73.2 and 74.2 m. The surface infiltration rate grid was prepared by using the soils map (see Figure 7) and the modified infiltration rates from Table 2. Potential evaporation rate from Figure 11 was used to specify evaporation from the (dynamic) inundated areas within the model domain. The effect of friction on inundation area was examined by performing two simulations initially, one each for Manning's n of 0.05 and 0.07 for an inflow of 6000 ML/day over 120 days. The results showed that an increment of ±0.01 from 0.05 resulted in ±4% difference in the inundation area (Figure 27a). In view of the vegetation patterns and geomorphology of the KPF floodplain, Manning's n value of 0.05 was considered appropriate and used for further analysis with MIKE 21.

Results from MIKE 21 simulations for the historical flood events of 1991, 1993 and 2000 are shown in Figure 27b–d, along with results from remote sensing analysis and the calibrated quasi-2D MIKE 11 model. All simulations show that up to about 28 000 ML/day the results from MIKE 21 closely match those from the remote sensing analysis and quasi-2D MIKE 11. Thereafter, the results from MIKE 21 show significantly higher inundation areas relative to those from quasi-2D MIKE 11. When flow in the Murray is 28 000 ML/day, about 2000 ML/day flow enters the KPF through the inlets. The conveyance of the runners gradually reduces and water starts spilling into the floodplain (see Figure 21). Analysis of the variation of conveyance of the runners in the KPF shows significant variation in different parts of the KPF; up to 2000 to 2500 ML/day the flow is largely constrained in one dimension along the north-west direction of flow. Thereafter, the overland flow process becomes 2D and transverse hydraulic gradients

substantially affect the inundation patterns. The overland flow process and the inundation patterns for high flow conditions are better represented in a fully 2D model (MIKE 21) as opposed to 1D model simulations imposed on the DEM (quasi-2D MIKE 11).

Figure 27. (a) Effect of friction on inundation area in MIKE 21 for 6000 ML/day flow in the KPF; (b–d) Comparison of inundation areas from remote sensing analysis and quasi-2D MIKE 11 and 2D MIKE 21 models of the 1991, 1993 and 2000 historical flood events in the Murray

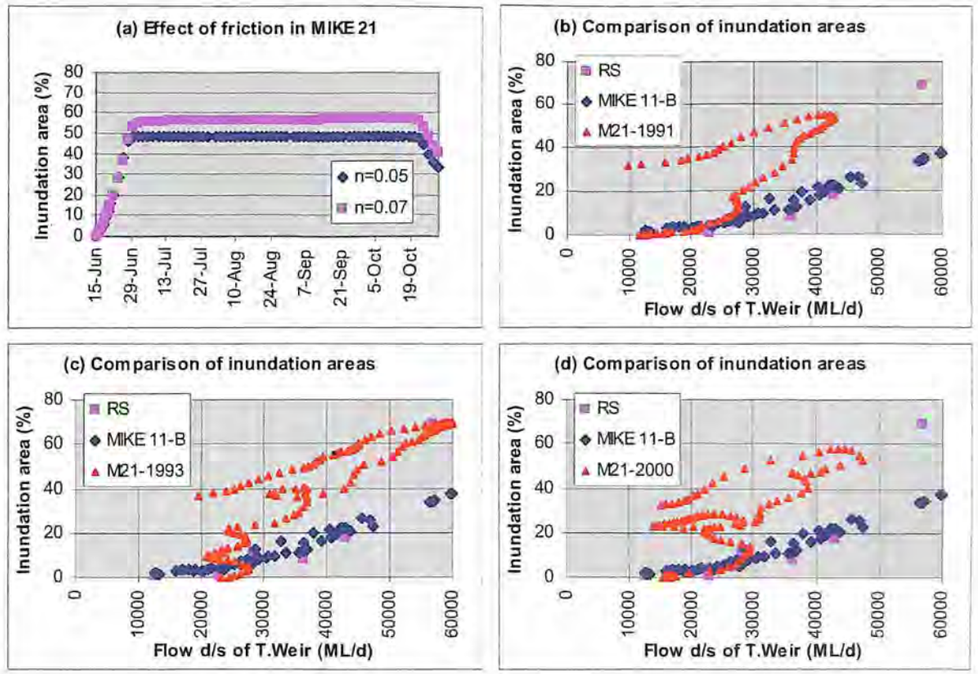

The remote sensing study estimated an inundation area of about 69% on 23 September 1993, corresponding to 56 970 ML/day flow in the Murray. Also, an inundation area of about 73% was mapped for the 1946 flood, corresponding to flow in the Murray of about 55 000 ML/day. The inundation area estimated for the 1993 event from the remote sensing analysis matches very well with the inundation areas simulated from MIKE 21 (Figure 27c) and compares well with the mapped inundation area for the 1946 flood event. The lower and upper parts of the inundation area curve from MIKE 21 in Figures 27b–d correspond to the rising and falling limbs of the hydrograph, and the difference results from storage within the system.

6.2.3. Stage 3—2D floodplain and 1D channel flow modelling using MIKE FLOOD

Inundation areas of the KPF floodplain are simulated well by the quasi-2D MIKE 11 model for low flow conditions in the Murray (20 000 to 28 000 ML/day). Simulations with MIKE 11 can be performed quickly, and the simulated water levels can be draped over a fine resolution DEM (e.g. 10 m DEM in this study). However, the approach forces a 1D simulation on a 2D process and markedly underestimates the inundation areas for high flow conditions when transverse gradients significantly affect the overbank flow and the inundation patterns. On the other hand,

a 2D simulation using MIKE 21 has significant numerical overheads, and compromise between the spatial and temporal resolution of the model and the simulation time is required.

In the case of KPF, 2D simulations could be performed at 40 m grid cell resolution and 10 s time step, even though the DEM at 1 m resolution is available. A close investigation of the conveyance of the runners in the KPF demonstrated that, in many areas, the runners are very well defined and can potentially carry between 8000 and 10 000 ML/day. Coarsening the DEM at 40 m resolution results in substantial smearing of the runners; conveyance of the runners in MIKE 21 is therefore under-represented. There are parts of the KPF floodplain where even under high flow conditions water will be channelled into the runners and will likely move faster through the forest. This situation is not represented adequately in the MIKE 21 model; therefore, it is expected that the inundation areas simulated by MIKE 21 may be somewhat higher than those obtainable from a model that captures runner dynamics in addition to accounting for floodplain behaviour. Additionally, information is needed on the threshold at which the process shifts from inundation of the runners and areas on the fringes of the runners to a fully 2D floodplain inundation process. The MIKE 21 results show that this threshold is about 28 000 ML/day (Figure 27b–d). However, the under-representation of the runner conveyance implies that this threshold may in fact be lower.

The MIKE FLOOD model was therefore developed to address the issues relating to under-representation of the runner conveyance in MIKE 21 and to analyse the threshold at which the inundation dynamics shift from runner-dominated behaviour to floodplain behaviour. The MIKE 21 model used in MIKE FLOOD is the same as that developed at 40 m resolution in Stage 2. A comprehensive MIKE 11 model was developed in Stage 3 at a fine resolution to capture the inundation dynamics and flow exchange between the runners and the floodplain. A total of six runners delineated by the D8 method were used (Figure 28). These runners are different from the runners used in the coarse MIKE 11 model in Stage 1. Unlike the wide cross-sections described in the coarse MIKE 11 at 40 m intervals and an average spacing of 824 m (Stage 1), cross-sections up to 200 m width, described at 1 m intervals and an average spacing of 226 m, were used in MIKE FLOOD (Stage 3). Critical cross-section locations were included in which the geometry changed substantially and could potentially involve significant exchange between the runners and the floodplain.

In view of the very long simulation times with MIKE FLOOD (up to 50 days), only two historical events for 1991 and 1993 were simulated. The boundary conditions used in the MIKE 21 component of the MIKE FLOOD model were exactly the same as those described in the MIKE 21 application (Stage 2). The surface infiltration rate and potential evaporation rate from inundated areas and the Manning's n used in the MIKE 21 component of MIKE FLOOD (Stage 3) were exactly the same as those used in Stage 2. Surface infiltration over the floodplain was incorporated through MIKE 21, and for this reason the leakage factor in MIKE 11 was set to zero. The calibrated Manning's n of 0.042 from the quasi-2D MIKE 11 modelling in Stage 1 was used for all six runners in MIKE FLOOD.

All inflow in MIKE FLOOD was included as point sources in MIKE 21 at the KPF inlets. The upstream end of each runner in MIKE 11 was specified to have a zero flow boundary condition. Runners 2, 3 and 5 connect with Runner 1 at the downstream end, which in turn connects with Runner 6 (Table 9 and Figure 28). Therefore, at the downstream end of Runners 4 and 6, a system-dependent boundary condition was used by specifying the rating curve, and the model estimates the flux (outflow) depending on the dynamic water level at the downstream boundary. In MIKE FLOOD water is permitted to leave the model domain through the outflow boundary as channel flow (Runners 4 and 6) as well as overland flow from the northern boundary (Thule outflow) and western boundary (Barbers Creek outflow).

Figure 28. Layout of the KPF MIKE FLOOD hydraulic model (floodplain runners generated by the D8 method are shown in blue)

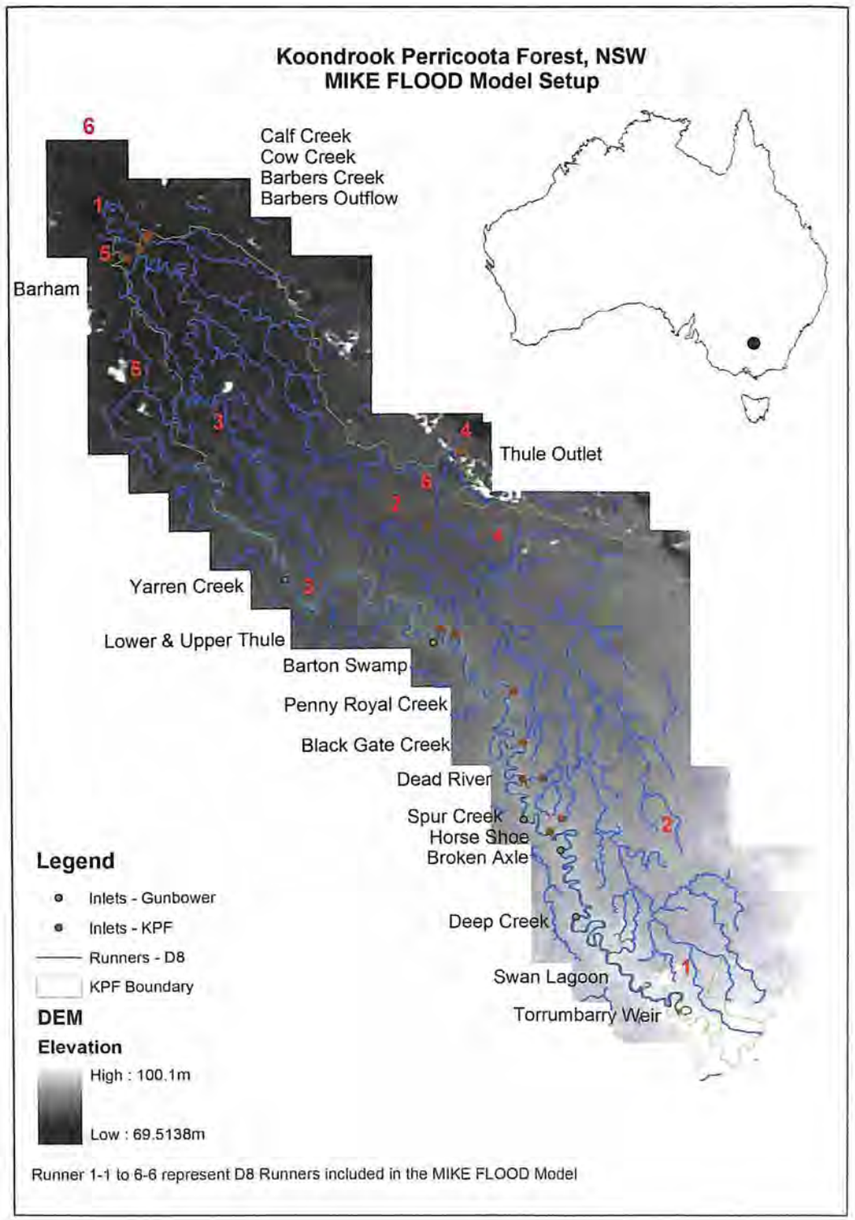

Table 9. Network details of the MIKE 11 component of the MIKE FLOOD model of the KPF (see Figure 28 for layout of the runners)

	No. of sections	Reach length (m)	Upstream connection		Downstream connection	
			Name	Distance (m)	Name	Distance (m)
Runner 1	396	81 510[*1]			Runner 6	31 000
Runner 2	122	30 250			Runner 1	37 010[*1]
Runner 3	55	13 000			Runner 1	51 260[*1]
Runner 4	52	13 000				
Runner 5	22	5000			Runner 1	74 760[*1]
Runner 6	162	40 000				
Total[*2]	809	182 760				

[*1]Runner 1 is defined between RD 9760 m and 91 270 m covering a reach length of 81 510 m. The downstream connection of Runners 2, 3 and 4 with Runner 1 represents the distance from the first cross-section of Runner 1 at RD 9760 m.

[*2]A total of 809 geo-referenced cross-sections represent a combined reach length of 182 760 m at an average spacing of 226 m.

Figure 29 (a), (b). Comparison of the variation of the areas inundated during the historical flood events with flow downstream (d/s) of Torrumbarry Weir, as determined by remote sensing analysis (RS) and the MIKE 11, MIKE 21 (M21) and MIKE FLOOD (MF) models.

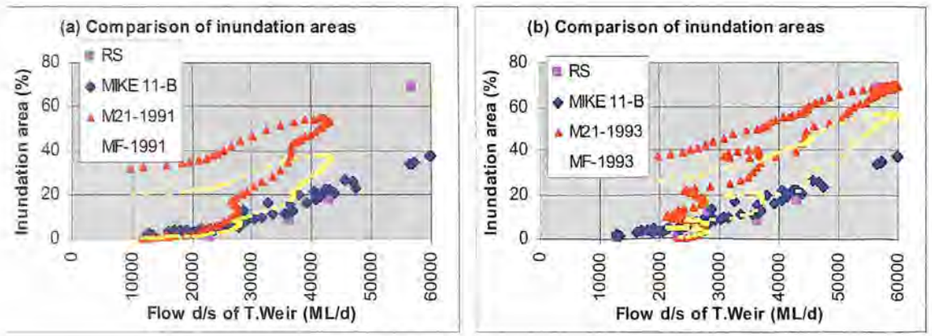

Lateral links along the left and right banks of the MIKE 11 cross-sections were included for each runner throughout the reach length. A cell to cell method was used for flow exchange between each reach length described by the MIKE 11 cross-sections and the overlapped MIKE 21 grid cells. MIKE 11 cross-sections were derived from a 1 m DEM at an average spacing of 226 m (Table 9). The bed level to be used for flow exchange at each overlapped 40 m grid cell in the reach length is internally defined in the model as the maximum of the 40 m grid cell elevation in MIKE 21 and the interpolated bank elevation from the MIKE 11 cross-sections. Therefore, MIKE FLOOD includes a good description of the runners and floodplain geometry through the use of lateral links between MIKE 11 and MIKE 21.

The results of MIKE FLOOD simulations of the historical flood events of 1991 and 1993, along with the results of the remote sensing analysis, quasi-2D MIKE 11 model and MIKE 21, are shown in Figure 29a, b, Figure 30 and Table 6. The inundation area versus flow

relationship simulated by MIKE FLOOD shows substantial reductions in inundation area estimates in comparison with those from MIKE 21 (Figure 29). MIKE FLOOD simulations for the 1993 (1991) event show a reduction of about 12.3% (17%) in the maximum inundation area of 69.3% (54.8%) simulated by MIKE 21. The numbers in parentheses indicate the corresponding values for the 1991 event. The reduction in the inundation area estimate in MIKE FLOOD results from appropriate representation of the conveyance of the runners, which was not represented in MIKE 21. Additionally, MIKE 21 simulations showed significant differences in the flow versus inundation area relationship at a threshold of about 28 000 ML/day, indicating a shift from a runner-dominated 1D process to a 2D floodplain inundation process. In contrast, the MIKE FLOOD simulations show that the shift from a 1D to a 2D inundation process begins around a threshold of 28 000 ML/day and increases gradually up to 36 000 ML/day, after which the process is largely 2D. Since the responses of all natural systems are generally highly damped because of large differences in storage relative to inflow and outflow, the gradual transition in inundation area simulated by MIKE FLOOD appears more realistic.

The 1991 flood event commenced on about 15 August 1991 with a single peak, and the Landsat TM image for 4 October 1991 corresponds to peak flow of 43 055 ML/day (see Figure 23). Comparison of the spatial inundation patterns from the remote sensing and MIKE FLOOD for 4 October 1991 shows good agreement (see Figure 30). However, the inundation areas east of the Thule outlet towards the northern boundary predicted by remote sensing do not compare well with those from MIKE FLOOD. Similar disagreement in the predicted inundation patterns also exist for the areas east of Thule outlet for 23 September 1993 and for the mapped inundation patterns on 7 August 1946. The corresponding flow of 56 790 ML/day is close to the peak flow of 59 944 ML/day on 14 October 1993, and the mapped flood inundation area for the 1946 flood event corresponds to a flow of about 55 000 ML/day. With the exception of some differences along the northern boundary east of Thule outlet, the broad inundation patterns across the KPF floodplain predicted by the two approaches compare well. For the lower flow of 36 319 ML/day on 22 August 1993, the inundation pattern from MIKE FLOOD is packed around the fringes of the runners that describe the lower parts of the floodplain, unlike the results of the remote sensing analysis, which show a wider distribution of the inundation areas around the runners.

During high flows in excess of 50 000 ML/day, there are two possible reasons for the differences in inundation patterns towards the northern boundary east of the Thule outflow. Firstly, some inflow into the KPF is sourced from the northeast, and this is not included in the MIKE FLOOD model wherein all water is sourced from the KPF inlets adjoining the Murray. Examination of the cross-sections of the KPF floodplain (see Figure 5) confirm that the northern boundary of the KPF is higher than the main floodplain; therefore, water sourced from the KPF inlets is unlikely to reach the northern boundary; this is confirmed by the remote sensing images (4 October 1991 and 23 September 1993) and the mapped inundation areas for the 1946 flood event. A close look at the results from the remote sensing of areas north and northeast of the KPF confirms this possibility. Secondly, the large amount of debris from dead trees during high flow events constrains flow in the runners, so that the inundation process is biased towards 2D floodplain inundation, as represented by MIKE 21. The flood inundation patterns from MIKE 21 compare better with those from remote sensing and the mapped 1946 flood event than with those from MIKE FLOOD (see Figure 30). The total inundation area of 65.9% estimated from MIKE 21 also compares well with the 68.8% inundation area from the remote sensing study, as against 51.9% simulated from MIKE FLOOD.

Figure 30. KPF flood inundation maps from remote sensing analysis, inundation mapping, and the MIKE FLOOD hydraulic model (continued)

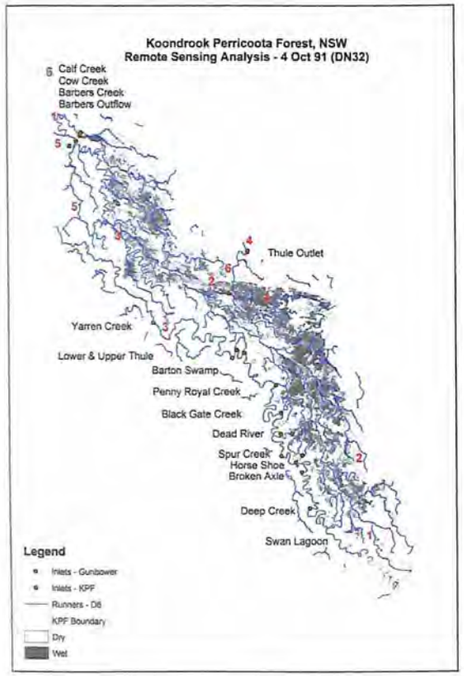

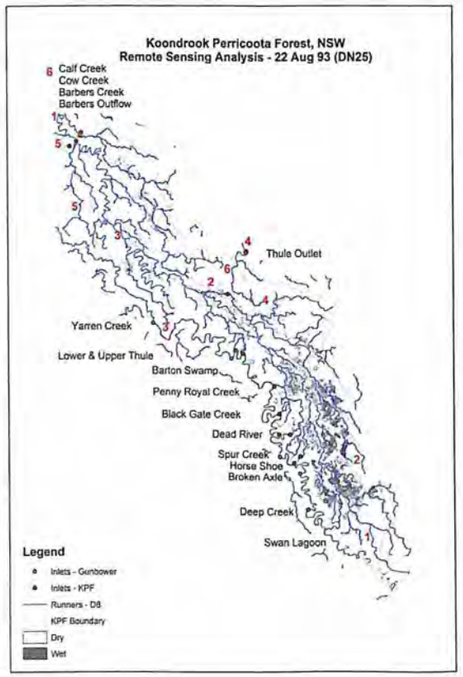

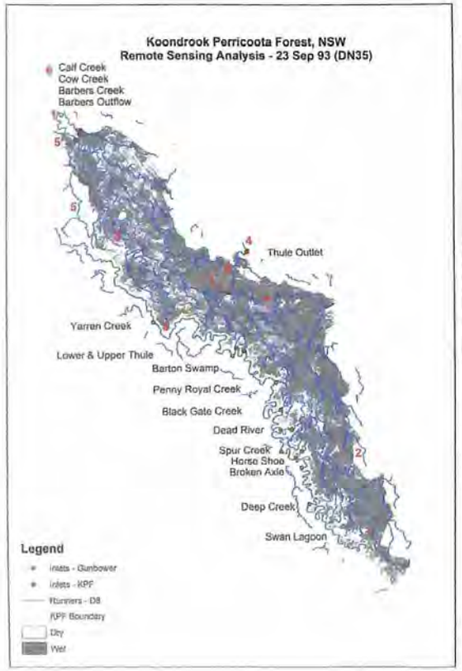

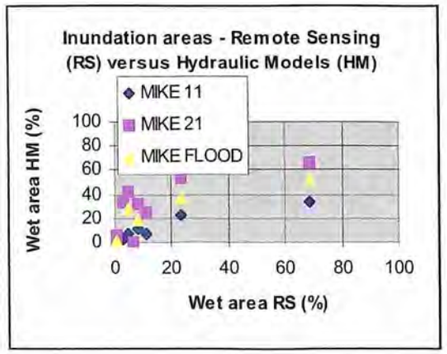

Figure 30. KPF flood inundation maps from remote sensing analysis, inundation mapping, and the MIKE FLOOD hydraulic model (continued)

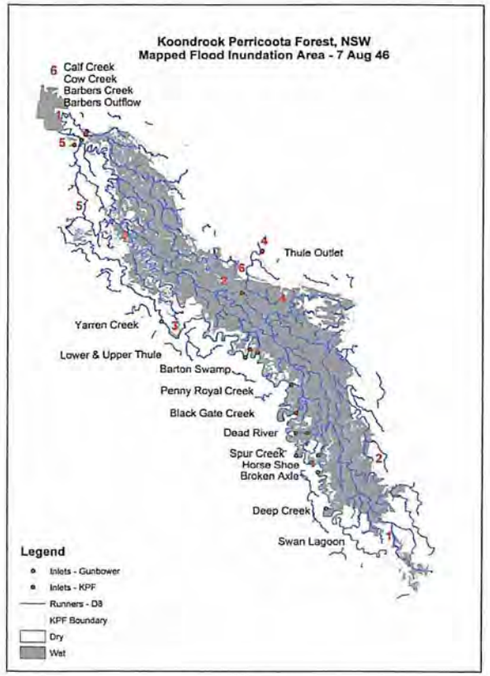

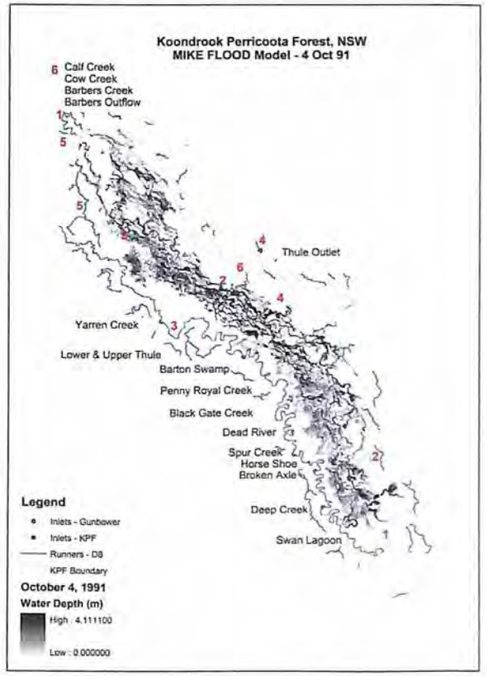

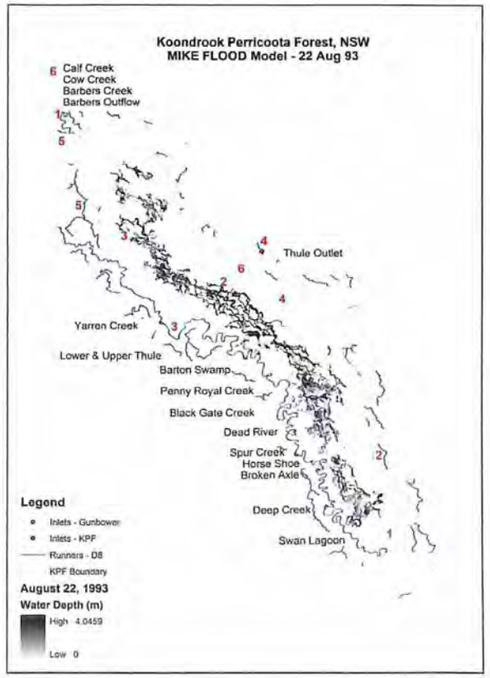

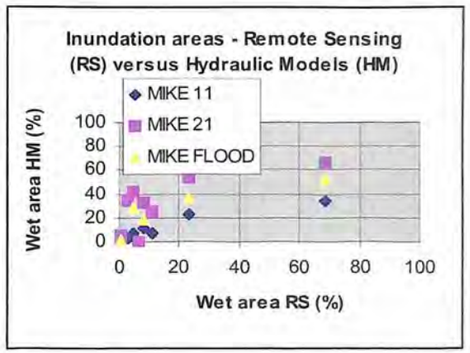

Figure 30. KPF flood inundation maps from remote sensing analysis, inundation mapping, and the MIKE FLOOD hydraulic model (continued)

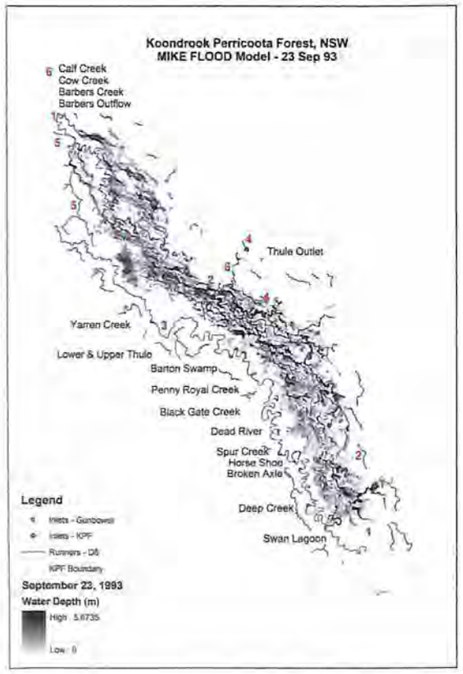

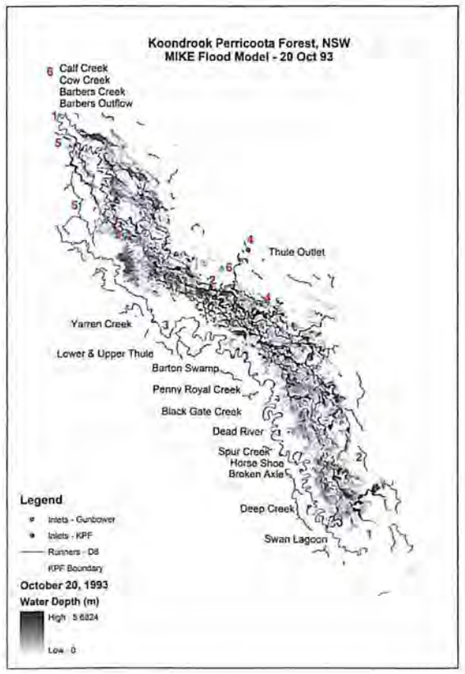

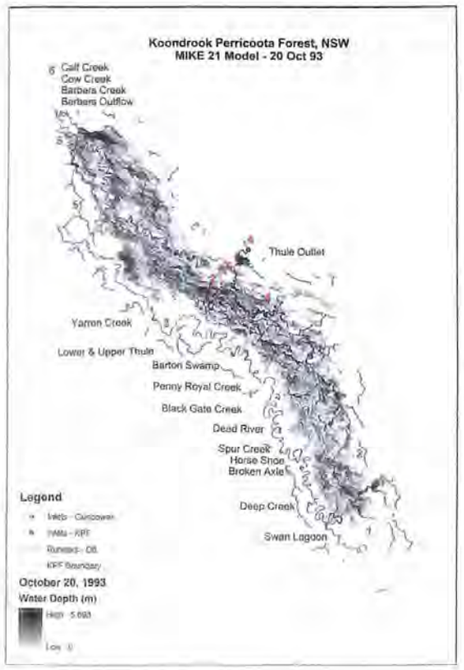

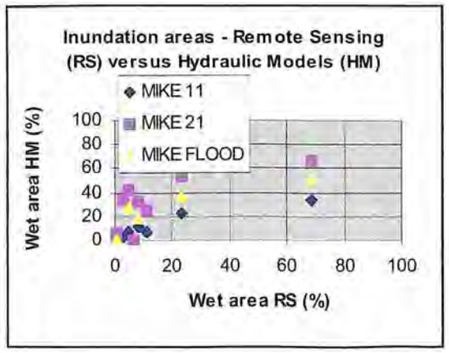

From the discussion above and Figures 29 and 30, it can be concluded that up to flows of about 28 000 ML/day, all three hydraulic models provide similar estimates of the inundation area in the range 0% to 10%. As the flow increases further, the results from the models tend to differ. Quasi-2D MIKE 11 substantially underestimates the inundation areas in comparison with the results from MIKE 21, MIKE FLOOD and the remote sensing analysis. MIKE 21, on the other hand, overestimates the inundation area by lack of representation of the conveyance of the runners when it is implemented at 40 m resolution (due to computational overheads). Up to a 45 000 ML/day flow and 45% inundation area, MIKE FLOOD provides the best estimates of the inundation area and patterns by suitably accounting for conveyance of the runners and the transition from a 1D runner-dominated flow process to the 2D floodplain process. Thereafter, high flows up to 70 000 ML/day can potentially involve constraints in the runners because of the presence of debris and the occurrence of possible flood flows from areas northeast of the KPF boundary; such flows are therefore better simulated by MIKE 21.

6.3 SCENARIO MODELLING, WATER BALANCE AND RETURN FLOW

The desired flooding regime in the KPF is at a frequency of 1 in 3 years and an areal extent of at least 30% of the forest. The design discharge capacity of the Torrumbarry Cutting was estimated to be between 5000 and 6000 ML/day on the basis of an analysis of the Murray flow data downstream of Torrumbarry Weir (see Section 4). MIKE FLOOD simulations were done for four scenarios with inflow boundary conditions of 2000, 3000, 5000 and 6000 ML/day for 45 days at the downstream end of the Torrumbarry Cutting (see Figure 3 for the alignment of the Torrumbarry Cutting). MHL modelling of the Torrumbarry Cutting using MIKE 11 indicated that a 500 ML/day flow will likely be available within the Bullock Head Creek outlet (upstream end of Runner 1), and the remaining portion of the diversion flow from the Murray will likely be available across the floodplain. Therefore, for each scenario, a specified flux inflow boundary condition of 500 ML/day was used at the upstream end of Runner 1 in MIKE FLOOD (see Figures 3 and 28). The remaining inflow (e.g. 5500 ML/day for the 6000 ML/day inflow scenario) was included in MIKE 21 as point sources distributed uniformly across a 1.6km width of the floodplain at the downstream end of the Torrumbarry Cutting. The hydrograph for each scenario was ramped up gradually over a week from zero to the maximum flow value. At the downstream end of the KPF (Runners 4 and 6), the same boundary conditions as in Stage 3 modelling were used. All other data and the parameters from Stage 3 modelling were also used in scenario modelling, and simulations were done for a 45 day period at 10 s time steps.

Flood inundation maps for the KPF from MIKE FLOOD simulations for each scenario are shown in Figure 31. The inundation areas in the KPF, simulated under steady-state conditions for flow diversions of 2000, 3000, 5000 and 6000 ML/day from the Torrumbarry Cutting for 45 days are 12%, 17%, 28% and 32%, respectively. The variation in the inundation area with time shows that a steady state is reached in about 3 weeks from commencement of the flow diversion from the Torrumbarry Cutting (Figure 31). Measured flow data in the Murray at Torrumbarry Weir and Barham shows that for flow in the Murray of about 40 000 ML/day, combined flow diverted naturally into the KPF and Gunbower is about 30% (see Figure 14). MIKE 11 modelling in the Murray shows approximately 50% partitioning of overbank flows into the KPF and Gunbower under historical conditions (i.e. 15% overbank discharge into each forest) (see Table 7). Therefore, a flow diversion of about 6000 ML/day from the Torrumbarry Cutting is equivalent to natural diversion from the Murray under historical conditions when flow in the Murray is about 40 000 ML/day. In the case of the 1991 historical event with a peak flow of about 43 000 ML/day, the maximum inundation area simulated using MIKE FLOOD is about 37.8% (see Figure 29).

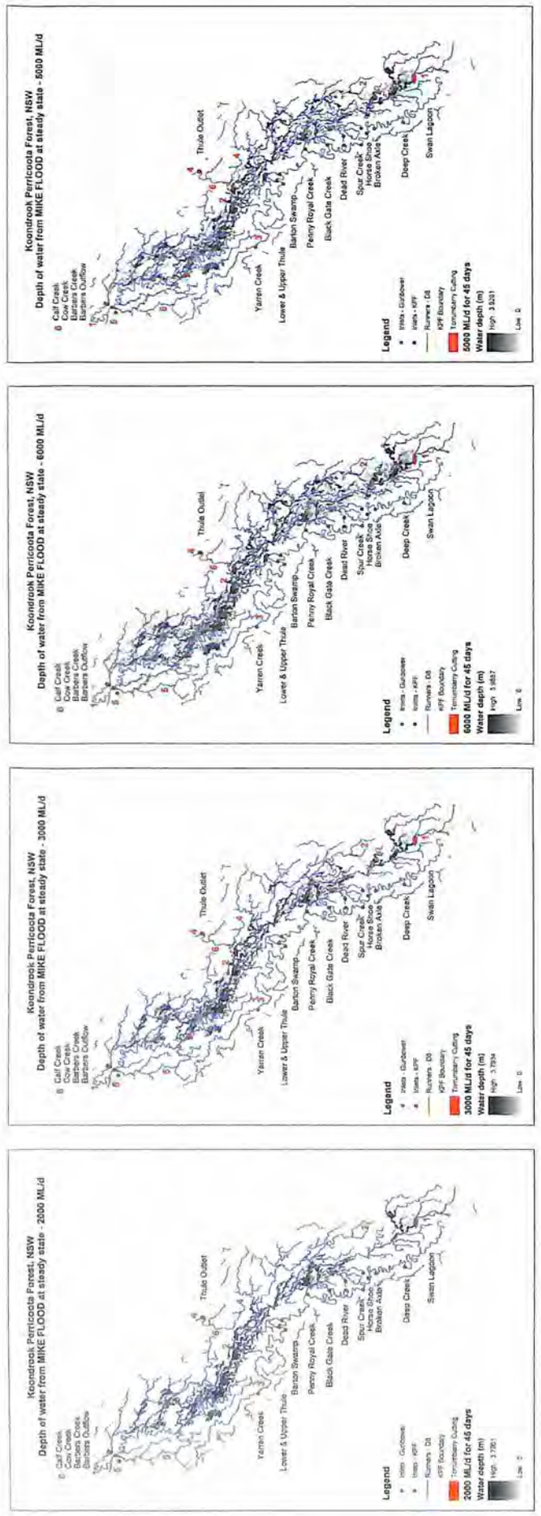

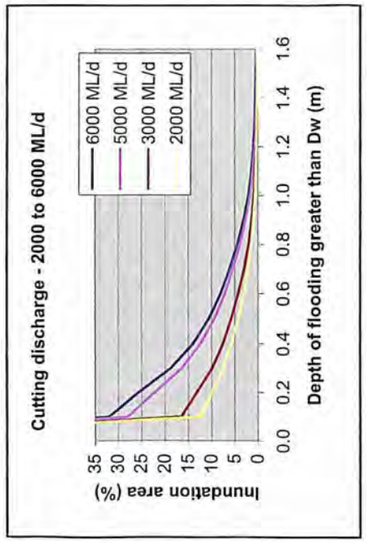

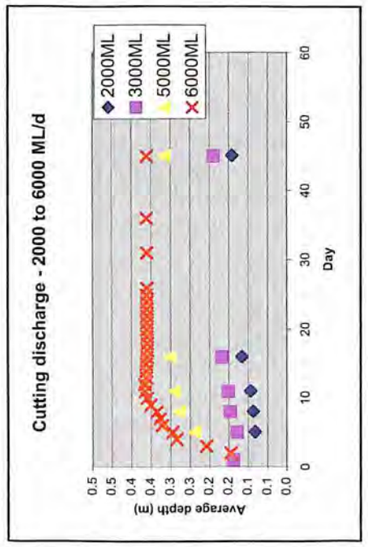

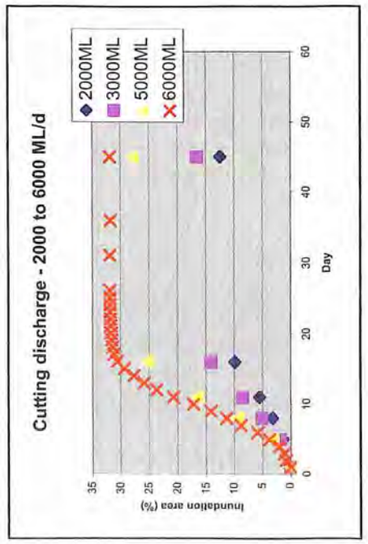

Figure 31. KPF flood inundation maps, inundation areas and depth variations from MIKE FLOOD simulations for a 2000- to 6000-ML/day discharge from the Torrumbarry Cutting over 45 days.

Figure 32. Water balance components from MIKE FLOOD simulations for a 2000- to 6000-ML/day discharge from the Torrumbarry Cutting over 45 days

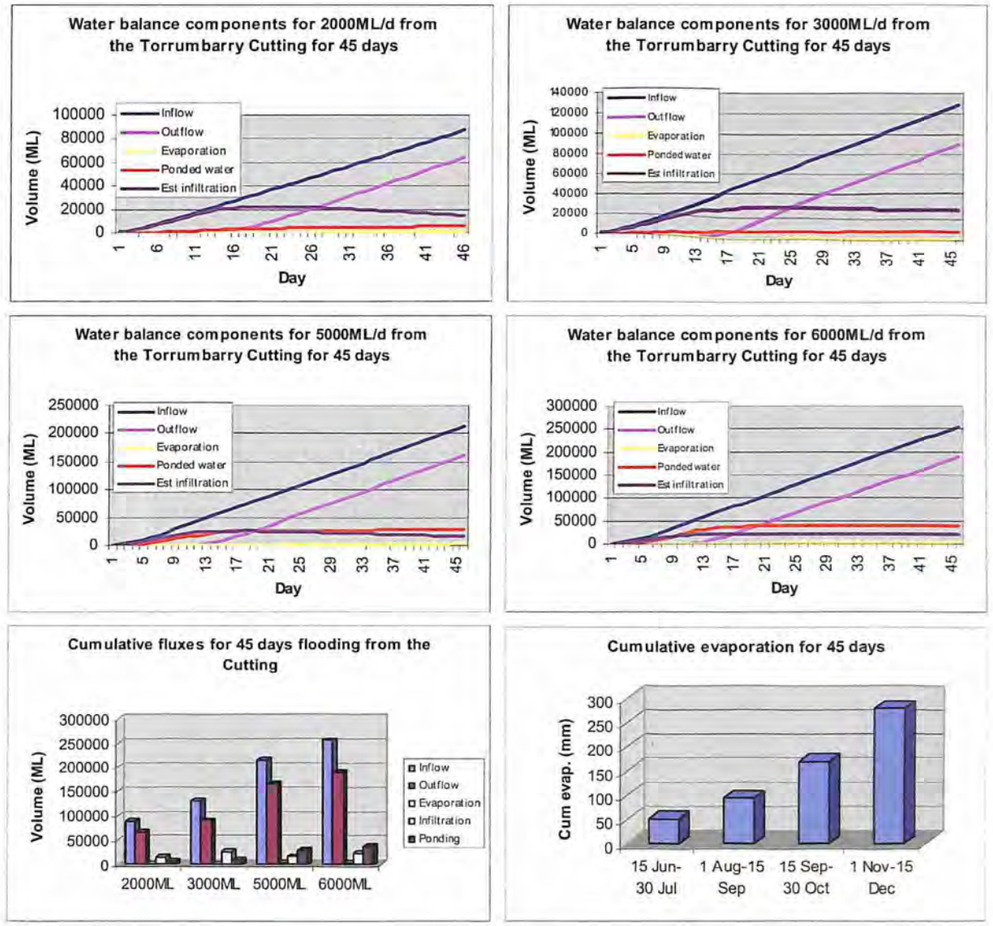

Therefore, an inundation area of 32% corresponding to a diversion flow of 6000 ML/day from the Torrumbarry Cutting is consistent with the results of the historical modelling (see Figure 29). The results indicate that a simulated inundation area of 28% corresponding to a 5000 ML/day diversion from the Cutting is close enough to the ecological target of 30% inundation of the KPF. Given the uncertainty around floodplain modelling and the possible impacts of debris constraining conveyance by the runners in the inundation area, it is possible that a 30% inundation target may be achievable with a diversion flow of 5000 ML/day via the Torrumbarry Cutting.

The depth of water from flooding for different scenarios of diversion flow via the Torrumbarry Cutting varies in the range 0 to 4m. Depth–inundation area curves for each scenario were prepared at 0.1 m depth intervals (Figure 31). The curves show the percentage inundation areas under water depths greater than or equal to D_w. As an example, for a 6000ML/day scenario 15% of the KPF area inundated from flooding will likely have a water depth greater

than or equal to 0.4m. The area weighted average depth of water across the KPF floodplain, and its variation with time, were obtained from the depth–inundation area curves (Figure 31). The area weighted depths of water equal to 0.141, 0.188, 0.315 and 0.36 m corresponded to 2000, 3000, 5000 and 6000 ML/day flow under steady state conditions.

Partitioned water balance components for the KPF are shown in Figure 32. The MIKE FLOOD model does not provide partitioned water balance components in the list of options for outputs. Therefore, these need to be obtained implicitly by using spatiotemporal fluxes such as inflow, outflow, potential evaporation, inundation depth and area. Inflow to the KPF is known from the imposed boundary condition. MIKE FLOOD model simulations provide outflow from the model domain for both of the component models, i.e. MIKE 21 as well as MIKE 11. Using the daily potential evaporation data in Figure 11 (pink line) and the simulated inundation area for each historical and future scenario in Figure 31, an evaporation volume can be obtained. To estimate the amount of ponded water, a depth versus inundation area curve was first prepared in ARC GIS at a depth interval of 10cm (Figure 31, bottom right). An area weighted average depth for each day was obtained for each scenario. Multiplying the area weighted depth by the respective inundation area gives a daily trace of the ponded volume. The cumulative infiltration volume can thus be estimated as inflow minus outflow minus evaporation minus ponded volume. Please note that the depth versus inundation area curve involves numerical approximation at 10cm intervals and that the standard deviation of the depth is high (see Figure 35). If this analysis were done at a very fine depth interval, then the ponded volume would increase a little more gradually (red line in Figure 32); consequently, the infiltration volume would keep increasing linearly until the steady state was reached, instead of tapering off. However, this transitional inconsistency does not affect the overall final estimate of return flow, because the volume of inflow minus outflow minus evaporation is fixed.

Cumulative fluxes for each scenario are shown in Figure 32. In the case of the 2000 ML/day and 3000 ML/day scenarios, the volume of ponded water is much smaller than the infiltration volume; therefore, the ecological objectives are unlikely to be met with these diversion flows. In the case of the 6000 ML/day diversion flow the volume of ponded water is greater than the infiltration volume. In the case of the 5000 ML/day diversion flow they are broadly similar in magnitude. Note that the 45-day simulation period used in the scenario modelling from 15 June to 30 July corresponds to low potential evaporative demand (see Figures 11 and 32). However, if environmental watering were done during a different period, then the inundation areas, as well as the water balance components, would be different. In general, an increase in potential evaporation will likely reduce the inundation area, depth of water and infiltration volume.

The volume of water infiltrating the soil surface would be further apportioned into three components: soil moisture storage, groundwater recharge and lateral through flow. Breakdown of the infiltration volume into these components is not possible without the use of an unsaturated zone eco-hydrological model. However, recharge to groundwater from the KPF floodplain is likely to be very small (Evans and Barnett 2007). Therefore, the bulk of the infiltration volume will likely be stored as soil moisture storage and water in excess of soil moisture storage would leave the KPF as lateral through flow and groundwater recharge. Soil moisture storage would in turn be available for evapotranspiration and help meet the ecological objectives.

Likely return flows from the KPF outflow boundaries under the historical and likely future conditions from all simulations are shown in Table 10. The results show that return flows from enhanced flooding in the KPF are likely to vary in the range 65% to 84%. MIKE FLOOD

simulations for diversion flows of 2000, 3000, 5000 and 6000 ML/day show return flows in the range 69% to 75%. Flood events for 1991 and 1993 extend over 76 days and 139 days, respectively, whereas the MIKE FLOOD simulations for scenario modelling extend over 45 days only. Therefore, the return flows from environmental flooding are likely to increase from about 70% for short-duration flooding over 40 to 50 days to about 84% for flooding durations of about 100 to 120 days.

Table 10. Predicted return flows from enhanced flooding in the KPF

	Quasi-2D MIKE 11	MIKE 21	MIKE FLOOD
Historical – 1991 event	66%	77%	84%
Historical – 1993 event	65%	83%	84%
Historical – 2000 event	66%	77%	
Future – 2000 ML/day			74%
Future – 3000 ML/day			69%
Future – 5000 ML/day			75%
Future – 6000 ML/day			73%

MIKE FLOOD implementation includes the effects of runner and floodplain dynamics and allows for flow exchange between the runners and the floodplain. The magnitude of flow exchange can be assessed from the plots showing variation of flow/incremental flow along the length of the runners for different scenarios (Figure 33). The runner reach lengths where flow increases indicates contribution from the floodplain to the runners; flow exchange is in the opposite direction when flow in the runner decreases. Variation of flow in Runners 1 and 6 indicates that there are reaches of significant length in Runners 1 and 6 that can carry up to 5000 ML/day, and it is this conveyance that results in the lower inundation area estimates from MIKE FLOOD as opposed to MIKE 21. The range of variation in flow in the runners is also shown in a schematic (Figure 34) for the 2000 ML/day and 6000 ML/day scenarios.

Average water depth and the standard deviation of water depth over each vegetation species are shown in Figure 35. The average water depths estimated for SQ1, SQ2, SQ3, Box, Red Gum/Box and open plains and swamps for 6000 ML/day are 0.214, 0.15, 0.06, 0.044, 0.118 and 0.2 m, respectively. The high standard deviation (up to 0.36 m) indicates the high variability in water depth across the KPF floodplain.

Figure 33. Variations of flow in Runner 1 under steady state conditions with a 6000 ML/day flow from the Torrumbarry Cutting

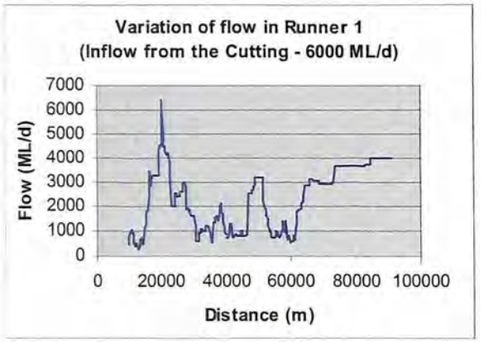

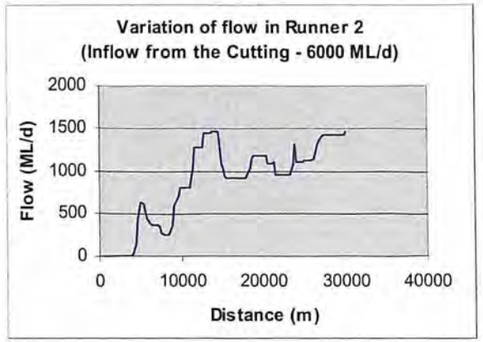

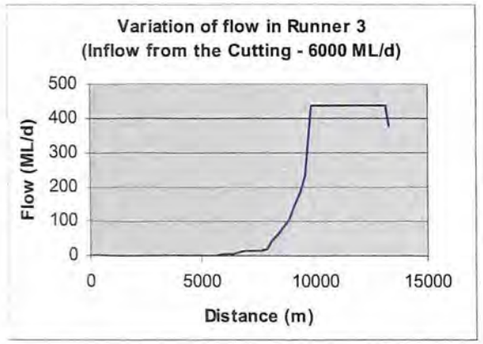

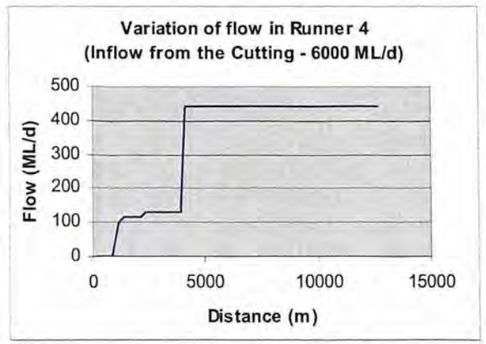

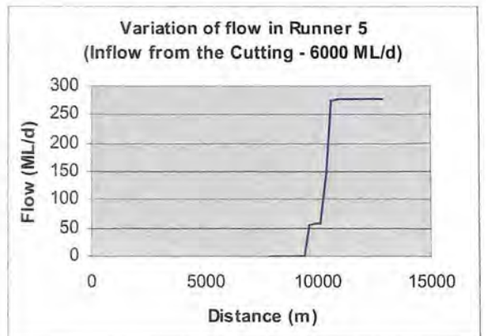

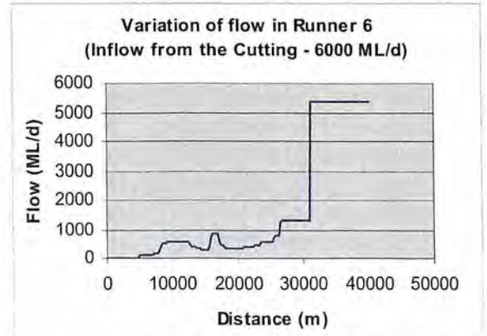

Figure 34. Variation of flow in the KPF runners under steady state conditions with 6000ML/day and 2000 ML/day flows from the Torrumbarry Cutting

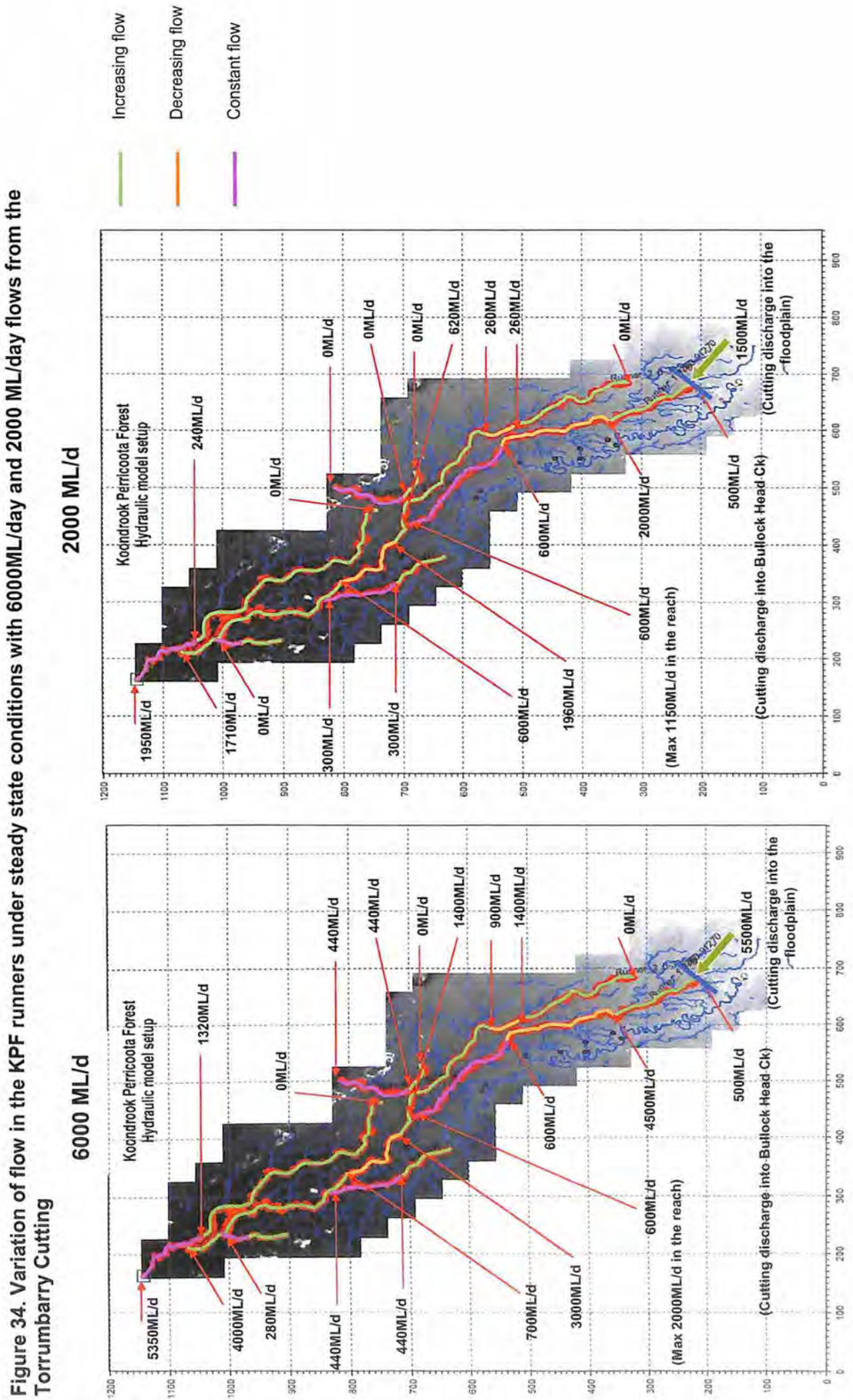

Figure 35. Average water depth and standard deviation of water depth across the vegetation species in the KPF

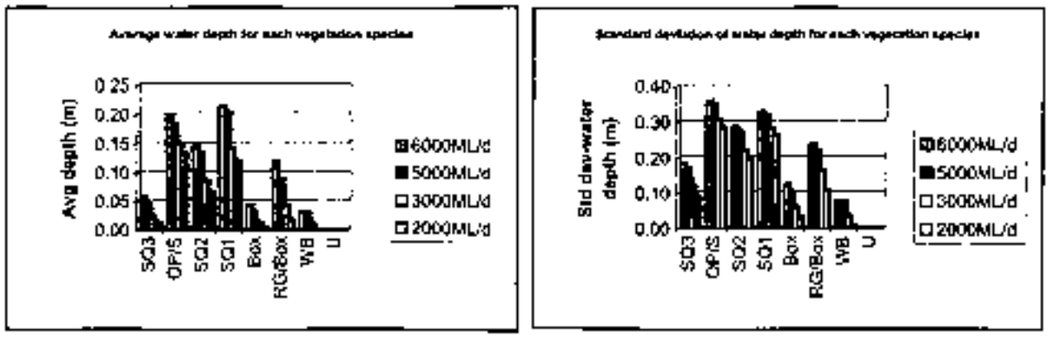

7 Flood inundation process and linkage of the hydraulic and hydrological models

7.1 HYSTERETIC FLOOD INUNDATION PROCESS

The MIKE FLOOD and MIKE 21 simulations of the historical events of 1991, 1993 and 2000 show a **hysteretic** floodplain inundation response (Figure 36). The historical flooding events in 1991 and 1993 consist of a single peak hydrograph, whereas the event in 2000 consists of multiple peaks (Figure 36a, b). In all cases, the inundation area versus flow relationship consists of two limbs that represent the wetting and drying phases of the KPF floodplain (Figure 36c, d). The wetting and drying limbs of the inundation response curves are consistent for all historical events.

The hysteretic inundation response can be conceptualised as in Figure 36e. The equilibrium inundation area at a given flow in the Murray is greater in the drying phase than in the wetting phase because of dynamic storage within the KPF. As flow in the Murray increases along the rising limb of the hydrograph, the inundation response follows the **primary wetting** curve (lower bound in Figure 36e). When the hydrograph recedes from a maximum flow value in the Murray (say 100 000 ML/day) that could potentially inundate the maximum floodplain area of the KPF, the inundation response curve follows the **primary drying** curve (upper bound in Figure 36e). The primary wetting and drying curves define the bounds of the KPF inundation response to flow conditions in the Murray, and all flooding in the KPF under a variety of hydrological conditions will be bound within these two extremes.

A number of **secondary wetting** and **secondary drying** curves are possible, depending on the magnitude and distribution of multiple peaks of the hydrograph (dotted lines in Figure 36e). As an example, consider the inundation response of the 2000 flooding event simulated by MIKE 21 and corresponding to the first peak with a maximum flow of 30 000 ML/day (M21–2000a, Figure 36c) and the second peak with a maximum flow value of 45 000 ML/day (M21–2000b, Figure 36c). As flow in the Murray increases to 30 000 ML/day (20 September), the simulated inundation area increases to 12% along the primary wetting curve. Flow in the Murray then drops to about 22 000 ML/day (29 September) but the inundation area increases to about 21%. The flow increases further to 28 000 ML/day (3 October) and then drops to 14 000 ML/day (23 October), and a corresponding reduction in inundation area from 29% to 23% occurs along the secondary drying curve. Thereafter, the curve of the inundation response to the second peak of the 2000 hydrograph follows a similar inundation response pattern along the primary wetting and drying curves as simulated for the 1991 and 1993 flood events (M21–2000b, Figure 36c).

The hysteretic inundation response of the KPF can be expressed in a simplified parametric form described by equation 6.

$$A = \begin{cases} A_r + \dfrac{A_s - A_r}{\left[1 + (\alpha(Q_s - Q))^n\right]^m} & Q < Q_s \\ A_s & Q \geq Q_s \end{cases} \qquad (6)$$

where, A = (inundation area/total area) (m^2/m^2), Q = flow (ML/day), Q_s = upper bound of the KPF inflow (ML/day), A_r = residual inundation area fraction (m^2/m^2), A_s = saturated inundation area fraction (m^2/m^2), α, n and m are the empirical parameters affecting the shape of the inundation response curve, and $m = 1 - 1/n$.

The form of the inundation response curve described by equation 6 is analogous to the van Genuchten (1980) equation, used extensively in soil physics to describe the relationship between soil moisture and matric suction. The parameters in equation 6 were optimised for the wetting and drying phases of the conceptualised KPF inundation response in Figure 36e. The fitted parameters are shown in Table 11 and the fitted models are shown in Figure 36f. The fitted models compare very well with the conceptualised inundation response curves, and R^2 values of 0.993 and 0.988 were obtained for the wetting and drying phases, respectively. The inundation response model in parametric form provides a simple and practical tool for assessment of the inundation area in the KPF under any hydrological flooding regime.

Figure 36(a–b). Observed and simulated flow in the Murray under 1991 and 2000 historical conditions. (c) Flow downstream of Torrumbarry Weir versus inundation area (RS: Remote sensing; MIKE 11B: Results with Manning's n = 0.042 and leakage factor = 7×10^{-7} s^{-1}; M21: MIKE 21 results under 1991, 1993 and 2000 conditions). (d) Flow downstream of Torrumbarry Weir versus inundation area (RS: Remote sensing; MIKE 11B: Results with Manning's n = 0.042 and leakage factor = 7×10^{-7} s^{-1}; M21: MIKE FLOOD results under 1991, 1993 and 2000 conditions). (e–f) Conceptualised and fitted hysteretic responses of the KPF to environmental flooding.

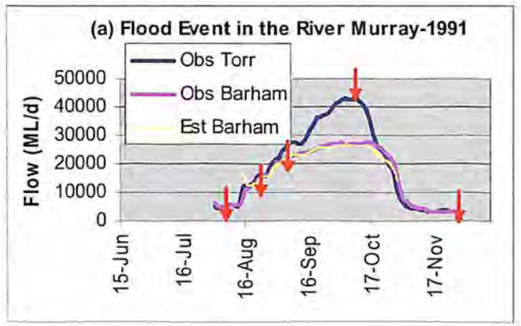

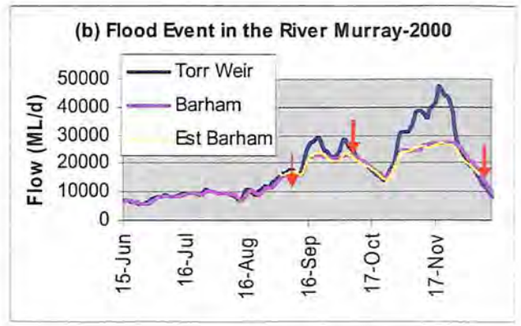

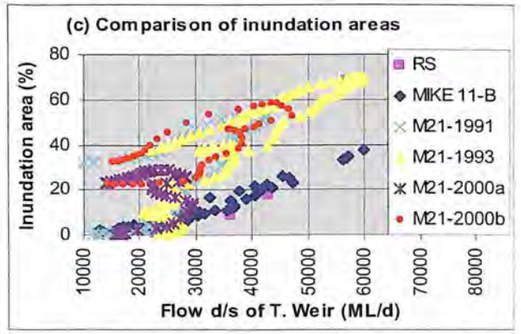

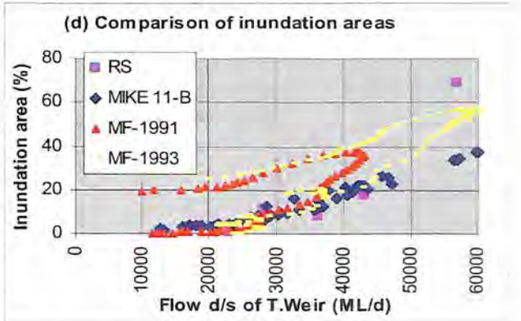

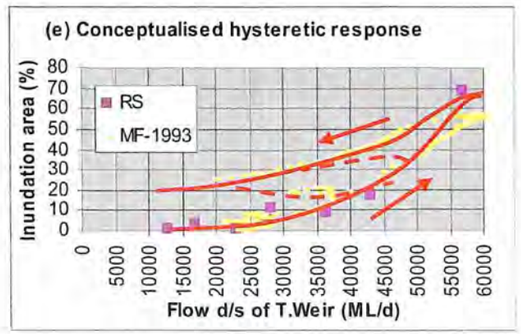

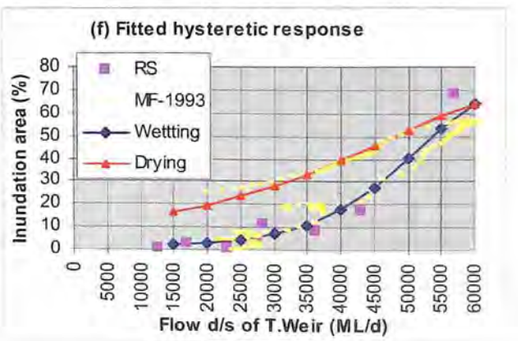

Table 11. Parameters of the KPF inundation response curve

	Wetting phase	Drying phase
A_r (m^2/m^2)	0	0
A_s (m^2/m^2)	0.7367	0.74168
α (day/ML)	0.00002	0.0000175
n (–)	7.78819	4.49187
Q_s (ML/day)	100000	100000
R^2	0.993	0.988

7.2 LINKING OF THE KPF HYDRAULIC MODEL WITH THE HYDROLOGICAL MODEL OF THE RIVER MURRAY

Hydrological models require *a priori* information on inflow, outflow and storage characteristics of the hydrological system so that the empirical model parameters can be calibrated. However, in the case of KPF this information is not available; therefore, the KPF hydraulic models need to provide this information to the MDBC hydrological model.

Lumped hydrological routing models disregard heterogeneity within the model domain and use the following two fundamental equations:

Mass balance: $$Q_{\inf low} - Q_{outflow} = \frac{dS}{dt} \quad (7)$$

Storage–outflow relationship: $$S - S_0 = KQ_{outflow}^{\beta} \quad (8)$$

where, $Q_{\inf low}$ = inflow (ML/day), $Q_{outflow}$ = outflow (ML/day), S = storage in the hydrological system (ML), S_0 = residual storage threshold required before outflow from the hydrological system commences (ML), K = time constant of the storage in the hydrological system or the scale parameter (day^{-1}) , and β = parameter describing the non-linearity of the hydrological system (–).

Losses in the mass balance equation of the hydrological model can be included either explicitly or through the use of constant or seasonally varying gain factors. In general, hydrological systems are large and the storage within the system is larger than the inflow to and outflow from the hydrological system. Therefore, the hydrological response is highly damped and the hydrological system can be approximated as linear, i.e. the parameter β equals unity. Substituting equation (8) into (7), Nash (1960) showed that, under the constraints of conservation, stability, high damping and the absence of feedback, the two parameter case described by equation (9) with η as integer and positive K is as general a case as the differential equation of the input–output system of unlimited order. Providing additional flexibility by allowing n to take fractional values, the impulse–response function has the ability to represent adequately almost all the impulse–response shapes commonly

encountered in the hydrological context. Although other parametric and non-parametric forms exist, the Gamma function routing model form is widely used for hydrological routing.

$$h(\tau) = \frac{1}{K\,\Gamma(\eta)} \exp\left(\frac{-\tau}{K}\right)\left(\frac{\tau}{K}\right)^{\eta-1} \quad (9)$$

where, $\Gamma(\eta) = \int_0^{\infty} \exp(-\tau)\,\tau^{\eta-1} d\tau$ is the incomplete gamma function (dimensionless).

Figure 37. (a) Storage versus outflow data for the KPF; (b) Relationship between threshold storage in the KPF and diversion flow from the Cutting before outflow commences from the KPF; (c) Storage versus outflow relationship, and table showing threshold storage S_0 and time constant K for different scenarios of diversion flow from the Torrumbarry Cutting

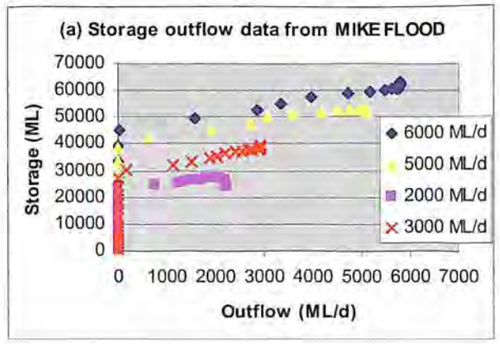

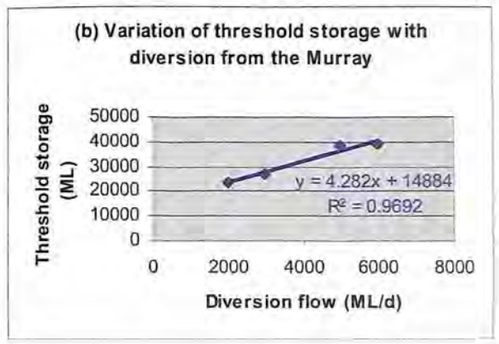

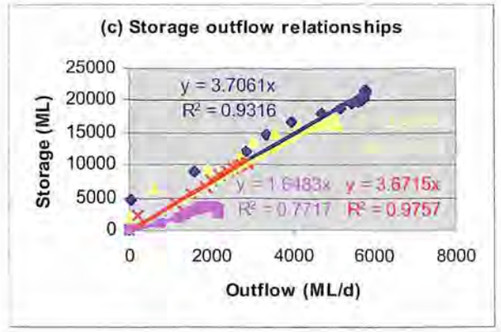

Diversion flow	S0 (ML)	K (d-1)	R2
2000 ML/d	23448	1.6483	0.77
3000 ML/d	27730	3.6715	0.98
5000 ML/d	36294	3.4855	0.79
6000 ML/d	40576	3.7061	0.93

If inflow to and outflow from the hydrological system are known, then the model described by equation (9) or its alternative model forms can be easily calibrated for the parameters K and η. In the case of KPF, inflow to and outflow from the KPF are unknown, and therefore information from hydraulic models needs to be used in the hydrological model. The flow duration curves at Torrumbarry Weir and Barham provide the information on total diversion flow from the Murray to the Gunbower and KPF (see Figure 14). The results from Table 7 provide information on partitioning between the KPF and Gunbower for historical conditions. The time series for these historical events from the MIKE 11 model of the Murray can be used to develop empirical relationships for the inflow into each forest. Return flows and partitioning of the water balance components for the historical and likely future conditions can be used as calibration datasets for incorporating the effects of enhanced flooding of the KPF into the MDBC's hydrological model for the Murray.

The storage–outflow relationship described by equation 8 was developed for the KPF by using the water balance components for each diversion flow scenario from the Torrumbarry Cutting (Figure 37a). The storage–outflow data in Figure 37a show that for each case of diversion flow from the Torrumbarry Cutting (2000 to 6000 ML/day), a threshold storage S_0 must be reached before outflow from the KPF commences. The plot also shows that once outflow commences the storage–outflow relationship is linear. Therefore, the following information is required for incorporating KPF results into the hydrological model: a relationship between threshold storage S_0 versus diversion flow from the Torrumbarry Cutting, and the time constant or slope K of the storage–outflow data.

The threshold residual storage S_0 for the KPF corresponding to a given diversion flow from the Torrumbarry Cutting can be estimated from the linear regression equation with a slope of 4.282 and an intercept of 14 884 (Figure 37b). Using the residual threshold estimate S_0 from the equation in Figure 37b, regression equations for the diversion flow scenarios of 2000, 3000, 5000 and 6000 ML/day flow were developed (Figure 37c). The time constant K in the range 3.48 to 3.7 day^{-1}, is recommended for the KPF storage–outflow relationship. The R^2 values for the regression equations vary between 0.77 and 0.98 (see the table in Figure 37 for details of the regression equations); therefore, the linear models developed can be confidently used in the hydrological model of the Murray. Finally, information on the evaporation losses can be obtained by using parametric forms of the inundation response model described by equation (6) and the appropriate inundation response model parameters corresponding to the wetting and drying phases of the KPF (Table 11).

8 Conclusions

Koondrook–Perricoota Forest is in the NSW part of the Ramsar listed Gunbower–Perricoota Forest and covers about 33 750 ha along the Murray River. The natural frequency of flooding for 3 to 5 months at a time in the KPF has decreased from once every 4 years to once every 10 to 12 years owing to regulation of the River Murray and increasing demand for water supply. Within the TLM and the TLM EWMP, it is proposed to construct a channel, called the Torrumbarry Cutting, in the KPF to allow water from Torrumbarry Weir to take its natural course through the forest, eventually returning the water to the Murray and its tributary Wakool.

This report describes the development and implementation of the MIKE suite of hydraulic models for the KPF. As far as the authors are aware, this is one of the most comprehensive and biggest hydraulic modelling studies in Australia to date. It is also the first study in Australia to propose a hysteretic inundation response of the Murray floodplain to variations in flow in the Murray during flooding events. A range of historical and likely future conditions for flow diversion from the Torrumbarry Cutting were assessed to explore whether the ecological target of 30% inundation of the KPF can be achieved. Additional issues discussed in the report include the design capacity of the Torrumbarry Cutting; partitioning of flow from the Murray into the adjoining KPF and Gunbower Forest; spatial inundation patterns and depth; partitioning of the water balance; and likely return flows from enhanced flooding of the KPF. An inundation response model has been developed and the relationships for coupling the results of the KPF hydraulic model into the MDBC hydrological model have been derived.

The hydraulic model for the KPF was developed by using the DEM at 1 m grid cell resolution obtained from the LiDAR survey conducted as part of the Hume–Euston Project (MDBC 2005). The average elevations along the width of the forest towards the eastern and western boundaries are 84.7 m and 76.56 m, respectively, and the overall relief is about 8.14 m (see Figure 3). The general flow direction in the KPF is north-west, and the slope of the KPF varies from 1 in 4613 towards the eastern boundary to 1 in 7310 towards the western boundary.

The vegetation species map delineates the main species in the KPF as Box, Box/Red Gum, Red Gum SQ1 (high productivity), Red Gum SQ2 (low productivity), Red Gum SQ3 (low productivity), Open Plains or Swamp (Figure 6). In general, the vegetation species map indicates the degree of wetness in the KPF, with more frequent wetting of the areas under SQ1 (downstream end) and least wetting under Box vegetation (upstream end).

Extensive soils investigations, including soil survey and surface infiltration experiments, were done in the KPF to support the hydraulic modelling work. Typically, the majority of the soils have a medium to heavy clay layer within the top 30cm of the profile. KPF soils were classified into six major soil hydrological groupings that reflect the relative infiltration rates of the most representative impermeable near-surface horizon (see Figure 7). Spatially distributed surface infiltration rates under positive hydraulic head were used in the hydraulic modelling (see Table 2). An area weighted infiltration rate of 25 mm/day was estimated across the entire KPF floodplain, which includes areas that may or may not be inundated. Infiltration rate varies in the range 5 to 20 mm/day across the bulk of the areas likely to be inundated under enhanced flooding conditions.

Floodplain inundation mapping was developed from a hard copy of the inundation maps and the prevailing vegetation patterns prepared from the aerial survey on 7 August 1946 by the

RAAF. Additional data used for producing the final inundation map included aerial photos from two sources at 1:50 000 and 1:15 000 scales, as well as from LiDAR data and SPOT imagery. This flood event corresponds to 55 000 ML/day flow in the Murray and forms a useful dataset. A total mapped inundation area equal to 73% of the KPF was estimated for the 1946 flood event (see Figure 30).

Remote sensing analysis of the KPF floodplain inundation was conducted using 12 images from the Landsat satellite for the flood events in 1991, 1993 and 2000 by the methodology of Shaikh et al. (2001, 1998). Density slicing, an image enhancement technique, was used to delineate spatial patterns of the inundation areas in the KPF. A DN threshold was used to produce a new image in which the pixels have a binary representation of wet and dry areas. A sensitivity analysis of the DN threshold was also conducted on three images to evaluate the impact of assumptions in the method on the overall inundation patterns in the KPF. The results of the inundation area estimates from the remote sensing analysis were found to compare well with the inundation information produced by Forests NSW from a reconnaissance survey during historical flood conditions in the KPF: i.e. 30-day minimum flow in the Murray versus percentage inundation area (see Figure 19, Table 6).

Water availability analysis was done to explore the opportunity for diverting a range of discharges into the Torrumbarry Cutting. A carrying capacity of the Torrumbarry Cutting in the range 4000 to 7000 ML/day could potentially achieve the desired ecological outcomes. On the basis of hydraulic efficiency, a design discharge capacity of 5000 to 6000 ML/day would appear reasonable for the Torrumbarry Cutting. The effectiveness of different diversion flow scenarios from the Torrumbarry Cutting (2000, 3000, 5000 and 6000 ML/day) to achieve the ecological objectives was assessed later from hydraulic modelling.

Natural flow diversion from the Murray into the KPF and Gunbower Forest commences at about 17 000 ML/day, and flow diversions increase substantially with an increase in flow in the Murray from 20 000 to 65 000 ML/day. When the observed flow downstream of Torrumbarry Weir is 20 000, 30 000, 40 000, 50 000 and 65 000 ML/day, the proportion of combined flow naturally diverted to the Gunbower and Koondrook–Perricoota Forests is 0%, 14%, 30%, 41% and 46%, respectively. A MIKE 11 model was set up for the Murray between Torrumbarry Weir and Barham to partition flows between the two forests on either side of the Murray. Very good model calibrations were achieved for the historical flood events of 1991, 1993, 2000 and 2003 (see Figure 23). For a given flood event, flow diversions between the KPF and Gunbower are broadly comparable. Simulated combined inflow from all inlets of the KPF for each of the flood events in 1991, 1993 and 2000 are much more than the volume of water in the range 4000 to 6000 ML/day planned for diversion into the KPF from the Torrumbarry Cutting (see Figure 24). Inflow hydrographs for each inlet, obtained from MIKE 11 modelling of the Murray, were used for hydraulic modelling of the KPF floodplain.

The KPF floodplain modelling was performed in three stages, moving progressively from simple to more complex forms. Knowledge of the KPF flood inundation processes was improved in each stage to better formulate more complex model forms. The primary reason for the choice of a staged approach was to account for the scale of the hydraulic modelling problem. The problem size is huge and involves significant numerical overheads. On the basis of prototype benchmarking, it was estimated that the simulation times for implementation of the MIKE FLOOD model would be very long (>30 days). It was considered mandatory to commence simulations with simple model forms using MIKE 11 (Stage 1: quasi-2D) and then conduct targeted simulations using MIKE 21 (Stage 2: 2D) and MIKE FLOOD (Stage 3: combined 1D flow in the runners and 2D flow in the floodplain).

An inundation response relationship comprising flow in the Murray versus percentage inundation area was developed, and the results from MIKE 11 were compared with those from the remote sensing study. The results showed a good match with those from the remote sensing study up to about 35 000 ML/day. Thereafter, the results drifted apart, and lower estimates of the inundation area were obtained from the model relative to those from the remote sensing study.

The MIKE 21 model set up for the KPF involves marked numerical overheads and the following considerations: spatial and temporal resolution of the model, memory requirements and processor speed, and the Courant criterion. On the basis of these considerations, MIKE 21 simulations were performed at 40 m grid cell resolution and 10 s time steps. Although the 40 m grid scale is considerably coarser than that of the available DEM data, it still pushes the model computations to limits while keeping simulation times within a practical range (5 to 15 days).

The results of the MIKE 21 simulations closely matched those of the remote sensing analysis and quasi-2D MIKE 11 up to about 28 000 ML/day (see Figure 27). Thereafter, MIKE 21 gave significantly higher inundation areas than those from quasi-2D MIKE 11. The remote sensing study estimated an inundation area of about 69% on 23 September 1993, corresponding to a 56 970 ML/day flow in the Murray. Also, an inundation area of about 73% was mapped for the 1946 flood, corresponding to flow in the Murray of about 55 000 ML/day. The inundation area estimated for the 1993 event from the remote sensing analysis matches very well with the simulated inundation areas from MIKE 21 and compares well with the mapped inundation area for the 1946 flood event.

The MIKE FLOOD model was developed to address the issues relating to under representation of the runner conveyance in MIKE 21 and to analyse the threshold at which the inundation dynamics shift from runner dominated behaviour to floodplain behaviour. The MIKE 21 model used in MIKE FLOOD was the same as that developed at 40 m resolution in Stage 2. A comprehensive MIKE 11 model was developed in Stage 3 at a fine resolution to capture inundation dynamics and flow exchange between the runners and the floodplain. Simulation times with MIKE FLOOD were up to 50 days on an Intel® Dual Core™ PC with 2.13-GHz processor speed and 3.25-GB RAM.

The inundation area versus flow relationship simulated by MIKE FLOOD showed substantial reductions in the inundation area estimates compared with those from MIKE 21 (see Figure 29). The MIKE FLOOD simulations for the 1991 and 1993 events showed a reduction of about 17% and 12.3%, respectively, in the respective maximum inundation areas of 54.8% and 69.3% simulated by MIKE 21. Additionally, the MIKE 21 simulations showed significant differences in the flow versus inundation area relationship at around a 28 000 ML/day threshold, indicating a shift from a runner dominated 1D process to a 2D floodplain inundation process. In contrast, the MIKE FLOOD simulations showed that the shift from a 1D to a 2D inundation process begins around a threshold of about 28 000 ML/day and increased gradually up to 36 000 ML/day, after which the process was largely 2D. Since the responses of all natural systems are generally highly damped because of large differences in storage relative to inflow and outflow, the gradual transition in the inundation area simulated by MIKE FLOOD appears more realistic.

Comparison of the spatial inundation patterns from remote sensing and MIKE FLOOD showed good agreement. However, during high flows (in excess of 50 000 ML/day), the inundation areas predicted by remote sensing east of the Thule outlet towards the northern boundary did not compare well with those from MIKE FLOOD. Two possible reasons for the

differences in inundation patterns towards the northern boundary east of the Thule outflow were identified. Firstly, some inflow into the KPF is sourced from the northeast, and this is not included in the MIKE FLOOD model wherein all water is sourced from the KPF inlets adjoining the Murray. A close look at the results from remote sensing for areas north and northeast of the KPF confirmed this possibility. Secondly, the large amounts of debris from dead trees during high flow events constrain flow in the runners; therefore, the inundation process is biased towards 2D floodplain inundation, as represented in MIKE 21.

On the basis of the results from the MIKE 11, MIKE 21 and MIKE FLOOD models, it was concluded that up to flows of about 28 000 ML/day, all three hydraulic models provide similar estimates of the inundation area in the range 0% to 10%. As flow increases further, the results from the models tend to differ. Quasi-2D MIKE 11 substantially underestimates the inundation areas in comparison with MIKE 21, MIKE FLOOD and the remote sensing analysis. MIKE 21, on the other hand, overestimates the inundation area owing to lack of representation of the conveyance of the runners when the model is implemented at 40 m resolution (because of computational overheads this was the grid cell resolution adopted). Up to 45 000 ML/day flow and 45% inundation area, MIKE FLOOD provides better estimates of the inundation area and patterns by suitably accounting for conveyance of the runners and transition from a 1D runner dominated flow process to a 2D floodplain process. Thereafter, high flows up to 70 000 ML/day can potentially involve constraints in the runners because of the effect of debris and possible flood flows from areas northeast of the KPF boundary; these high flows are better simulated by MIKE 21.

MIKE FLOOD simulations were done for four scenarios with inflow boundary conditions of 2000, 3000, 5000 and 6000 ML/day for 45 days at the downstream end of the Torrumbarry Cutting. The inundation areas in the KPF, simulated under steady state conditions for flow diversions of 2000, 3000, 5000 and 6000 ML/day from the Torrumbarry Cutting for 45 days, were 12%, 17%, 28% and 32%, respectively. The variation in the inundation area with time shows that the steady state is reached in about 3 weeks after the commencement of flow diversion via the Torrumbarry Cutting (Figure 31). It was shown that the 1991 historical event, with a peak flow of 43 000 ML/day, is close to the diversion flow of 6000 ML/day from the Torrumbarry Cutting. The simulated inundation area of 37.8% for the 1991 event from MIKE FLOOD compares well with the 32% inundation area estimated for the 6000 ML/day diversion flow from the Torrumbarry Cutting.

Area weighted water depths equal to 0.141, 0.188, 0.315 and 0.36 m were obtained, corresponding respectively to 2000, 3000, 5000 and 6000 ML/day flows under steady state conditions. Variation in the water balance components with time was obtained for each scenario, and the volume of water in ponding, evaporation loss, surface infiltration and return flow was estimated (see Figure 32). In the case of the 2000 ML/day and 3000 ML/day scenarios, the volume of water in ponding was much smaller than the infiltration volume; therefore, the ecological objectives are unlikely to be met with these diversion flows. In the case of 6000 ML/day diversion flow, the volume of ponded water was greater than the infiltration volume. The two were broadly similar in magnitude in the case of 5000 ML/day diversion flow. The 45-day simulation period used in the scenario modelling from 15 June to 30 July corresponds to low potential evaporative demand (see Figures 11 and 32). However, if environmental watering were done during a different period, then the inundation areas as well as the water balance components would be different. In general, an increase in potential evaporation would be likely to reduce the inundation area, depth of water and infiltration volume.

The results showed that return flows from enhanced flooding in the KPF are likely to vary in the range 65% to 84% (see Table 10). MIKE FLOOD simulations for diversion flows of 2000, 3000, 5000 and 6000 ML/day showed return flows in the range 69% to 75%. The flood events in 1991 and 1993 extended over 76 days and 139 days, respectively, whereas the MIKE FLOOD simulations for scenario modelling extended over 45 days only. Therefore, return flows from environmental flooding are likely to increase from about 70% for short duration flooding over 40 to 50 days to about 84% for flooding durations of about 100 to 120 days.

The average water depth estimated for SQ1, SQ2, SQ3, Box, Red Gum/Box, and open plains and swamps at 6000 ML/day were 0.214, 0.15, 0.06, 0.044, 0.118 and 0.2 m, respectively (see Figure 35). The high standard deviation (up to 0.36m) indicated high variability in water depth across the KPF floodplain.

Finally, the results from complex hydraulic modelling of the KPF were synthesised into simple and practical tools for use by environmental water managers and to help implement basin scale hydrological models (e.g. the MDBC model for the Murray), thus incorporating the effects of environmental flow diversions within the TLM Initiative. A storage-outflow relationship was developed for the KPF for use in the hydrological model (see equation 8 and Figure 37). The results show that, for the purposes of lumped hydrological modelling, the KPF storage can be approximated as a linear reservoir with a time constant K of about 3.5 to 3.7 day^{-1} and a threshold storage dependent on flow in the Murray, as defined by a calibrated linear form (see Figure 37b).

A hysteretic inundation response model comprising flow in the Murray versus percentage inundation area was proposed for the KPF, and the accuracy of the calibrated parametric form of the response model was about 99% (see Figure 36 and equation 6). The proposed inundation response model consists of primary wetting and drying curves that define the lower and upper bounds of the wetland inundation; all possible wetland inundation processes dependent on hydrological conditions in the Murray can be defined by the secondary wetting and drying curves. We believe that the parametric form is robust and applicable to any wetland (especially the Murray wetlands). If developed further and extended to other areas, this model can greatly help water managers to assess the ecological benefits from the environmental watering of wetlands.

9 References

Abbott, M.B. 1979. Computational Hydraulics – Elements of the Theory of Free Surface Flows. Pitman, London.

Abbott M.B., McCowan A. and Warren I.R. 1981. Numerical Modelling of Free-Surface Flows that are two-dimensional in Plan. In H.B. Fischer (Editor), Proceedings of a Symposium on Predictive Ability of Transport Models for Inland and Coastal Waters. New York, Academic Press.

Abbott M.B., Damsgaard A. and Rodenhuis G.S. 1973. A Design System for Two-Dimensional Nearly-Horizontal Flows. J. Hydr. Res. 1, 1973.

Abbott M.B., Bathurst J.C., Cunge J.A, O'Connell P.E. and Rasmussen J. 1986. An introduction to the European hydrological system – Système Hydrologique Européen SHE, 1. History and philosophy of a physically-based distributed modelling system. J. Hydrol. 87, 45–59.

Anderson M.G. and Bates P.D. 2001. Model Validation: Perspectives in Hydrological Science. J. Wiley, Chichester, New York. ISBN 0471985724.

Band L.E. 1986. Topographic partition of watersheds with digital elevation models. Water Resour. Res. 22(1), 15–24.

Bates, P.D., and Anderson, M.G. (1993). A two-dimensional finite element model for river flood inundation. Proc. R. Soc. Lond., Ser. A, 440, 481–491.

Bates, P.D. and Anderson M.G. (1996). A preliminary investigation of the impact of initial conditions on flood inundation conditions using a time/space distributed sensitivity analysis. Catena, 26, 115–134.

Bates P.D. and De Roo A.P.J. 2000. A simple raster-based model for floodplain inundation. J. Hydrol. 236, 54–77.

Bates, P.D., Anderson, M.G., Baird, L., Walling, D.E. and Simm, D. 1992. Modelling floodplain flows using two-dimensional finite element model. Earth Surf. Process. Landf., 17, 575–588.

Bates P.D., Anderson M.G., Price D., Hardy R. and Smith, C. 1996. Analysis and development of hydraulic models for floodplain flows. In Anderson M.G., Walling D.E. and Bates P.D. (Eds) Floodplain Processes. John Wiley and Sons, Chichester, pp. 215–254.

Bates P.D., Horritt M.S., Smith C.N. and Mason, D. (1997). Integrating remote sensing observations of flood hydrology and hydraulic modelling. Hydrol. Process. 11, 1777–1795.

Bates P.D., Stewart M.D., Desitter A., Anderson M.G., Renaud J.-P. and Smith J.A. 2000. Numerical simulation of floodplain hydrology. Water Resour. Res. doi: 10.1029/2000WR900102.

Bates P.D., Matthew D.W., Horritt M.S., Mason D., Holden N. and Currie A. (2006). Reach scale floodplain inundation dynamics observed using airborne synthetic aperture radar imagery: data analysis and modelling. J. Hydrol. 328, 306–318.

Bennett M.W.A. 1987. Rapid monitoring of wetland water status using density slicing. In D. Bruce (Editor), Proceedings of the 4th Australasian Remote Sensing Conference, Adelaide, 14–18 September 1987, pp. 682–691.

Beven K.J. 2000. On the future of distributed modelling in hydrology, Hydrol. Process. 14(16–17), 3183–3184.

Beven K.J. 2001. On hypothesis testing in hydrology, Hydrol. Process. 15, 1655–1657.

Beven K. and Freer J. 2001. A Dynamic TOPMODEL. Hydrol. Process. 15, 1993–2011.

Beven K.J. and Binley A.M. 1992. The future of distributed models: model calibration and uncertainty prediction, Hydrol. Process. 6, 279–298.

Beven K.J. and Kirkby M.J. 1979. A physically-based variable contributing area model of basin hydrology. Hydrol. Sci .Bull. 24, 43–69.

Binley A.M. and Beven K.J. 1993. Three dimensional modelling of hillslope hydrology. In Beven K. and Moore I. (Eds) Terrain Analysis and Distributed Modelling in Hydrology. John Wiley and Sons, Chichester, pp. 107–120.

Bishop K.H., Grip H. and O'Neill A. 1990. Origins of acid runoff in a hillslope during storm events. J. Hydrol. 116 (1–4), 35–61.

Blöschl G. and Sivapalan M. 1995. Scale issues in hydrological modelling: a review. In Kalma J.D. and Sivapalan M. (Eds) Scale Issues in Hydrological Modelling. John Wiley, Chichester, pp. 9–48.

Borin M., Bonaiti G. and Giardini L. 2001. Controlled drainage and wetlands to reduce agricultural pollution – a lysimetric study. J. Environ. Qual. 30, 1330–1340.

Bouwer H. 1986. Intake rate: cylinder infiltration In Klute A. (Ed.) Methods of Soil Analysis, Monograph No. 9, Am. Soc. Agron. Madison, WI.

Brooks A.N. and Hughes T.J.R. 1982, Streamline upwind/Petrov-Galerkin formulations for convection dominated flows with particular emphasis on the incompressible Navier-Stokes equations. J. Compul. Meth. Appl. Mech. Eng. 32, 199–259.

Cantya M., Nielsen A.A. and Schmidt M. 2004. Automatic radiometric normalization of multitemporal satellite imagery. Rem. Sens. Environ. 91, 441–451.

Carey G.F. and Jiang B.N. 1986. Element-by-element linear and non-linear solution schemes. Comm. Appl. Numer. Meth. 2, 45–153.

Charman P.E.V. and Murphy B.W. (Eds) 2000. Soils – Their Properties and Management, A Soil Conservation Handbook for NSW. 2nd edition, Oxford University Press, Oxford. ISBN 0 19 550994 3.

Cirmo C.P. and McDonnell J.J. (1997). Linking the hydrologic and biogeochemical controls of nitrogen transport in near-stream zones of temperate-forested catchments: a review. J. Hydrol. doi: 10.1016/S0022–1694(96)03286–6.

Claxton A.J., Bates P.D. and Cloke H. 2003. Mixing of hillslope, river and alluvial groundwaters in lowland floodplains. Ground Water 41(7), 926–936.

Cloke H.L., Anderson M.G. and Renaud J-P. 2006. Development of a modelling methodology for the investigation of riparian hydrological processes. Hydrol. Process. 20(1) 85–107.

Costa-Cabral, M. and Burges S.J. 1994. Digital elevation model networks (DEMON): a model for flow over hillslope for computation of contributing and dispersal areas. Water Resour. Res. 30(6), 1681–1692.

Craze B., Hofman G., Chapman G.A. and Stone M.J. 2003. Soil Survey Standard Test Methods. Department of Land and Water Conservation, Sydney. http://www.dlwc.nsw.gov.au/care/soil/soil_pubs/soil_tests/soil_test_methods.html. Accessed November 2005.

DHI 2007. MIKE FLOOD – combined 1D and 2D hydrodynamic modelling (based on MIKE 11 and MIKE 21) for detailed inland flooding and storm surge studies. 2007 Release by DHI Water and Environment. Agern Allé 5, DK-2970 Horsholm, http://www.dhigroup.com. Accessed March 2008

DOC 2006, Koondrook Perricoota Forest Cutting 1D Hydraulic Model setup report, Manly Hydraulic Laboratory, NSW Department of Commerce, Sydney. Report No. MHL1489, Commerce Report No. 06024, MHL File No.FH6-00057.

Dooge J.C.I. 1980. Flood routing in channels. Unpublished lecture notes, Department of Civil Engineering, University College, Dublin, Ireland.

Dooge J.C.I. and Harley B M. 1967. Linear routing in uniform open channels, Proc. Intern. Hydrology Symp., Fort Collins, Colorado, Sept 6–8, pp. 57–63. Colorado, USA, Colorado University Press.

Dooge J.C.I. and Napiórkowski J.J. 1987. Applicability of diffusion analogy in flood routing. Acta Geophys. Polon. 35(1): 66–75.

Evans R. and Barnett P. 2007. Assessment of salinity impacts of enhanced flooding in the Koondrook Perricoota Forest on the Wakool and Murray Rivers – Final Report. Technical report prepared by Salient Solutions Pty Ltd and submitted to the NSW Dept of Natural Resources, Queanbeyan.

Fairfield J. and Leymarie P. 1991. Drainage networks from grid digital elevation models. Water Resour. Res. 27(5), 709–717.

Gee D.M., Anderson M.G. and Baird L. 1990. Large scale floodplain modelling. Earth Surf. Process. Landf., 15, 512–523.

Grayson R.B., Moore I.D. and McMahon T.A. 1992. Physically based hydrologic modelling. 2. Is the concept realistic? Water Resour. Res. 28(10), 2659–2666. doi. 10.1029/92WR01259.

Green D.L., Shaikh M., Maini N., Cross H.C. and Slaven J. 1998. Assessment of Environmental Flow Needs for the Lower Darling River. Report CNR 98.028, Centre for Natural Resources, Department of Land and Water Conservation, Parramatta.

Green W.H. and Ampt G. 1911. Studies of soil physics, part I – the flow of air and water through soils. J. Agr. Sci. 4, 1–24.

Hervouet, J.-M. 1992. Element-by-element methods for solving shallow water equations with FEM. Proc. 9th International Conference on Computational Methods in Water resources. Denver, USA.

Hervouet J.-M. 2000. TELEMAC Modelling System: an overview. In: Hervouet J.-M. and Bates P (Eds). Special Issue: The TELEMAC Modelling System. , Hydrol. Process. (13), 2209–2210.

Horritt M.S. 2006. A methodology for the validation of uncertain flood inundation models. J. Hydrol. doi: 10.1016/j.jhydrol.2005.10.027.

Isbell R.F. 1996. The Australian Soil Classification. CSIRO Publishing, Collingwood, Victoria.

Jeffrey S.J., Carter J.O., Moodie K.B. and Beswick A.R. 2001. Using spatial interpolation to construct a comprehensive archive of Australian climate data. Environ Model. Softw. 16, 309–330.

Jenkins B., Vaze J., Tuteja N.K. and Teng J. 2006. Soils Report for Koondrook–Perricoota Forest Hydraulic Modelling: Soil Survey, Data Provision, Soils Map and Soils Testing. NSW Department of Natural Resources and Murray Darling Basin Commission, Australia. ISBN 0 7347 5798 0.

Jenson S.K. 1991. Applications of hydrologic information automatically extracted from digital elevation models. Hydrol. Process. 5(1), 31–44.

Jenson S.K. and Domingue J.O. 1988. Extracting topographic structure from digital elevation data for geographic information system analysis. Photogramm. Eng. Rem. S. 54(11), 1593–1600.

Johnston R. and Barson M.M. 1993. Remote sensing of Australian wetlands: an evaluation of Landsat TM data for inventory and classification. Aust. J. Mar. Freshw. Res. 44, 235–252.

Kazezyılmaz-Alhan C.M., Miguel A.M. Jr and Curtis J.R. 2007. A wetland hydrology and water quality model incorporating surface water/groundwater interactions. Water Resour. Res. 43, W04434, doi: 10.1029/2006WR005003.

King I.P. and Roig L.C. 1988. Two-dimensional finite element models for floodplains and tidal flats. In Niki K. and Kawahara M. (Eds), Proc. Int. Conf. on Computational Methods in Flow Analysis, Okayama, Japan, pp. 711–718.

Knight D.W. and Shiono K. 1996. River channel and floodplain hydraulics. In Anderson M.G., Walling D.E. and Bates P.D. (Eds), Floodplain Processes. John Wiley and Sons, Chichester, pp. 139–181.

Lane S.N., Richards K.S. and Chandler J.H. 1994. Application of distributed sensitivity analysis to a model of turbulent open channel flow in a natural river channel. Proc. R. Soc. Lond. Ser. A 447, 49–63.

Lynch D.R. and Gray W.G. 1980. Finite Element simulations of flow deforming regions. J. Comput. Phys. 36, 35–153.

Mark D.M. 1988. Chapter 4: Network models in geomorphology. In Anderson M.G. (Ed.) Modelling in Geomorphological Systems. John Wiley, New York. pp. 73–97.

Mark D.M., Dozier J. and Frew J. 1984. Automated basin delineation from digital elevation data. Geo. Process. 2, 299–311.

Martz L.W. and Garbrecht J. 1992. Numerical definition of drainage network and subcatchment areas from digital elevation models. Comput. Geosci. 18(6), 747–761.

McDonnell J.J., Stewart M.K. and Owens I.F. 1991. Effect of catchment-scale subsurface mixing on stream isotopic response. Water Resour. Res. doi: 10.1029/91WR02025.

MDBC 2002. Setting up of MSM-BIGMOD Modelling Suite for the River Murray System. Technical Report No. 2002/5, November. Murray Darling Basin Commission, Canberra, Australia.

MDBC 2006. The Gunbower–Koondrook–Perricoota Forest Icon Site Environment Management Plan 2006–2007, Murray Darling Basin Commission, Canberra. Publ. No. 32/06, ISBN 1 921038 98 5.

MDBC 2007. Setting up of the Murray Simulation Model (MSM) for Auditing the CAP in the Murray and Lower Darling River Systems. Technical Report 2006/11, Murray Darling Basin Commission, Canberra, Australia, May.

MDBC 2005. Evaluation of remote sensing technologies for high resolution terrain mapping: LiDAR vs photogrammetry. A report to the Murray Darling Basin Commission prepared by Spatial Information and Infrastructure, Department of Sustainability and Environment, Victoria.

MIL 2004. Torrumbarry Cutting Project – Stage 1 Report. Murray Irrigation Limited, Deniliquin, NSW.

Mitchell G.F., Hunt C.L. and Su Y.M. 2002. Mitigating highway runoff constituents via a wetland. Transp. Res. Rec. 1808, 127–133.

Moore R., Schulz C.M., Cooper S., Smith S. Jr and Rodgers J.H. (2002). Mitigation of chlorpyrifos runoff using constructed wetlands. Chemosphere 46(6), 827–835.

Morris D.G. and Heerdegen R.G. 1988. Automatically drained catchment boundaries and channel networks and their hydrological applications. Geomorphology 1, 131–141.

Napiórkowski, J.J. 1992. Linear theory of open channel flow. In O'Kane J.P. (Ed.) Advances in Theoretical Hydrology – A Tribute to James Dooge. European Geophysical Society Series on Hydrological Sciences. Elsevier, Amsterdam.

Nash J.E. 1960. A unit hydrograph study with particular reference to British catchments. Proc. Inst. Civ. Eng. 17, 249–282.

O'Callaghan J.F. and Mark D.M. 1984. The extraction of drainage networks from digital elevation data. Comput. Vis. Graph. Image Process. 28, 328–344.

Peroux K.M. and White I. 1988. Design for disc permeameter. Soil Sc. Soc. Am. J. 52, 1205–1215.

Pleysier J.L. and Juo A.S.R. 1980. A single extraction method using silver-thiourea for measuring exchangeable cations and effective CEC in soils with variable charges. Soil Sci. 129, 205–211.

Ponce V.M., Li R.M. and Simons D.B. 1978. Applicability of kinetic and diffusion models. J. Hydraul. Div. ASCE 104(HY3), 353–360.

Quinn P., Beven K, Chevallier P. and Planchon O. 1991. The prediction of hillslope flow paths for distributed hydrological modelling using digital terrain models. Hydrol. Process. 5, 59–80.

Rayment G.E. and Higginson F.R. 1992. Australian Laboratory Handbook of Soil and Water Chemical Methods – Australian Soil and Land Survey Handbook. Inkata Press, Melbourne and Sydney.

Richardson C.J., Qian S., Craft C.B. and Qualls R.G. 1997. Predictive models for phosphorus retention in wetlands. Wetlands Ecol. Manage. 4, 159–175.

Ritchie J.A. 1963. Earthwork tunnelling and the application of soil testing procedure. J. Soil Cons. NSW 19, 11–129.

Romanowicz R. and Beven K. 2003. Estimation of flood inundation probabilities as conditioned on event inundation maps. Water Resour. Res. 39(3), 1073, doi: 10.1029/2001WR001056, 2003.

Siebert J. and McDonnell J.J. 2002. On the dialog between experimentalist and modeler in catchment hydrology: use of soft data for multicriteria model calibration. Water Resour. Res. 38 (11), 1241. doi: 10.1029/2001WR000978.

Shaikh M., Brady A.T., and Sharma P. 1998. Applications of remote sensing to assess wetland inundation and vegetation response in relation to hydrology in the Great Cumbung Swamp, Lachlan Valley, NSW, Australia. In McComb A.J. and Davis J.A. (Eds) Wetlands for the Future. Gleneagles Publishing, Adelaide. pp. 595–606.

Shaikh M., Green D. and Cross H. 2001. A remote sensing approach to determine environmental flows for wetlands of the Lower Darling River, New South Wales, Australia. Int. J. Remote Sens. 22(9), 1737–1751.

Singh V.P. 1996. Kinematic Wave Modelling in Water Resources: Surface Water Hydrology. Wiley, New York.

Smith L.C. 1997. Satellite remote sensing of river inundation area, stage, and discharge: a review. Hydrol. Process. 11, 1427–1439.

Summerell G.K., Tuteja N.K., Grayson R.B., Hairsine P.B. and Leaney F. 2006. Contrasting mechanisms of salt delivery to the stream from three different landforms in South Eastern Australia. J. Hydrol. doi: 10.1016/j.jhydrol.2006.05.002.

Talsma T. and Hallem P.M. 1980. Hydraulic conductivity measurements of forest catchments. Aust. J. Soil Res. 18, 139–148.

Tarboton D.G. 1997. A new method for the determination of flow directions and upslope areas in grid digital elevation models. Water Resour. Res. 33, 309–319.

Tarboton D.G. 1989. The analysis of river basins and channel networks using digital terrain data. ScD Thesis, Department of Civil Engineering, M.I.T., Cambridge, MA. (Also available as Tarboton D.G., Bras R.L. and Rodriguez-Iturbe I. (Same title), Technical report no. 326, Ralph M. Parsons Laboratory for Water resources and Hydrodynamics, Department of Civil Engineering, M.I.T., September).

Tarboton D.G., Bras R.L. and Rodriguez-Iturbe I. 1988. The fractal nature of river networks. Water Resour. Res. 24(8), 1317–1322.

Tuteja N.K. and Close A. 2006. Koondrook–Perricoota Flood Enhancement Project I15 – Water Availability Study. Interim report submitted to the Murray Darling Basin Commission and Project Steering Committee, 29 September. Project I15, The Living Murray.

Tuteja N.K., Beale G.T.H., Summerell G.K. and Johnston W.H. 2002. Development and validation of the catchment scale salt balance model CATSALT version 1. NSW Department of Land and Water Conservation, Parramatta. CNR 2001.031 ISBN 0 7347 5244 X.

Tuteja N.K., Vaze J., Teng J. and Mutendeudzi M. 2007. Partitioning the effects of pine plantations and climate variability on runoff from a large catchment in south-eastern Australia. Water Resour. Res. 43, W08415, doi: 10.1029/2006WR005016, 2007.

URS 2004. Tornumbarry Cutting – Hydraulic Modelling Report. Final Report 50018/005 October 2004. Prepared for Murray Irrigation Limited, Deniliquin, NSW.

van Genuchten M.Th. 1980, A closed form equation for predicting the hydraulic conductivity of unsaturated soils. Soil Sc. Soc. Am. J. 48, 703–708.

Watson F.G.R., Grayson R.B., Vertessy R.A., Peel M.C. and Pierce L.L. 2001. Evolution of a hillslope hydrological model. International Conference on Modelling and Simulation MODSIM 2001, Canberra, Australia, 10–13 December 2001, pp. 461–467.

Wigmosta M.S., Vail L.W., Lettenmaier D.P. 1994. A distributed hydrology-vegetation model for complex terrain. Water Resour. Res. 30(6), 1665–1679.

Woolhiser D.A. and Ligget J.A. 1967. Unsteady one-dimensional flow over a plane: the rising hydrograph. Water Resour. Res. 3(3), 753–771.

Yen B.C. (1979) Unsteady flow mathematical modelling techniques. In Shen H.W. (Ed.) Modelling of Rivers. Wiley Interscience, New York, pp. 13.1–13.33.

Zeilke W. and Urban W. 1981. Two-dimensional Modelling of Rivers with Floodplains. Numerical Modelling of River Channel and Overland Flow for Water Resources and Environmental Applications. IAHR, Delft, The Netherlands.